№1, 2024

ISSN 2706-977X

MATERIAL AND MECHANICAL ENGINEERING TECHNOLOGY

Material and Mechanical Engineering Technology | MMET

Editorial board of the journal

Content

DOI 10.52209/2706-977X_2024_1_3 **IRSTI 55.31.01** **UDC 621.92**

Features of Engineering Methods of Research Results on Butt Welding on Metal Pipelines

Mardonov B.T. [1], Sherov K.T. [2]*, ToirovM.Sh. [1], Makhmudov L.N. [1], Yakhshiev Sh.N.[1], Kongkybayeva A.N.[2], Shezhau K. [2]

[1]Navoi State Mining and Technologies University, Navoi, Uzbekistan
[2]Seifullin Kazakh Agrotechnical Research University, Astana, Kazakhstan
*corresponding author

Abstract. This article discusses the use of flash butt welding (FBW) for increased labor productivity in pipeline construction. However, despite its promise, FBW technologies and equipment have limitations in creating defect-free welded joints. The Ishikawa diagram is used to systematize and analyze factors that cause defects, which are then ranked on a Pareto diagram. The main causes of defects are found to be associated with human factors, such as the qualifications of workers, as well as imperfections in machinery and equipment, material deviations, and technology and measurement limitations. A correlation matrix is used to analyze the causes of the decrease in quality and determine that improving methods and means of FBW processes, along with FBW technologies, is the solution. However, a complete computer model of FBW processes has not yet been created due to difficulties in describing energy release and other energy phenomena. A physical and mathematical model is necessary to take into account energy processes in the welding zone.

Keywords: Defects in welded joints, Ishikawa diagram, Pareto diagram, human factor, qualification of performers

Introduction

For a significant increase in labor productivity in the construction of pipelines, it is very promising to use flash butt welding of FBW [1]. Unfortunately, modern FBW technologies and the equipment used do not allow to fully create defect-free welded joints [2, 3]. Analysis of the causes of defects is difficult to implement due to their diversity [4]. One of the effective tools for systematization and analysis of significant factors that cause any consequence is the Ishikawa diagram [5].

Traditionally, all possible causes on the Ishikawa diagram [8] are categorized according to the principles: (human) - due to the human factor; (machines, equipment) - associated with equipment; (materials) - related to materials; (methods, technology) - related to the technology of work, with the organization of processes; (measurement, control) - related to methods of measurement and quality control. Subsequently, these reasons were ranked on the Pareto diagram [6]. On Figure 1 shows the Ishikawa diagram indicating the main cause-and-effect relationships for ensuring the quality of welded joints during the implementation of the FBW process.

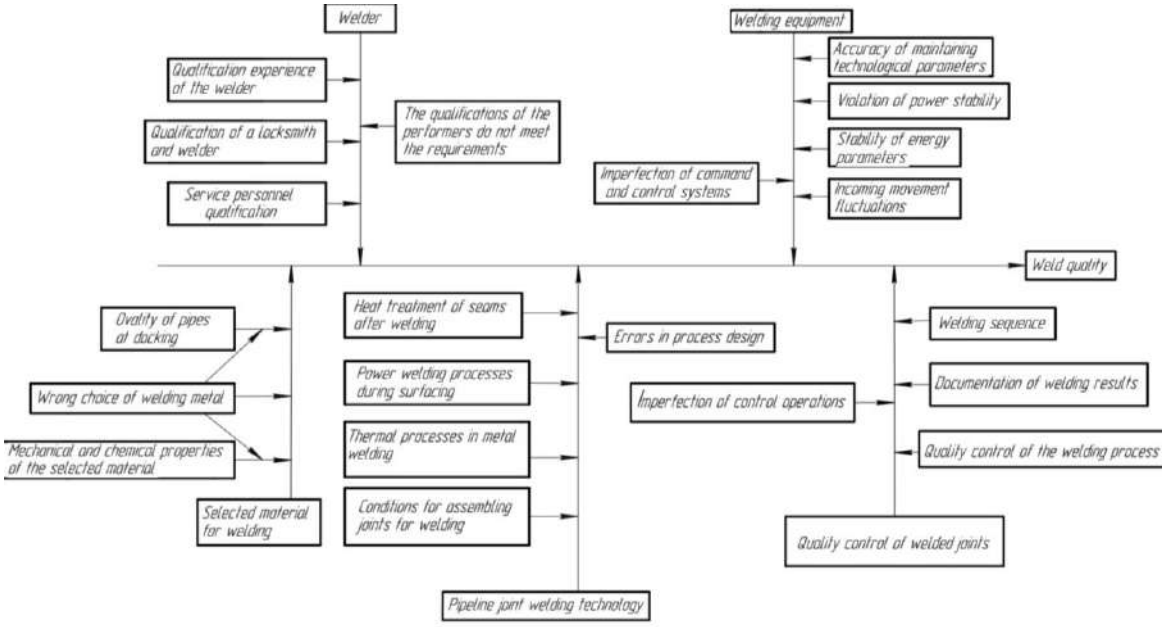

Fig. 1. - Ishikawa diagram of the implementation of the FBW process, indicating the cause-and-effect relationships

It has been established that the common cause of defects in the implementation of FBW processes associated with the human factor (human) is the qualification of the performers that does not correspond to the complexity of the process. The Pareto diagram showed that the absence of process monitoring systems and the possibility of

adjusting modes, assembly and installation problems of the welding machine at the joint, as well as machine failures and vague wording in the RE also contribute to the occurrence of defects.

The main reasons for the occurrence of defects due to imperfections (machines, equipment) are the instability of the welding mode parameters, the energy parameters of the process, the supply current, as well as the design flaws of the equipment. The Pareto diagram showed that the main among them are the instability of the technological parameters of the welding mode and the instability of the upsetting mechanisms. Among the reasons for the decline in product quality associated with (materials) are deviations in the ovality of pipes and their initial mechanical properties, the presence of internal and surface defects and contamination of the pipe cavity. The Pareto diagram showed the primary influence on the occurrence of defects of the ovality of pipes and their initial mechanical properties, the presence of internal defects.

There are still a number of problems grouped into the category (methods, technology), including the lack of the possibility of intervening in the welding process, difficulties in flashing and upsetting, the need for maintenance to improve the mechanical properties of the welds and the HAZ. The Pareto diagram shows that the main ones are the impossibility of prompt intervention in the welding process. In many respects, determine the quality of FBW.

1. Methodology

The Pareto diagram shows that the main disadvantages associated with methods for measuring and controlling the quality of welded joints are the inability to predict the quality of welds directly in the welding process and the lack of a system for monitoring deviations in the assembly of joints.

For further in-depth analysis, a correlation matrix was built between the causes of a decrease in the quality of welded joints and the conditions for performing welding work, which made it possible to determine that the integral way to solve most of these problems is to improve the methods and means of all stages of the FBW process with simultaneous improvement of FBW technologies based on high-quality and quantitative analysis of phenomena occurring during welding. It is known that the necessary properties of welded joints are ensured by setting the optimal parameters of the welding mode using computer analysis methods [7]. However, a sufficiently complete computer model of the processes occurring in the contact zone has not yet been created. This is due to the problems of describing the heat release in the contact zones, the formation of a permanent connection in the liquid-solid phase, and structural transformations in the weld and HAZ.

Since heat release is a system-forming factor, exclusive attention is paid to it [8]. Powerful heat release in the joint is due to the flow of current through numerous bridges of liquid metal in the joint, which randomly appear and explode, which leads to the removal of a significant amount of metal in the form of spatter. Therefore, the main problem of computer simulation of the FBW process is to take into account the basic energy phenomena in the physical and mathematical description. The main technological factors are the reflow rate V , allowances for reflow δ and upsetting Δ, at the installation reach L (distance from the machine clamps to the joint), as well as the open-circuit voltage U (Figure 2).

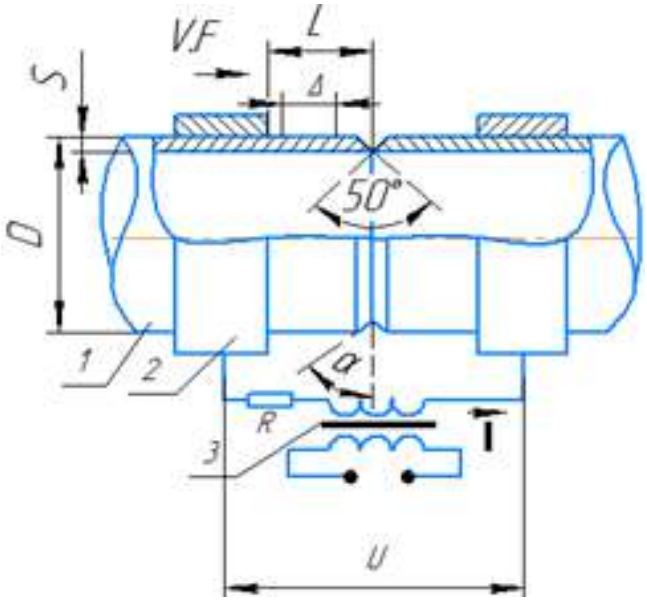

Fig. 2. - Scheme of the flash welding process. 1 - weldable structure, 2 - clamps, 3 - welding transformer

In this regard, the physical and mathematical model should take into account the energy processes occurring in the zone immediately adjacent to the joint (Figure 3).

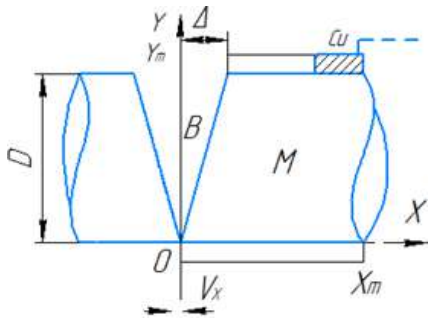

Fig. 3. - Reflow process zone: M - steel of the pipe wall, Cu - copper retainer (current lead), B - air

Since the welded joint is symmetrical, the processes in the end part of one of the pipes are characteristic of the second. Taking into account the fact that all axial sections of the pipe are the same, the process was considered only in one of these sections in the Cartesian coordinate system *x*, *y*. The center of coordinates was placed in the corner of the contact zone of the pipes. During melting, this center is immobile, and the metal moves at the melting speed along the $v_x x$ coordinate. Since the shape of the joint changes during reflow, the free space into which the metal moves is included in the modelling space. The zone occupied by metal is designated *M*, free - *B*. The main physical dependencies necessary for the development of a mathematical model of the FBW process, including the temperature distribution in the simulation zone by solving the heat equation, the boundary conditions for the heat exchange of the simulation zone with the surrounding space, as well as the distribution of heat generation in the metal from the flow of electric current through it and heat generation from arcs - of the spark process in the joint at the break of the jumpers are presented in [9].

2. Results and Discussions

It is known [10] that FBW processes can be divided into 5 stages, which are implemented in the following sequence: initial short circuit in the joint, preliminary heating of the edges during the arc- spark process, obtaining a steady temperature distribution in the joint, forcing flashing before upsetting and upsetting of the joint with subsequent cooling. Since at stage 1 the process is in the resistance welding mode under conditions of continuous edge approach, the main parameters of this process are the short-circuit current of the joint, the v_x edge approach speed and the edge preparation angle α. Figure 4 shows the dependence of the heating time of the contact metal on the angle of cutting edges at different values of the speed of their convergence, the initial short circuit in the joint. The obtained results of modelling the initial stage of the process show that at angles of cutting over 15° the flashing is stably excited at real speeds of the initial stage of flashing 0.1…0.3 mm/s. Therefore, the cutting angle α = 15° can be considered optimal.

Preliminary heating of the edges during the arc-spark process at stage 2 is accompanied by removal of edge metal Since the beginning of this stage occurs at cold metal, then it is characterized by an increased intensity of heat extraction in the arc zone spark process. Therefore, it is the shape of the groove that determines the rate of increase in the area of the melted metal as the edges approach each other.

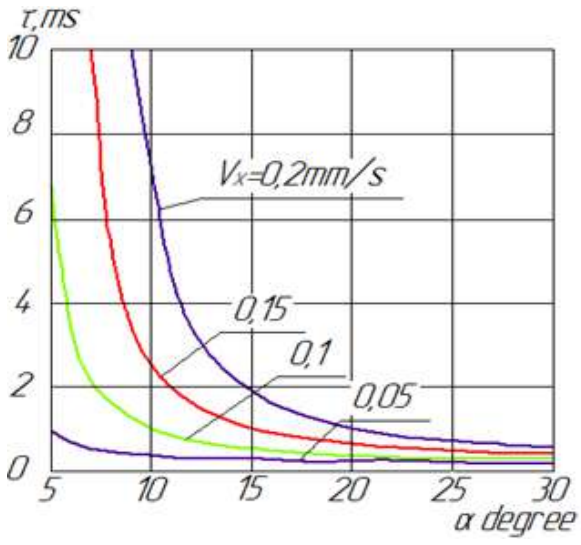

Fig. 4. - Dependence of the τ heating time of the butt metal to the melting temperature on the angle of α cutting edges at different speeds v_x their convergence

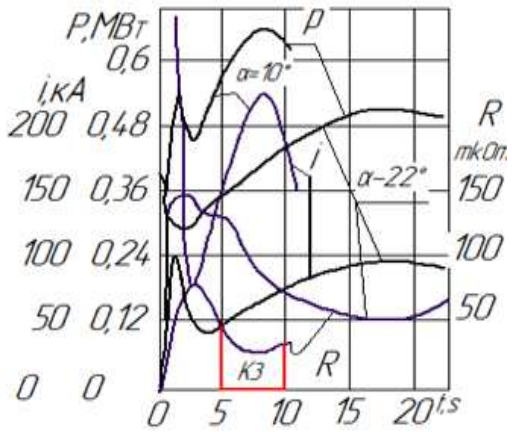

Fig. 5. - Influence of the bevel angle on the power, current and electrical resistance of the joint in the initial phase of the process at a melting speed of 0.14 mm/s

On Figure 5 shows the change in heat dissipation power and joint resistance in the initial phase of the process at different values of the angle of cutting edges. The power consumed for melting is determined by the amount of heat carried away by the drops metal and heat flow into the metal of the joint. At the beginning of reflow, the power of the thermal flow into metal which has a low temperature. As the metal warms up, this power decreases, and the total power of the process and the welding current decrease accordingly. The power carried away by the drops increases as the growth of the reflow area faster than the decrease in the heat flux in edges.

Therefore, after the initial decrease in current, its increase begins. Maximum current and power is reached when the fusion has removed the grooves and covered the entire cross section.

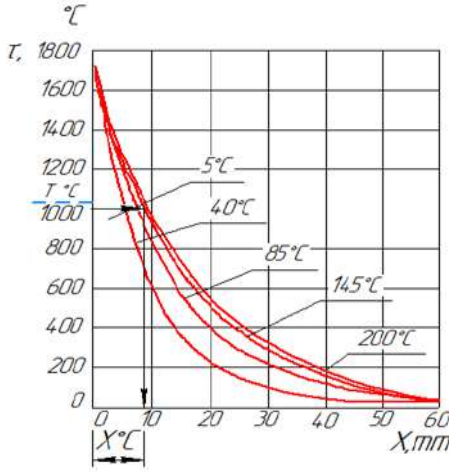

Fig. 6. - Temperature distribution over the depth of the metal at different times of melting and determination of the allowance for upsetting X_{oc} by the temperature Toc of metal deformation during joint upsetting

Stage 3 is characterized by a steady temperature distribution in the joint. Since at this stage the melting covers the entire cross section of the joint, the power of the heat flux into the metal gradually decreases, and the temperature distribution stabilizes. In this case, the optimal combination of the edge approach rate and the energy parameters of the process should ensure a uniform temperature distribution without chaotic arc breaks and short circuits. If at this stage the heat input is excessively high, and the edge convergence rate is too low, then there is a high probability of occurrence of local tearing of the metal, which increases the risk of defects in the formation of the seam.

On Figure 6 shows the change in the temperature distribution over the depth of the metal during melting. The resulting temperature distribution makes it possible to determine the optimal value of the melting allowance. This allowance is determined by the optimum temperature for completing the deformation of the metal during upsetting. When welding steels, this temperature is 1000 ... 1200 ° C. It is also desirable that the precipitation temperature be below the phase transition temperature (760 0 C), which excludes the formation of hardening structures. According to the value of the deformation temperature during upsetting Toc and the resulting temperature distribution, it is possible to determine the allowance for reflow Xos, fig. 6. According to the tensile strength τos at the selected temperature Tos , Figure 7, and the cross-sectional area of the joint - upsetting force.

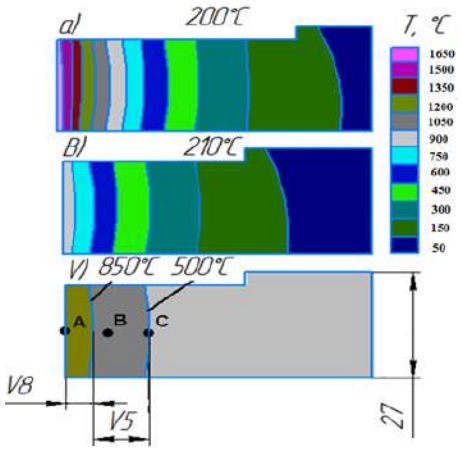

Fig. 7. - Temperature distribution in the wall of a steel pipe at the moment end of melting (a), at the moment of end of upsetting (b) and location of zones of complete (X8, T>850 °C) and partial (X5, 850 °C >T >500 °C) structural transformation (c)

To ensure the fusion of the joint at stage 4, flashing is forced before upsetting. To do this, the speed is increased to the maximum allowable value of the power of the machine. On Figure 8 shows the influence of the value Vx4 of the flashing speed at the stage of its forcing on the power P of heat release in the joint, on the welding current I and on the resistance of the joint R. at a speed of 0.4 mm/s, the resistance of the joint drops below 50 μΩ, the internal resistance of the machine.

Therefore, it is more rational to stepwise increase the reflow rate: at the first stage - Vx3 to the limit value at which the stability of the process is maintained, and at the second stage, the value of Vx4 to the maximum for the power source with varying the reflow interval. Based on the results obtained, which are in good agreement with the data of [11,12,13,14], a cyclogram with Vx4 = 1.2 mm/s was adopted. At stage 5, joint settlement and cooling occur. Sludge plays an important role in weld quality as it forces molten metal and contaminants out of the joint. The duration of upsetting is determined by the capabilities of the upsetting mechanism of the welding machine and should be as short as possible, since after short circuit the temperature of the metal decreases rapidly (Figure 8).

Conclusions

The performed analysis made it possible to determine how the main physical and technological conditions for the flow of FBW affect the possibility of obtaining defect-free welded joints of joints in large-diameter main pipelines, including the bevel angle of the joint edges, allowance for flashing, forcing flashing and upsetting. The presented research methods can also be used to solve other problems of welding production, for example, the creation of intelligent control systems.

References

[1] Zhuravlev S. I., Konovalov N. A. Features of the construction of main pipelines using flash butt welding // Materials of the International Scientific and Practical Conference "Problems and Methods for Ensuring the Reliability and Safety of Oil, Oil Products and Gas Transportation Systems. - Ufa: State Unitary Enterprise "IPTE", 2013, P. 206–207.

[2] Zhuravlev S. I. Ways to solve the problems of introducing flash butt welding on main pipelines of large diameters //*Izvestia of higher educational institutions. Engineering,* vol. 8, 2013, P. 64-71.

[3] Konovalov N. A., Tretyakov E. S. Using methods of expert assessments in improving equipment and technologies for flash butt welding of pipelines //Proceedings of the VI All-Russian Conference of Young Scientists and Specialists "The Future of Mechanical Engineering in Russia, Moscow, 2013, P. 108–109.

[4] Zhuravlev S. I., Konovalov N. A., Poloskov S. I. Technological features of flash butt welding of pipelines of large diameters", Sat. scientific papers of the VII International scientific and technical conference "Modern problems of mechanical engineering". Tomsk: Publishing House of the Tomsk Polytechnic University, 2013, P. 180–185.

[5] Ishikawa K. La gestion de la qualité, outils et applications pratiques. Traduit par Jean-Marie Douchy. Paris: L'Usine Nouvelle, 2007. - 242 p.

[6] Reed W. J. The Pareto, Zipf and other power laws //Economics Letters, vol. 74, 2001, P. 15 - 19. https://doi.org/10.1016/S0165-1765(01)00524-9

[7] Ichiama Y., Satio T. Factors affecting flash weldability in high strength steel - a study on toughness improvement of flash welded joints in high strength steel //Welding International, vol. 18, no. 6, 2004, P. 436 - 443. https://doi.org/10.1533/wint.2004.3255

[8] Erofeev V. A. Prediction of the quality of electron beam and laser welding based on computer simulation: Monograph. - Tula: TulSU, 2002. - 140 p.

[9] Zhuravlev S. I., Erofeev V. A., Poloskov S. I. Physico-mathematical model of flashing in the process of flash butt welding //Welding and Diagnostics, vol. 4, 2013, P. 26–30.

[10] Mardonov B. T., Toirov M. S. Reliable evaluation of strength effects of welding defects for steel pipes and tube systems //Science and technology magazine "Development of science and technology" - Fergana polytechnic institute. vol. 1, 2023, P. 20-25.
[11] Kuchuk -Yatsenko S.I. Flash butt welding. Kiev: Naukova Dumka, 1992. - 236 p.
[12] Kuchuk-Yatsenko S.I ., Shvets Yu. V., Zagadarchuk et al. Flash butt welding of thick-walled pipes made of high-strength steels of strength class K56 //*Automatic* V. F. *welding*, vol. 5, 2012, P. 5–11.
[13] Sherov K.T., Mussayev M.M., Zharkevich O.M. Features of chip formation during thermal friction milling. Material and Mechanical Engineering Technology, №3, 2021, P. 17-21. DOI https://doi.org/10.52209/2706-977X_2021_3_17
[14] Akulovich L.M., Sergeev L.E., Mendaliyeva S.I., Sherov K.T. Features of Magnetic Field Modeling for Magnetic-Abrasive Treatment of Complex-Profile Surfaces. Material and Mechanical Engineering Technology, №4, 2022, P.37-42. DOI https://doi.org/10.52209/2706-977X_2022_4_37

Information of the authors

Bakhtiyor Mardonov, doctor of technical sciences, professor, Navoi State Mining and Technologies University.
e-mail: mbt69@mail.ru
Karibek Sherov, doctor of technical sciences, professor, Seifullin Kazakh Agro-Technical Research University
e-mail: shkt1965@mail.ru

Murtoza Toirov, PhD, Navoi State Mining and Technologies University
e-mail: murtoza.toirov@mail.ru

Lutfiddin Makhmudov, doctoral student, Navoi State Mining and Technologies University
e-mail: lmn_76@mail.ru

Sherali Yakhshiev, PhD, Navoi State Mining and Technologies University
e-mail: sheraliyaxshiyev1978@mail.ru

Arailym Kongkybayeva, doctoral student, Seifullin Kazakh Agro-Technical Research University
e-mail: arai_janaarka@mail.ru

Kadylet Shezhau, doctoral student, Seifullin Kazakh Agro-Technical Research University
e-mail: kadylet.2011@mail.ru

DOI 10.52209/2706-977X_2024_1_9 **IRSTI 55.15.09** **UDC 615.49203.07**

Studying the Depth of Carbonifying Castings Obtained by the Lost Foam Casting Method with a Complex Polystyrene Composition

Kovalyova T.V.*, Issagulov A.Z.
Abylkas Saginov Karaganda Technical University, Karaganda, Kazakhstan
*corresponding author

Abstract. At present, lost foam casting method is an updated, long-term and the most economically feasible method in the foundry industry. Despite the fact that the casting technique is relatively simple, high demands are placed on the model materials. Carburization of the surfaces of steel castings obtained by the lost foam casting method is one of the main and the most significant problems in the use of this casting method. One solution is to use a complex composition of the material: a combination of cast and construction polystyrene. It was determined that the complex composition of the cast and construction polystyrene model in the ratio of 60 to 40% helps to reduce the depth of carburization and the percentage of internal defects. In addition, the cost of 1 kg of the complex composition models is 25% lower than the cost of 1 kg of models made of cast polystyrene.

Keywords: complex polystyrene, carburization, quality, roughness, casting defects.

Introduction

Producing the domestic high-precision castings for any country is a task of strategic importance, because it ensures economic independence and determines the basis for the development of national mechanical engineering. According to [1], now in Kazakhstan the share of imported foundry products is about 80%. Meanwhile, the country has both sufficient raw material resources and basic means for manufacturing foundry products for various purposes, including high-precision castings.

Recently, much attention has been paid to the technology of producing castings with the use of the lost foam casting method (LFC), and in Kazakhstan this technology is beginning to spread. The Parkhomenko KMZ LLP in Karaganda was the first to introduce the LFC method. The method showed that its scope can cover almost all the traditional sand molding. This is especially true in single and small-scale production.

The lost foam casting method is a low-waste production. One of the disadvantages of this technology is the carburization of the surface of the castings during the destruction of polystyrene. For most parts, a layer of steel containing a high carbon content is a defect, since such a layer is brittle and hard, removes the cutting tool during processing, and during operation of the part can lead to its destruction. The casting polystyrenes PSV-1L currently used in production in Kazakhstan, despite fairly complete gasification, are sources of increasing the carbon content of the surface of the castings to a depth of 1.5-2 mm. At the same time, cast polystyrene foam, which has small grains, has a relatively high density. It is known that reducing the density of the model reduces the depth of the loaded layer of steel castings [2-3]. In this case, it becomes possible to obtain a complex composition of a polystyrene foam model from a mixture of casting and construction polystyrene granules, which have a lower density. At the same time, the cost of the model will also be lower, since construction polystyrene is 30-40% cheaper than foundry polystyrene. It is proposed to use PSV-1L grade polystyrene, traditional for the Karaganda region.

1. Methods and Experiments

According to the proposed technology [4], in the foundry shop of the Parkhomenko KMZ LLP (Karaganda) there were carried out studies of the quality of castings made by the LFC method with the use of the complex composition of the gasified model.

A new composition of the model material for LFC was proposed:

- construction polystyrene PPS-20–40%. The size of the granules is 0.5-0.8 mm;
- cast polystyrene PSV-1L – 60%. The size of the granules is 0.2-1.2 mm.

The models were produced from a mixture of cast polystyrene with fractions of 0.7...1.0 mm (the size of the supplied granules) in an amount of 60% and construction polystyrene foam granules up to 3.0 mm in size (the main dimensions of construction polystyrene granules) in an amount of 40%. Polystyrene, according to the technology adopted at the plant, was pre-foamed with steam and dried, then blown into a mold, which was kept in an autoclave until the polystyrene granules were sintered [5].

The studies were carried out on the "Case" casting made of 35L steel. The melt was obtained in an induction furnace, pouring was carried out at a temperature of 1540-1560 ^{0}C.

Use sand grades 1K02 and 1K016 as filler for the casting mold in a ratio of 70 to 30 in order to increase the density and strength of the mold.

Metallographic studies to assess the quality and properties of metal materials were carried out using an Altami POLAR 3 microscope (Russia).

After the castings were made, samples were cut out from them with the use of a disk cutter. They were used to prepare thin sections to evaluate the microstructures. Quantitative and qualitative assessment of microstructures was carried out using the ThixometPro program (Russia).

The discontinuities in castings were studied with the use of an ultrasonic flaw detector USD-50 (Russia).

It is known that when a model obtained by LFC interacts with the molten metal, the following combustion products are formed: water vapor, liquid phase, solid residue and gas that contains the elements of hydrogen, hydrocarbon, carbon monoxide, and carbon. The content of the solid phase relative to the gaseous phase increases with increasing the temperature and at steel pouring temperatures it exceeds 70%. Carbon and soot constitute the solid phase, which contribute to the carburization of the casting both on the surface and in the volume of the ingot as a whole [6, 7].

Using the compositions indicated in Table 1, casting models “Case” were made (Figure 1). Studying the castings showed that the castings obtained with the use of the new technology had high geometric accuracy (allowances of 0.5-1%), low roughness (Rz 60-90), and there were no external and internal defects.

The trend of transition from casting in sand-clay molds to lost foam casting models is explained by the fact that this contributes to sharp reduction in the total labor costs, the metal intensity of the resulting castings, and the achievement of high and often fundamentally new physical and mathematical characteristics and operational properties of cast products.

a)

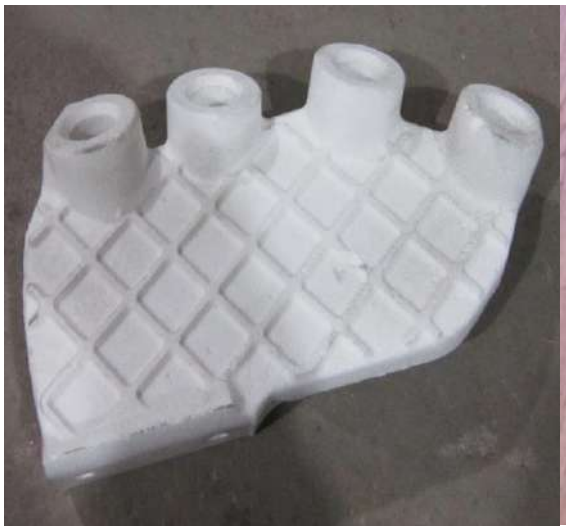

b) c)

Fig. 1. – Manufacturing the “Case” casting: a) compression mold; b) model; c) casting

1. Results and discussion

There were studied three castings obtained with different composition of polystyrene models (Table 1).

Table 1. The composition of polystyrene models

Sample No.	Cast polystyrene, %	Construction polystyrene, %
1	80	20
2	100	-
3	60	40

In the first series of experiments, the effect of the model density on the depth of carburization was assessed (Table 2).

It is obvious that reducing the model density has a beneficial effect on minimizing carburization of the casting surface. However, the use of a combination of construction and cast polystyrene leads to the most optimal placement of granules. Thus, the rate of burnout and removal of gases from the mold cavity occurs consistently, which is almost comparable to the burnout rate of casting polystyrene [8].

Table 2. The model density effect on the carburization depth

Sample No.	Density, g/cm^3	Maximum carburization depth, μm
1	0.31	62.2
2	0.37	68.5
3	0.44	82.3

There were also radially placed risers at equal intervals on the surface of the model and considered the feasibility of their use from the point of view of carburization (Table 3). The risers were placed with the diameter of 6 mm.

Table 3. The number of risers in the casting mold effect on the carburization depth

Sample No.	Number of risers	Maximum carburization depth, μm
1	0	79.9
2	2	66.1
3	4	64.5

As studies have shown, the presence of risers generally reduces the depth of carburization, however, increasing the number of risers does not affect carburization.

The microstructure of the sample surface layer depth is shown in Figure 2.

It can be seen in the microstructure that the maximum depth of carburization when using the complex composition of polystyrene reaches 56.4 microns. It is known from a number of studies [2-3] that the depth of carburization of steels with the carbon content of 0.3-0.4% averages 76-105 microns, which is significantly greater than the depth of carburization with the use of the proposed technology due to decreasing the density of the model with the use of construction polystyrene. This generally reduces the amount of carbon generated as a result of the model destruction. Thus, the proposed complex composition of the polystyrene model with the use of the proposed technological modes for specific types of castings solves the problem of carburization of the surface layer of the casting.

The carried out studies suggest that the use of polystyrene composition 3 for the model contributes to the formation of a homogeneous structure throughout the entire volume of the melt, helps to exclude slag, gases, etc. from the melt.

This was also confirmed by studying the discontinuities with the used of an ultrasonic flaw detector.

The analysis and studies of the technological process of lost foam casting allowed making a reasonable comparison of the technological, operational, economic and environmental indicators of the casting processes in sand-clay molds and in sand molds of the LFC method (Tables 4-7).

Table 4. Performance indicators

Indicator	LFC with the use of cast polystyrene for models	LFC with the use of the complex polystyrene composition for models
Technological		
Mixture composition	Single-component	Multi-component
Carburization	More than 100 μm	Less than 80 μm
Ga permeability	High	High
Roughness	Low	Low
Burning	Medium	Low
Operational		
Power consumption	Low	Low
Current operation	Medium	Medium
Area occupied by the equipment	Small	Small

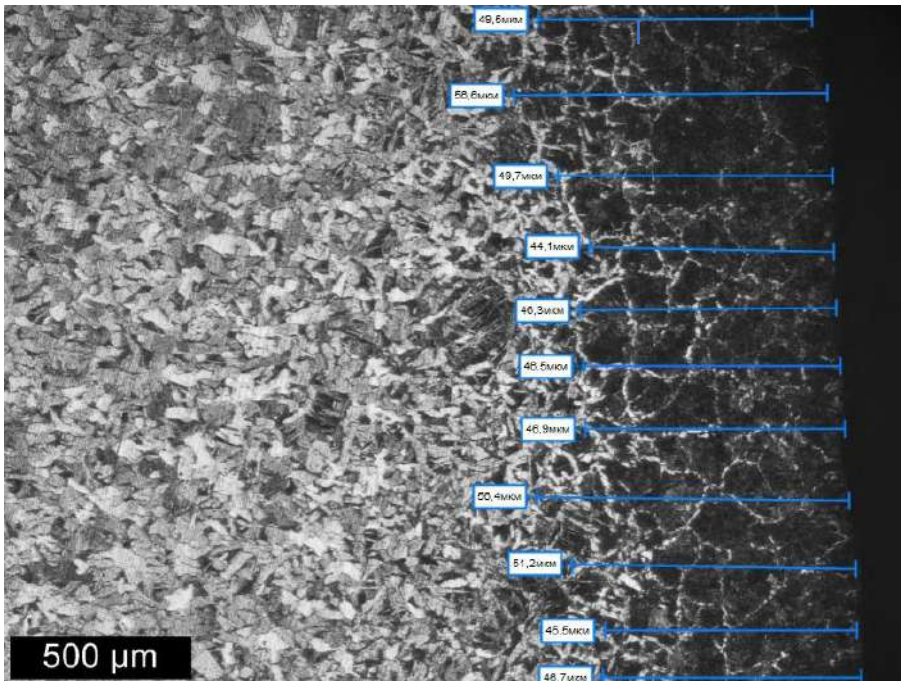

a)

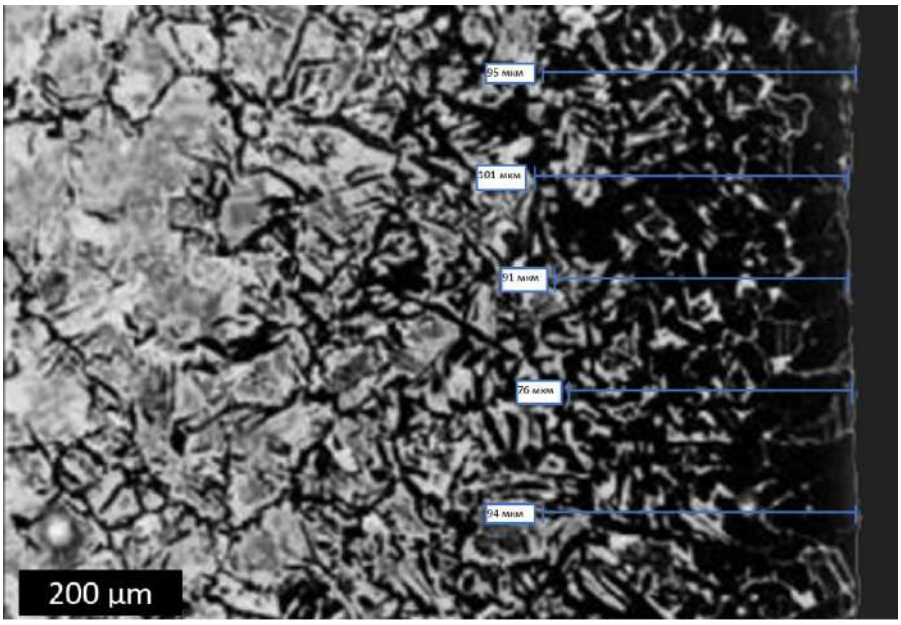

b)

Fig. 2. - Microstructure of the St 35L casting and determining the carburization depth of the surface layer using the ThixometPro program, obtained by the lost foam casting method with complex polystyrene (a) and cast polystyrene (b)

Table 5. Statement of capital investments in molding sand and models for LFC with the use of cast polystyrene for the model

Material	Cost of one *kg* or one *l*, tenge	Quantity of the material, *kg* or *l*	Total amount, tenge
Sand of the K0315A grade, SS 2138-84, kg	12	50	600
Cast polystyrene PSV-1L, kg	3000	25	75000
Paint	1000	10	10000
TOTAL			85600

Table 6. Statement of capital investments in molding sand and models for LFC (comparison)

Material	Cost of one *kg* or one *l*, m^3, tenge	Quantity of the material, *kg* or *l*	Total amount, tenge
Sand of the K02A grade, SS 2138-84	10	15	1500
Sand of the K0315A grade, SS 2138-84	12	35	420
Cast polystyrene PSV-1L	3000	15	45000
Construction polystyrene PPS-20	1200	10	12000
Paint	800	9	7200
TOTAL			66120

The charge materials are no different.

A comparative analysis of defects in castings and molds when using LFC molds is presented in Figure 3.

In total, the percentage of defects during LCM using cast polystyrene for a model is ~1.8% of the casting volume, and during LCM using polystyrene of a complex composition for a model, it is significantly lower and amounts to less than 1.0% of all manufactured castings.

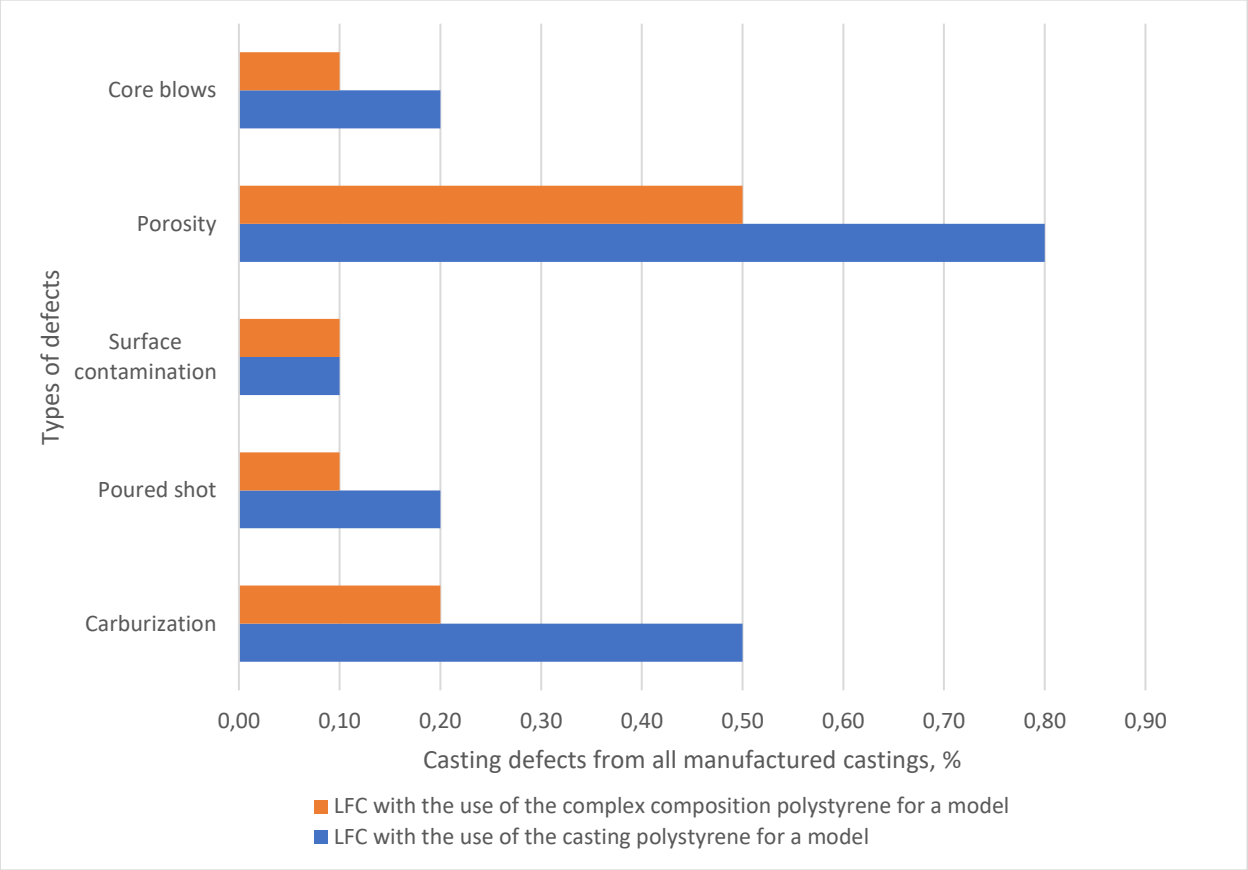

Fig. 3. - Types of defects in LFC with the use of models of various compositions

Conclusions

Research has shown that the use of a casting and construction polystyrene model composition in a ratio of 60 to 40% contributes to the formation of a homogeneous structure throughout the entire volume of the melt, helps to exclude slag and gases from the melt, which is confirmed by a decrease in the percentage of castings rejected by porosity and cavities.

The depth of carburization is also reduced if the technological conditions of pouring (number of blows, pouring speed) and melt temperature are observed (for steel grade 35 L it is 1540-1560 ^{0}C). This occurs due to a decrease in the density of the model and its faster gasification

At the same time, the introduction of construction polystyrene into the model reduces its cost and, as a consequence, the cost of castings.

Acknowledgements

These studies were carried out as part of implementing grant funding from the Science Committee of the Ministry of Science and Higher Education of the Republic of Kazakhstan under the project AP15473207 "Developing the technology of producing defect-free homogeneous castings by the lost foam casting method" (agreement with the Committee on Scientific Education of the Ministry of Education and Science of the Republic of Kazakhstan No. 337/ZhG-3-22-24 dated 11 November 2022).

References

[1] Issagulov A.Z., Kulikov V.Yu., Tverdokhlebov N.I., Shcherbakova Ye.P., Kovalyova T.V. Obtaining castings by the loas foam casting method using molds of construction polystyrene // University Proceedings, Publishing House of KSTU, Karaganda, 2017, No. 3, P. 30-32.

[2] https://on-v.com.ua/novosti/texnologii-i-nauka/kak-snizit-nauglerozhivanie-pri-lgm/

[3] Khaydorov A.D., Kondratyev S.Yu. Formation of the steel casting structure obtained by the lost foam casting method with subsequent heat treatment // Procurement production in mechanical engineering No. 12, 2014, P. 3-9.

[4] Issagulov A.Z., Kulikov V.Yu., Kvon Sv.S. Kovalyova T.V. The composition of the polystyrene mold effect on the properties of the "Through Lid" casting // Foundry Production, Foundry Production Publishing House, M., 2021, No. 3, P. 25-28.

[5] Kulikov V.Yu., Issagulov A.Z., Kovalyova T.V. Study of the properties of polystyrene with the addition of secondary granules of construction polystyrene // Bulletin of the Magnitogorsk State Technical University named after. G.I. Nosova, 2017, T. 15, No. 4, P. 40-46.

[6] Kovalyova T.V. Thermodynamic modeling of an alloy with the use of lost foam casting method // Proceedings of the International scientific and practical online conference "Integration of science, education and production as the basis for implementing the Nation's Plan" (Saginov's Readings No. 13), dedicated to the 30th anniversary of Independence of the Republic of Kazakhstan, June 17-18, 2021 Karaganda Technical University. Karaganda: KTU Publishing house, 2021, P. 1313-1314.

[7] Issagulov A.Z., Kulikov V.Yu., Tverdokhlebov N.I., Shcherbakova E.P., Kovalyova T.V. The influence of paint on the quality of cast iron and steel castings of complex configurations during forestry and metallurgy //Foundry production, 2015, No. 7, P. 17-19.

[8] Kovalyova T.V., Issagulov A.Z. Modeling temperature fields of castings with the use of lost foam casting method // Mechanical engineering: new concepts and technologies. Collection of articles of the All-Russian scientific and practical conference of students, graduate students and young scientists. - Krasnoyarsk: Siberian State University named after M.F. Reshetnyova, 2020. - P. 79-83.

Information of the authors

Issagulov Arictotel Zeinullinovich, d.t.s, professor, executive director, Abylkas Saginov Karaganda Technical University
e-mail: mlpikm@mail.ru

Kovaleva Tatyana Viktorovna, m.t.s., senior research fellow of the KazMIRD, teacher, Abylkas Saginov Karaganda Technical University
e-mail: sagilit@mail.ru

DOI 10.52209/2706-977X_2024_1_15 IRSTI 55.22.19 UDC 669.2

Structure and Physical Properties of High Entropy Coatings on Surfaces of Weapons and Military Equipment Parts

Berdibekov A.T.*, Yurov V.M., Gruzin V.V., Dolya A.V.
National defense university named after the First President of the Republic of Kazakhstan - elbasy, Astana, Kazakhstan
*corresponding author

Abstract. The method of spraying CGDN coatings we propose is universal for repairing military equipment in the field. We carried out the method using a Dimet-425 installation and an IPG Photonics laser. The increase in heat resistance and adhesion of the coated sample relative to the uncoated sample is explained by the fact that the modified surface layer of the sample is a transition layer that has a sharp boundary with the base material or transition zone, consisting of a diffusion zone and a thermal-affected zone. The characteristic adhesion value obtained for CGDN coatings is 20 - 80 MPa, and the powder utilization rate reaches 50 - 80%.

Keywords: coating, sputtering, laser, particle speed, particle impact, deformation, adhesion.

Introduction

In 2008, the MIL-STD-3021 standard "Sputtering of materials. Cold gas dynamic spraying", which describes the process of operation of the CGD method, as well as methods for testing coatings and is used in the restoration of military equipment using CGD [1]. This area of coating is also being explored by developers from Japan, the Republic of Korea, India, Austria and Australia [2]. A review of high-entropy (HEC) coatings on parts of various industries, including aviation, rocket and military equipment, has been carried out in recent years in reviews [3-7]. To increase the service life of both artillery and small arms barrels, coatings are used, most often chromium with a thickness of 50 to 180 microns, which increases the service life by 2.5-3 times [8-10] - for example, for small arms from conventional 10 thousand to 25-30 thousand shots. To increase the wear resistance of barrels, chemical-thermal treatment of the inner surface, in particular nitrocarburization, is also used [11].

In this article we will consider the structure and physical properties of high-entropy coatings on the surfaces of weapons and military equipment.

1. Methodology

Research on the application of coatings using the cold gas dynamic spray (CGDN) method began in the first half of the 1980s. In the period from 1980 to 2022, more than 200 patents were received for various design modifications of spraying installations, as well as in the field of applying metal coatings for various functional purposes. The main energy source in the processes of formation of CGDN coatings is the kinetic energy of high-speed particles in the solid phase. The main physical mechanism of CGDN is the high-speed deformation of sprayed particles upon impact, leading to intense shear flows of the material along the contact boundaries and the formation of adhesive-cohesive bonds. As a result of experiments, coatings of almost all types of metals (Al, Cu, Zn, Mo, Ta, Ti, Cr, Nb, Zr, Ag, Fe and many others) and alloys widely used in industry were successfully applied [12-14] .

Before moving on to our technology, let's consider the interaction of particles with the base, which we will further represent as military steel (Fig. 1).

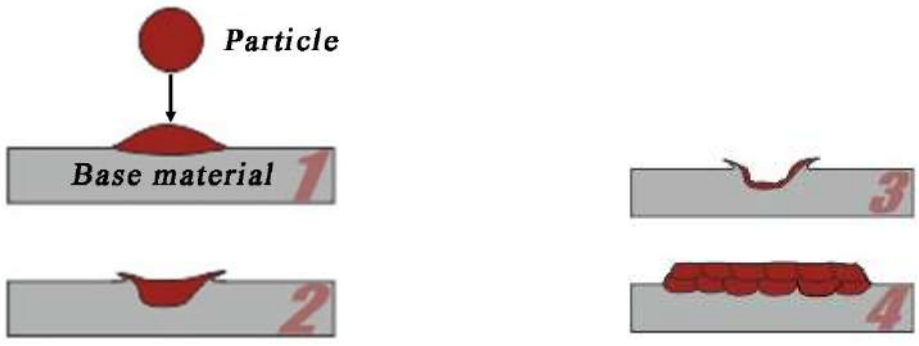

a) b)

Fig. 1. - Effect of particle velocity on coating quality

Scheme in Fig. 1 boils down to this:

1. The coating particle has reached the minimum impact speed, which is necessary to excite the mechanism of interaction with the surface of the substrate (processed sample). This so-called “critical speed” affects the properties of the coating material.

2. Since the impact speed is higher than the critical speed, the deformation and quality of adhesion of the particles increase.

3. If the impact velocity is too high (the "erosion rate"), more material is destroyed than added. No coating is formed.

4. In order for a dense and formed coating to form, the particle impact velocity value must be between the values of the critical velocity and the erosion rate.

We applied HES coatings using the CGDN method with a supersonic supply of a gas-powder mixture using the Dimet-425+Laser installation (Fig. 2). The installation included an IPG Photonics fiber laser with a wavelength of 1064 nm and a maximum power of 6 kW. The installation of HES coatings using the CGDN method (Fig. 2) contains a chamber 1, a nozzle 2, a substrate 3 for supplying a gas-powder mixture, and a laser 4.

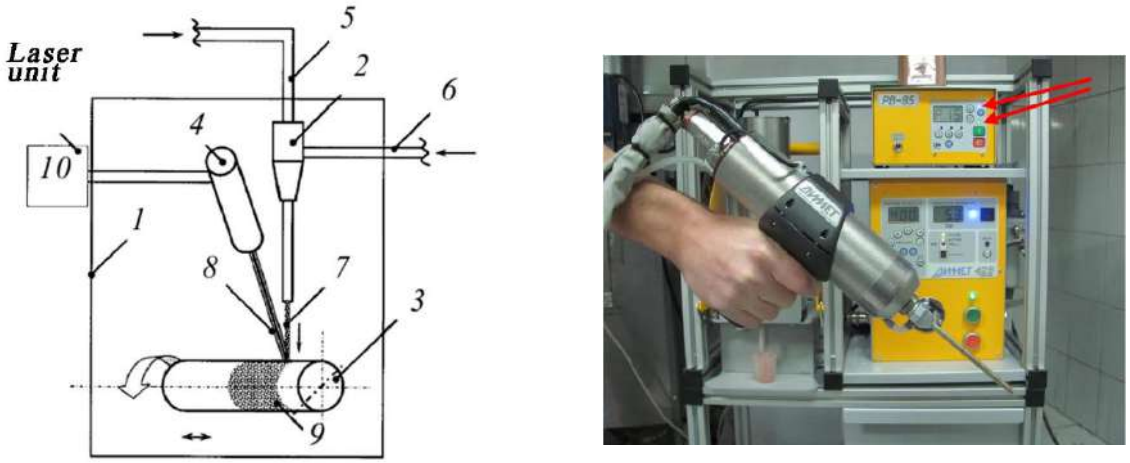

Fig. 2. - Installation of HES coatings using the CGDN method (left); powder feeder from the Dimet-425 installation (right)

Nitrogen is supplied to spray nozzle 2 using pipe 5, and powder is supplied to spray nozzle 2 using pipe 6. The gas-powder mixture 7 emerging from the nozzle 2 and the laser beam 8 are directed to the surface 9 of the substrate 3. The laser unit 10 is an electronic unit that controls the power of the laser radiation of the laser 4. Movement can be carried out, for example, manually or mechanically using gear or worm mechanisms transfers. Mechanically, the transmission moves the substrate 3 relative to the spray nozzle 2. As a result, a coating 9 is formed on the surface of the substrate 3. During the application of the gas-powder mixture 7, the substrate moves mechanically using gear mechanisms. One of the main features of the device is the ability to change the angle of inclination of the laser head, as well as shift the focus of the laser spot relative to the focus spot of the powder on the surface of the sample. The device we assembled based on the Dimet-425 installation is similar to the installation described in the Patent [15]. A similar installation is proposed in the Patent [16].

Results and discussion

In the works listed above, it was found that such criteria as the critical speed in the gas jet, the flow rate, and the speed of the sprayed particles increased. Also, the issue of the influence of particle speed in the CGDN process on the number of fixed powder particles when interacting with an obstacle was considered. In [2], it was found that an increase in the spraying speed to 780 m/s leads to the formation of not only craters from rebounded powder particles, but also to the fixation of the powder material, and a subsequent increase in the speed of the part to 850 m/s when using pure helium contributes to an increase the proportion of fixed parts is up to 0.5. An analysis of the nature of particle deformation at different deposition rates showed that an increase in the speed of particle movement leads to the ejection of metal along the periphery.

It turned out that by increasing the particle consumption it is possible to switch from substrate erosion to deposition. The main features of the spraying process in the mode of low impact speeds are the presence of a critical particle flow rate Qi, below which a coating is not formed at any time of exposure to a two-phase jet, as well as a very low value of the spraying coefficient $\Delta m/M = 10^{-3} \div 10^{-4}$. In addition, coatings obtained in this mode differ significantly in their properties from coatings obtained at $\upsilon_h > \upsilon_g$. At $\upsilon_{ch} < \upsilon_g$, when single particles are not fixed on the substrate, the process of formation of coatings at sufficiently high particle flow rates $Q_i > Qi_п$ can be explained by an increase in the temperature of the substrate surface due to heat release during particle impacts, activation of the substrate surface, as well as the presence of the effect of particle interaction - double impacts. The optimization calculations carried out confirmed the fairly high efficiency of using nozzles with a critical section size of 2 - 3 mm

and a length of 100 - 200 mm to accelerate particles 5-30 microns in size, which are poured into the hopper of the Dimet-425 installation in the amount of 80-100 g (Fig. 2b).

It is easier to judge the surface of military equipment from the AFM images of wind-electronic coatings shown in Fig. 3.

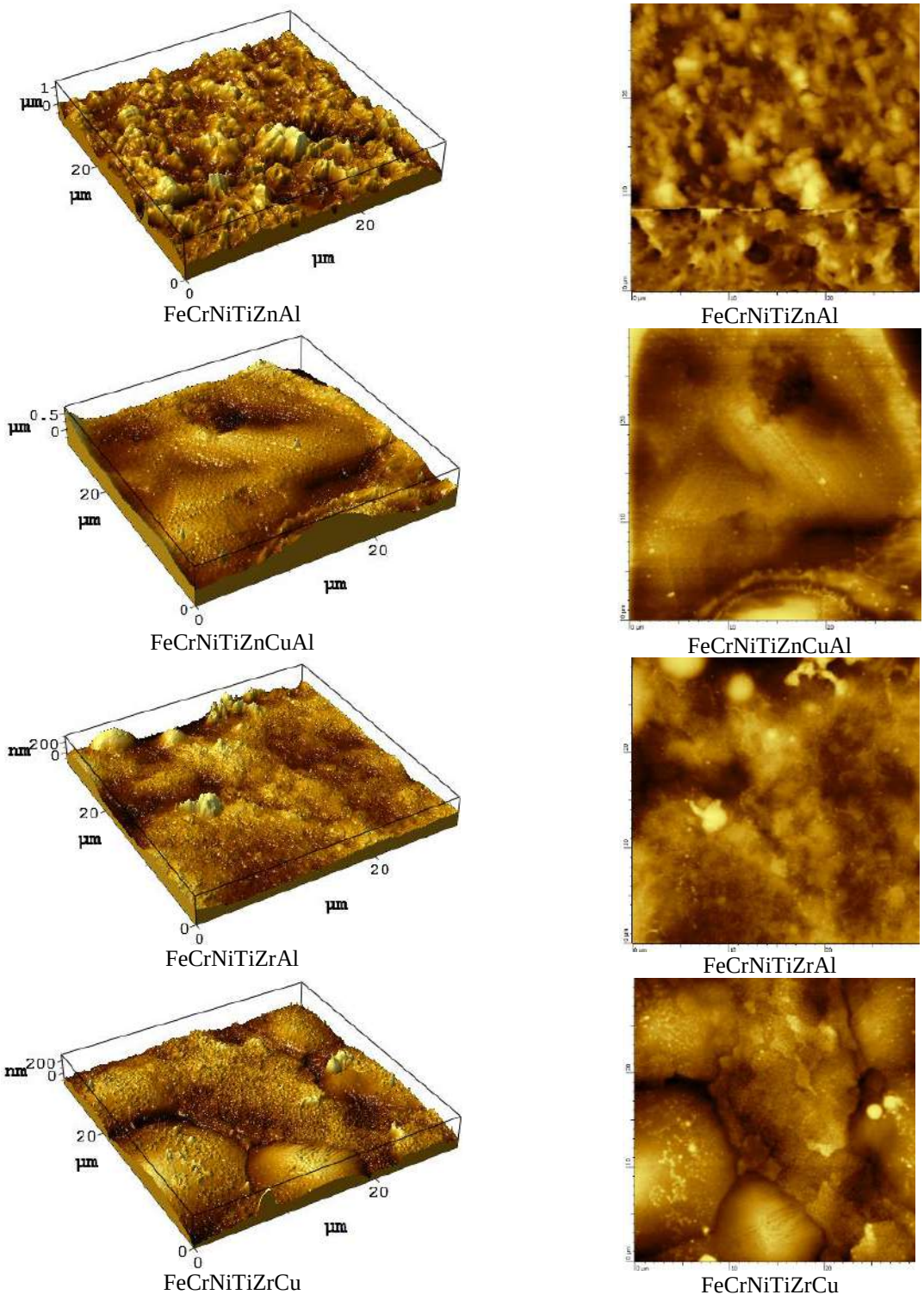

Fig. 3. - AFM images of HES coatings in 3D and 2D projections

Let us now cut the coverings in Fig. 3, using the Quanta 200 3D system. In Fig. 3 and 4 show images of a cellular and pencil structure, similar to Benard cells. A special feature of the surface, including multi-element coatings, is the fact that the surface is a nanostructure.

For the surface, surface energy σ (J/m^2) plays a significant role, determining such an important characteristic of the coating as adhesion energy, which is responsible for the destruction of the coating.

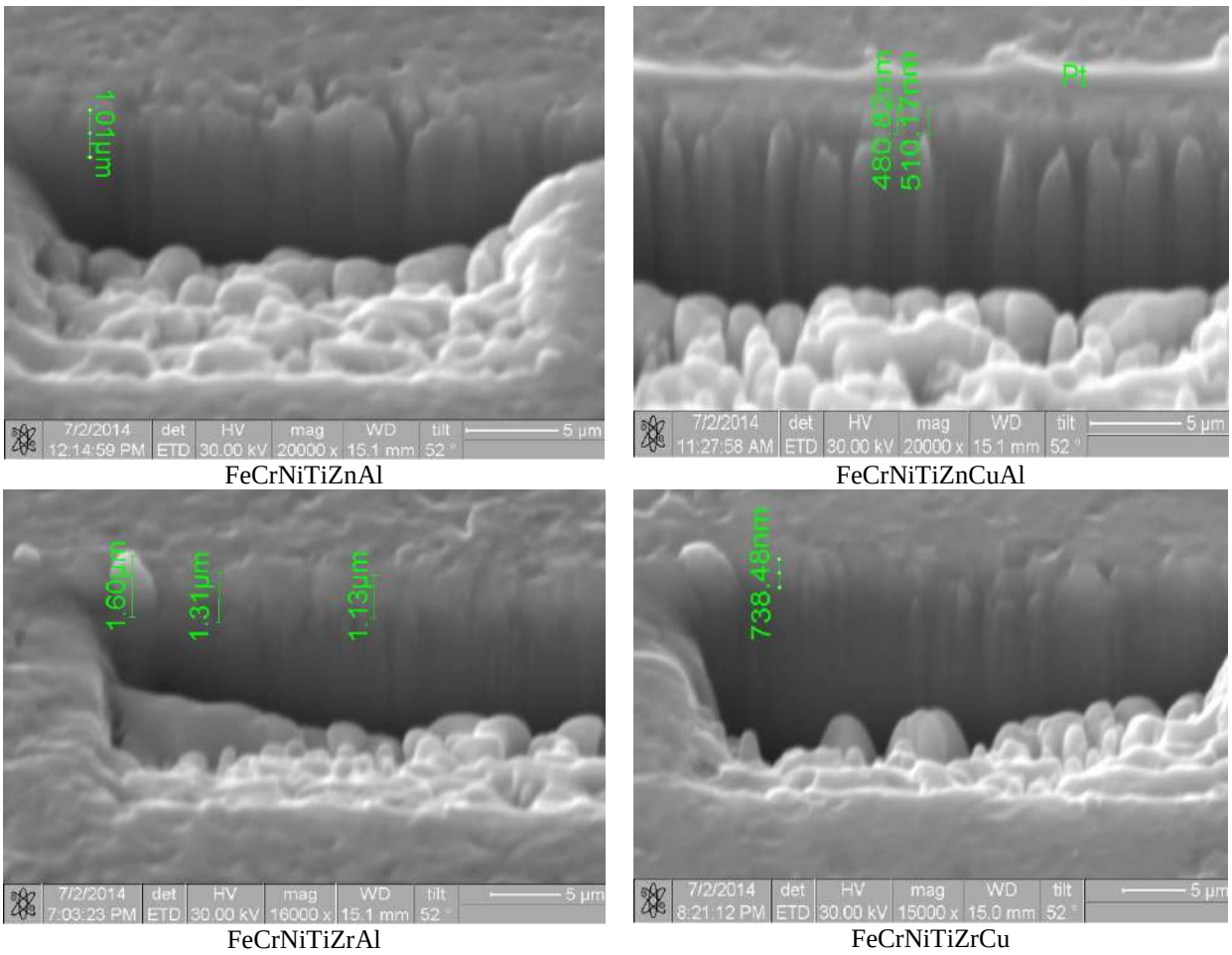

FeCrNiTiZnAl FeCrNiTiZnCuAl

FeCrNiTiZrAl FeCrNiTiZrCu

Fig. 4. - Cutting of HES coatings

The intensity of material destruction is determined by the adhesion energy at the interface:

$$W_{à} = 2\sigma \cdot S \ \ [J/m^2]$$

Here S is the surface area of the sample. Table 1 presents the adhesion energy for the coatings shown in Fig. 3 or 4. We determined the surface energy σ using the method described in [17]. The essence of this method was the dimensional dependence of the thickness of the coating on its microhardness or some physical property, for example, the resistivity of the coating.

Table 1. Surface energy and coating adhesion energy

Coating	σ, J/m^2	W$_a$, J/m^2
FeCrNiTiZnAl	1.05	2.10
FeCrNiTiZnCuAl	1.16	2.32
FeCrNiTiZrAl	1.17	2.34
FeCrNiTiZrCu	1.19	2.38

When the coating is formed, internal stress-strain states (SSS) arise in it. In a coating, SSS creates an energetic state that prevents adhesion and promotes peeling of the coating. SSS energy can be estimated using the formula [18]:

$$W_{SSS} = (\sigma_{SSS}^2 / 2Å) \cdot S \cdot h \, .$$

Here σ_{SSS} is the internal stress (Pa), E is Young's modulus (Pa), h is the coating thickness. Let us estimate W_{SSS} according to the data in Fig. 3, and take the coating thickness h from Fig. 4. Let's take Young's modulus from steel 12X18H10T – E = 205 10^9 Pa, h = 7 10^{-6} m, $\sigma_{SSS} \approx 1\ 10^9$ Pa, then we get $W_{SSS} \approx 0.02$ (J/m^2). This means that our coating Wa >> W_{SSS} is much greater than the energy of coating separation.

We carried out heat resistance tests in accordance with GOST 6130-71. Before testing, all test samples were thoroughly cleaned. The heat resistance tests themselves were carried out in electric resistance furnaces of the G-30 type in an air atmosphere, with automatic temperature control with an accuracy of ±10 °C. During the tests, special ceramic crucibles were used. The samples were placed in a crucible, which was then sent into a furnace. Heat resistance was assessed by the mass of oxidized material. Weighing of samples before and after heat treatment was carried out on an analytical balance with an accuracy of 0.1 mg. The research results are presented in table 2.

Table 2. Loss of coating mass after heat treatment at 1100 °C

Coating	Mass of oxidized coating, mg	Coating	Mass of oxidized coating, mg
Sample without coating, steel 12X18H10T	56,8	FeCrNiTiZrAl	5,4
FeCrNiTiZnAl	14,4	FeCrNiTiZrCu	4,1
FeCrNiTiZnCuAl	6,6	-	-

From Table 2 it follows that the highest heat resistance of the coatings we studied is the FeCrNiTiZrCu coating, and the lowest is FeCrNiTiZnAl. The increase in heat resistance of a coated sample relative to an uncoated sample is explained by the fact that the modified surface layer of the sample is a transition layer, which has a sharp boundary with the base material or transition zone, consisting of a diffusion zone and a heat-affected zone. The transition layer is formed both by the direct transfer of material during CGDN to the substrate, and as a result of the chemical interaction of the coating and substrate materials with each other and with the environment. The transition layer obtained as a result of CGDN on a steel substrate contains austenitic and martensitic phases, carbides, nitrides, intermetallic compounds, oxides of the base and alloying electrode. Coatings formed by FeCrNiTiZrCu form unlimited solid solutions with the substrate and are characterized by high continuity and low porosity. And most importantly, the transition layer formed by these metals and the substrate, after laser exposure, remains practically unchanged.

The use of preliminary (before CIB) thermal activation of the surface makes it possible to increase the adhesion of the coating to the base and increase the homogeneity of its structural structure. As a result, the increase in weight gain due to oxidation is minimal. This fact allows us to conclude that surface activation is an important part in the technological process of producing HE coatings.

If we compare the values in Table 2 with Table 1, we come to the conclusion that a heat-resistant coating also corresponds to a high surface energy.

The wear resistance of coated parts was identical: for cutting tools, which was ensured by testing in the CNC machine shop using the same machining programs. The test results are shown in Table 3.

Table 3. Increase in wear resistance of coatings I%

Coating	I%	Coating	I%
FeCrNiTiZnAl	15	FeCrNiTiZrAl	40
FeCrNiTiZnCuAl	25	FeCrNiTiZrCu	65

If we compare the values in Table 3 with Table 1, we come to the conclusion that a wear-resistant coating also corresponds to a high surface energy.

Conclusion

The highest heat resistance of the coatings we studied is the FeCrNiTiZrCu coating, and the lowest is FeCrNiTiZnAl. The increase in heat resistance of a coated sample relative to an uncoated sample is explained by the fact that the modified surface layer of the sample is a transition layer, which has a sharp boundary with the base material or transition zone, consisting of a diffusion zone and a heat-affected zone.

The use of preliminary (before CIB) thermal activation of the surface makes it possible to increase the adhesion of the coating to the base and increase the homogeneity of its structural structure. As a result, the increase in weight gain due to oxidation is minimal. This fact allows us to conclude that surface activation is an important part in the technological process of producing HES coatings.

Acknowledgments

This scientific article was published within the framework of the scientific program of program-targeted funding for 2021-2023, IRN No. BR1090150221 “Development of technology for protective coatings of surfaces of weapons and military equipment for protection from aggressive environmental factors and operating conditions” (the research is funded by the Science Committee of the Ministry of Science and higher education of the Republic of Kazakhstan).

References

[1] Rokni M.R., Nutt S.R., Widener C.A. et al. Review of relationship between particle deformation, coating microstructure, and properties in high-pressure cold spray // J. of Thermal Spray Technology, 2017, Vol. 26. - P. 1-6.
[2] Irissou E., Legoux J.-G., Ryabinin A. et al. Review of cold spray process and technology: part I - intellectual property // Journal of Thermal Spray Technology, 2008, Vol. 17. No. 4. - P. 495-516.
[3] Rogachev A.S. Structure, stability and properties of high-entropy alloys // Physics of metals and metal science, 2020, vol. 121, no. 8. - P. 807-841.
[4] Pachurin G.V., Gushchin N.A., Pachurin K.G., Pimenov G.V. Technology for a comprehensive study of the destruction of deformed metals and alloys under different loading conditions. - N. Novgorod: Nizhny Novgorod. state univ., 2005. - 141 p.
[5] Gromov V.E., Shlyarova Yu.A., Konovalov S.V., Vorobyov S.V., Peregudov O.A. Application of high-entropy alloys // News of Higher Educational Institutions. Ferrous metallurgy, 2021, T. 64, No. 10. - P. 747-754.
[6] Gromov V.E., Konovalov S.V., Peregudov O.A., Efimov M.O., Shlyarova Yu.A. Coatings made of high-entropy alloys: state of the problem and development prospects // News of Higher Educational Institutions. Ferrous metallurgy. 2022, Vol. 65, No. 10. - P. 683-692.
[7] Kambarov Ye.Ye., Uazyrkhanova G.K., Rutkowska-Gorczyca M., Kussainov A.Ye. Overview of the high-entropy alloys concept // Bulletin of the National Nuclear Center of the Republic of Kazakhstan, 2013, No. 3. – P. 25-39.
[8] Salakhova R.K. Corrosion resistance of 30KhGSA steel with "trivalent" chromium coating in natural and artificial environments // Aviation materials and technologies, 2012, No. 2. - P. 59-66.
[9] Kuzmin Yu.A. State and directions of development of armored vehicles in foreign countries // Foreign Military Review, 2015, No. 3. - P. 55-59.
[10] Eliseev E.A., Tonysheva O.A., Yakusheva N.A. Materials and development of technologies that ensure the service life of barrels of artillery, tank and small arms weapons systems (review) // Proceedings of VIAM, 2017, No. 9(57). – P. 19-26.
[11] Kopeiko S. Military sniper weapon // Kalashnikov. Weapons, ammunition, equipment, 2012, No. 1. - P. 46–52.
[12] Hall P., Yang L., Brewer T., Buchheit T. Preparation and Mechanical Properties of Cold Spray Nanocrystalline Aluminum // Proc. Int. Therm. Spray Conf. Maastricht, 2008. - P. 479-480.
[13] Sansoucy E., Jodoin B., Kim G.E. Mechanical Characteristics of Al-Co-Ce Coatings Produced by the Cold Spray Process // Journal of Thermal Spray Technology, 2007, vol. 16. P. 651-660.
[14] Ajdelsztajn L., Zuniga A., Jodoin B., Lavernia E.J. Cold Spray of AlCuMgFeNi Alloy with Sc Addition // Journal of Thermal Spray Technology, 2006, vol. 15. - P. 184-190.
[15] Gilmutdinov A.Kh., Gorunov A.I. A method for laser cladding of coatings on a sample and a device for its implementation. - Patent No. 2656906 Russian Federation: MPK 23K 26/342 (2014.01), B23K 26/144 (2014.01)
[16] Jensen E.D., Kruger U., Ullrich R. Method of cold gas-dynamic spraying. - Patent No. 2394940 Russian Federation: IPC C23C 24/08 (2006.01), 07.20.2010 Bull. No. 20.
[17] Berdibekov A.T., Yurov V.M., Gruzin V.V., Dolya A.V. The influence of the external environment on microcracks in parts of military equipment //Interindustry scientific and technical journal "Defense complex - scientific and technical progress of Russia", 2023, No. 2. – P. 45-50.
[18] Ainbinder S.B., Panch A.S. The influence of the relative mechanical properties of metals on the formation and destruction of adhesion at low sliding speeds. In the book: Dry friction. Riga, 1961. - P. 64-79.

Information of the authors

Berdibekov Aidar Toktamysovich, PhD, associate professor, National Defense University named after the First President of the Republic of Kazakhstan - Elbasy
e-mail: berdibekovat777@mail.ru

Yurov Viktor Mikhailovich, c.ph.- m.s, associate professor, Nazarbayev Intellectual School
e-mail: exciton@list.ru

Gruzin Vladimir Vasilyevich, d.t.s, professor, National Defense University named after the First President of the Republic of Kazakhstan - Elbasy
e-mail: gruzinvv@mail.ru

Dolya Alexandr Valerievich, doctoral student, National Defense University named after the First President of the Republic of Kazakhstan - Elbasy
e-mail: iskander_kst@mail.ru

DOI 10.52209/2706-977X_2024_1_21 **IRSTI 55.19.13** **UDC 621.452.3**

Processing of a Part Such as a Composite Bearing Housing on a Milling Machine With a Digital Control Program

Nikonova T.Yu.*, Kabidenov D.K., Abdugalieva G.B., Berg A.S., Imasheva K.I.
Abylkas Saginov Karaganda Technical University
*corresponding author

Abstract. In the era of the industrial revolution of ndustry 4.0, the Republic of Kazakhstan is rapidly introducing automated robots and digital control programs in many of its production facilities. In this context, special attention is paid to modern technologies, and AKIRA SEIKI milling machines with FANUC control software stand out as advanced technologies in this process. They are becoming the most popular in the CIS countries due to the economic efficiency and intellectual support of the Taiwanese manufacturer.

Practical aspects of constructing CNC milling machines and their practical use are presented in this article. Particular attention is paid to the functionality of milling machines using the example of processing such a part as a composite bearing housing. In addition, the process of writing processing operation codes in the CIMKO computer program is described. The code is provided with brief descriptions to help you understand the compiled workpiece processing operations.

With the growing need for efficiency and precision in production, many companies and industrial plants in the Republic of Kazakhstan are considering AKIRA SEIKI milling machines with FANUC control software as a major investment. These machines not only provide high productivity, but also help automate complex technological processes. CIMKO, among other things, allows the development and optimization of machining code, which complements the efficiency and accuracy of the machines.

Keywords: CNC, CIMKO, dump truck, bearing, CAM system, industry 4.0, milling, processing tools.

Introduction

Enhancing the productivity of machine-based manufacturing can be accomplished by employing cutting-edge machinery and tools capable of implementing resource-efficient technologies on a large scale. These approaches are particularly pertinent in the manufacturing of intricate components [1].

In recent decades, the new stage of the industrial revolution - Industry 4.0 - has been paying close attention to new technologies and production automation, and great changes are taking place in the world. This concept involves the integration of advanced technologies such as the Internet, artificial intelligence, automation and cloud computing into production and economic processes. Since the Republic of Kazakhstan is a country striving for modern development, it is among the countries that pay deep attention to the implementation of the principles of Industry 4.0 in various areas of their economy [2].

One of the main areas where Kazakhstan seeks to implement the concept of Industry 4.0 is the manufacturing industry. Modern automation and robotics technologies can significantly increase the efficiency of production processes, reduce labor costs and improve product quality. An example is the automotive industry, where automated assembly lines and robots speed up production and reduce the likelihood of errors.

Industry 4.0 - a new stage of industrial and economic development - is based on the introduction of advanced technologies into production processes. Among the main components of this concept are CNC machines. These advanced devices, which enable automation and flexibility in production, play an important role in the successful implementation of Industry 4.0.

CNC machines are a combination of mechanical systems and electronics that allow high-precision programming and control of material processing. The use of CNC machines is becoming a key factor in achieving the goals of Industry 4.0:

- flexibility and automation of production;
- productivity increase;
- monitoring and data collection;
- integration with other technologies;
- training and development of personnel;
- economic impact.

Goal of the work - implement processing of a part such as a composite bearing housing using a CNC system. The processing will be carried out on a Taiwanese Akira Seiki Oi-MF milling machine equipped with a Japanese numerical control program (FANUC).

1. Methodology

The Akira Seiki Oi-MF is a high-tech CNC router that comes with many impressive features and capabilities. This machine (Figure 1) is a perfect combination of mechanical design, electronics and software to ensure high productivity and quality processing.

Fig. 1. - Assembling an Akira Seiki machine with Fanuc control software

One of the main features of the Akira Seiki Oi-MF is its precise mechanical system. Modern components and advanced technologies ensure high stability and precision of machine movement. This is especially important when performing complex machining operations that require minimal deviation from specified parameters. The base of the machine (Fig. 1) is placed on the bed as shown, the first of which is to install the bed on a 40 cm concrete field, the side of which is limited by vibration, and after installing the bed, its mechanisms are cleaned with kerosene from solid oils that have been smeared by the manufacturer in to protect the frame from rust during transportation of the machine. The machine column is installed on a completely cleaned bed (Fig. 1). The column tray is secured to the frame with a torque wrench, maintaining a known torque using M24 screws. After securing the column to the frame, a turret is installed in the secured column (Fig. 1). The turret is designed for 28 tools and has tool mounting points. After installing the turret, the hydraulic and pneumatic hoses of the machine are tightened and the machine frame is assembled, as shown in Fig. 1, c. The spacer between the frames is sealed with sealant to prevent cooling water from spilling outside the machine, and then fixed with screws. When assembling the machine frame, an electrical cabinet is also installed. When all the elements shown in the diagram are installed, the last thing to install is the machine door and the conveyor carrying the coolant and processed material (chips), as well as the coolant tank [3] and [4].

Computer numerical control (CNC) machines are central to the modern manufacturing world. One of the most widespread and innovative manufacturers of such machines is Fanuc. Fanuc machine programming is based on the use of G-codes and M-codes, which allows precise control of geometric operations and auxiliary functions of the machine. G-codes, or geometric codes, are commands that tell a machine how to move and perform operations in three-dimensional space. These codes define various actions such as moving the X, Y, and Z axes, setting the feedrate, and rapid traverse. For example, the G00 command means rapid motion, which allows the tool to move quickly between points without cutting the material. The G01 and G02 codes define linear and rotary motions respectively, allowing the machine to perform various types of machining. M codes, or auxiliary function codes,

control various aspects of machine operation, including spindle rotation, cooling, lubrication, and other auxiliary operations. For example, command M03 rotates the spindle to the right, and M08 turns on the cooling system. These codes allow programmers to precisely control the operating conditions of the machine according to the requirements of the material being processed.

Programming a Fanuc machine begins by creating a program text file containing a sequence of G-codes and M-codes. The programmer determines tool movements, feed rates, tool types, and other parameters required to complete the machining task. This file is then downloaded to the device's digital controller [5] and [6].

It is important to understand that programming Fanuc machines requires precision and attention to detail. A small error in the code can cause the tool to move incorrectly or even cause damage to the machine and workpiece. Therefore, programmers must have a deep understanding of G-codes and M-codes, as well as the specifications of the specific Fanuc machine they are working on.

Fig. 2. - The main Fanuc unit for controlling the Akira Seiki milling machine

When processing any product, a processing program is written for it. CAM (computer-aided manufacturing) software systems such as MasterCAM, SolidCAM, PowerMILL are used in mechanical engineering to write machining programs. CAM programming is the process of creating machining programs that optimize manufacturing operations on CNC machines. This eliminates the need to manually enter each G-code and M-code, reducing the likelihood of errors and simplifying the programming process. Instead, the programmer works with a CAD model of the part and creates a CAM program that automatically generates the G-codes and M-codes needed for machining.

Advantages of CAM programming in mechanical engineering:

CAM programs allow you to achieve high precision machining of parts. Once a program is created, it can be reused on the same parts, ensuring product consistency.

CAM software can optimize workflows and select the best tools and feed rates to speed up production processes.

Transferring complex calculations and code generation to the CAM system reduces the likelihood of errors associated with manual code entry.

If there are changes to the part design, the CAM program can be easily adapted without having to rewrite all the code by hand.

CAM programming programs for CNC machining are of great importance to modern industry. They increase accuracy, repeatability, optimize production and reduce the risk of errors. Despite the challenges, CAM programming remains a key factor in manufacturing improvement and product quality.

2. Results and discussion

The above sketch shows the processing coordinates, including the dimensions of the workpiece. Processing coordinates simplify the compilation of program code, which is written during the processing of the product. The drawing was made in the AutoCAD program, the code for the machine will be written in the CIMKO program, and the initial simulation is written in the same program. The point (X0;Y0) shown in the drawing is the starting point of the product on this machine. That is, the program is written in accordance with these starting points.

Before writing any program, it is advisable to plan the processing operation completely in advance. That is, planning the types of operations and processing modes used during processing, as well as the types of tools required in accordance with these modes, helps the technologist to prevent many errors. Let's plan the operations performed when processing the product shown in Figure 3.

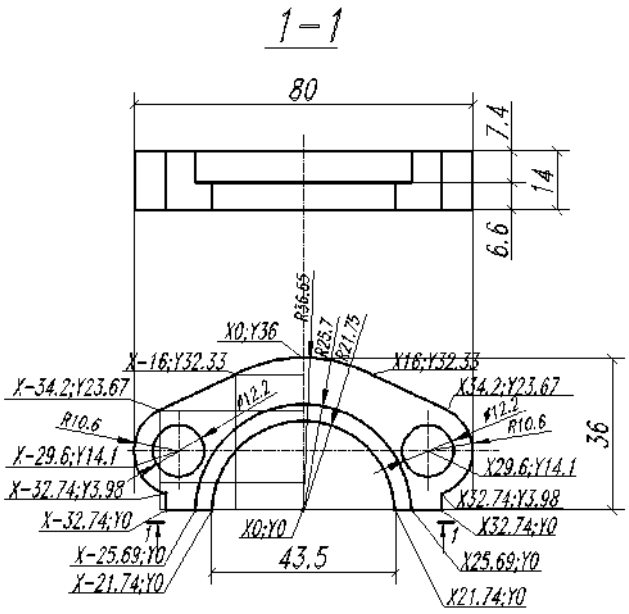

Fig. 3. - Sketch of a component type of compound bearing housing

The plan started with the selection of the required workpiece, if we select the workpiece, then the dimensions of the workpiece will be 90x50x30mm, because for the machining work, we will clamp the workpiece on a support (vice) by 5 mm, and grind another 5. mm on top of it with an end mill (Figure 4).

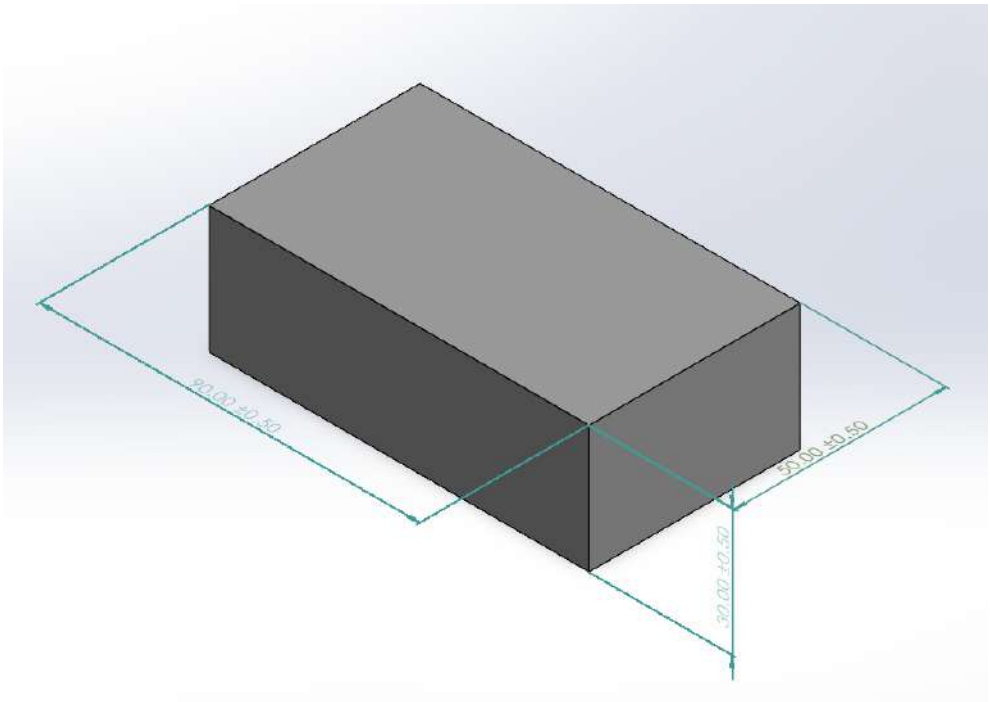

Fig. 4. - 3D model of the workpiece

We will leave an allowance of 2.5 mm at the edges for finishing the contour of the workpiece. According to the plan, processing this workpiece will require 3 main operations (Figure 5):

- milling the upper surface (required tool – end mill ∅50 mm);
- contour milling with an end mill (end mill ∅16 mm);
- drilling holes (required tools ∅14 mm).

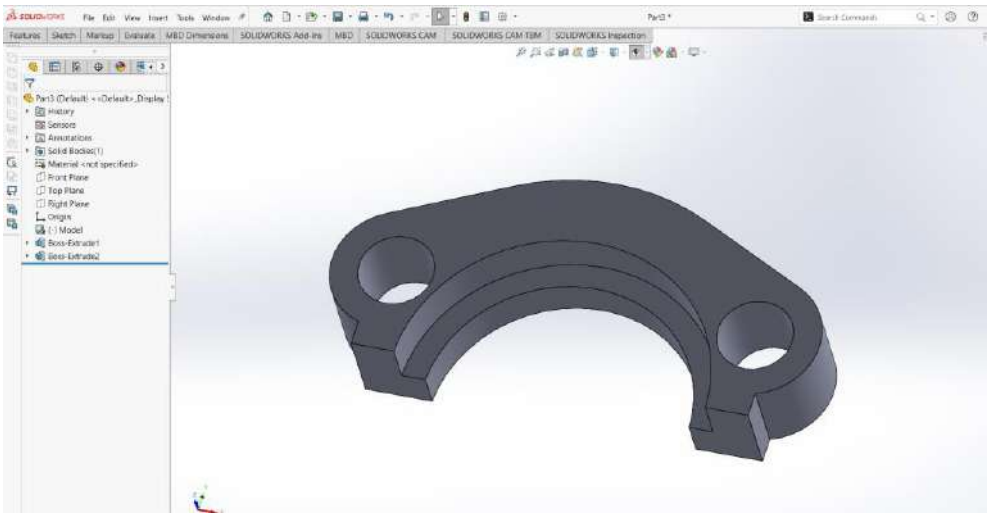

Fig. 5. - 3D model of the finished part

Having previously planned the writing of the program, we write the necessary program in the CIMKO program and check the correctness of the program. The CIMKO program is cheaper compared to other CAM system programs, since it only shows code visualization with program functions. Other programs in the CAM system supply the first visual processing with the most necessary information from the drawn 3D model, that is, from the type of tool used to the cutting modes of the machining tools, and automatically prepare their own program for the required tool accordingly. These programs are very suitable for processing complex products, but due to their high price, are not economically feasible for use in small-scale production unless multi-batch processes are available. Therefore, it is useful to write the code and check its visualization in the CIMKO program.

If we consider the program written above, then «O0007» in the first line is the name of the program, in the code system «O0001 - O7999» is considered a list of programs written by the operator or can be changed by the operator, and «O8000 - O9999» is written by the service personnel during setup program code whose settings cannot be changed by the operator (Figure 6).

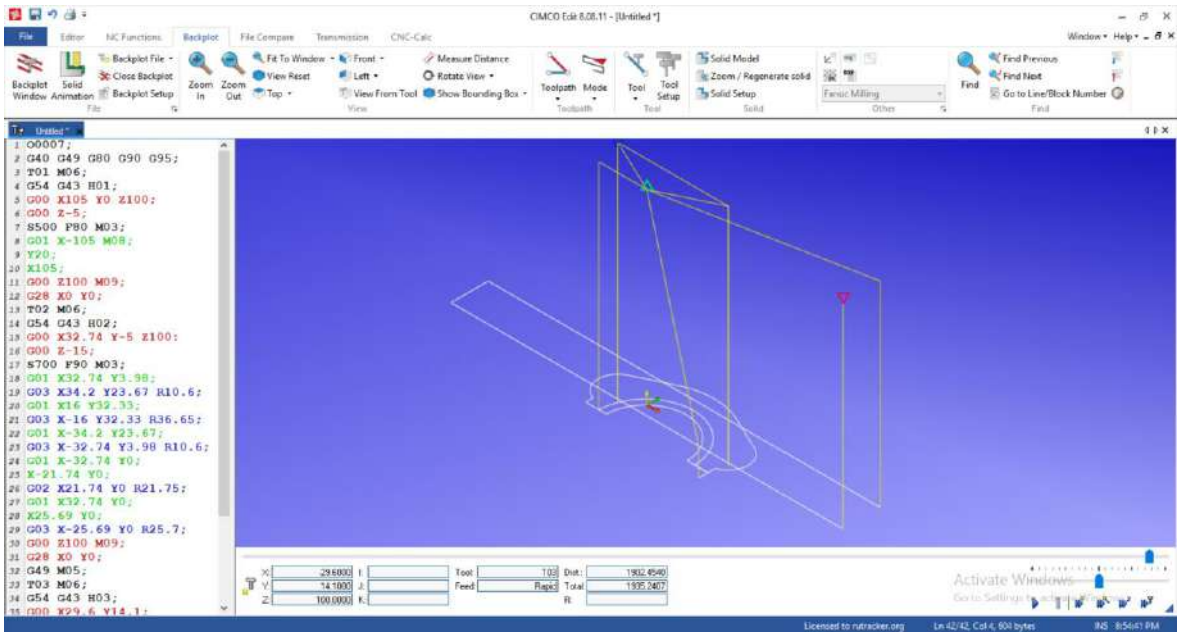

Fig. 6. - Processing codes for a CNC machine written in the CIMKO program

The G40 G49 G80 G90 commands on the second line are commands that reset the lever settings to their original state, recording the command system as a precaution to erase commands that were not erased in previous operations. T01 is the serial number of the tools in the turret, and command M06 is the command to change the spindle to another tool (Figure 7).

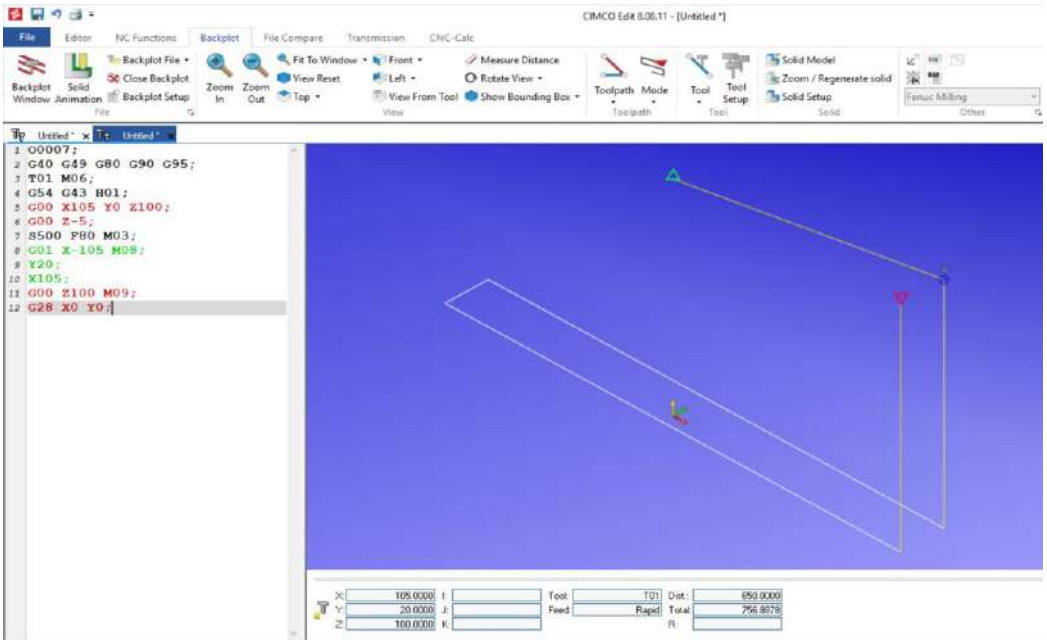

Fig. 7. - Codes for processing a product with a side mill (end mill)

G54 in the next line G43 command H01 G54 – selection of the workpiece coordinate system, G43 – setting tool length compensation by positive or negative offset, H01 – correction of the deviation of the selected tool, that is, if the processing tool is worn out, the digital tool handle makes corrections to improve the accuracy of machining operations . The G00 and G01 commands are the commands that provide the movement of the side cutter, and the direction of these commands is determined by the X,Y,Z coordinate.

After the first operation is completed, the spindle is moved to the starting point (safe point for tool change) by command G28 X0 Y0, and the next end mill is selected at this point by command T02 M06 (Figure 8).

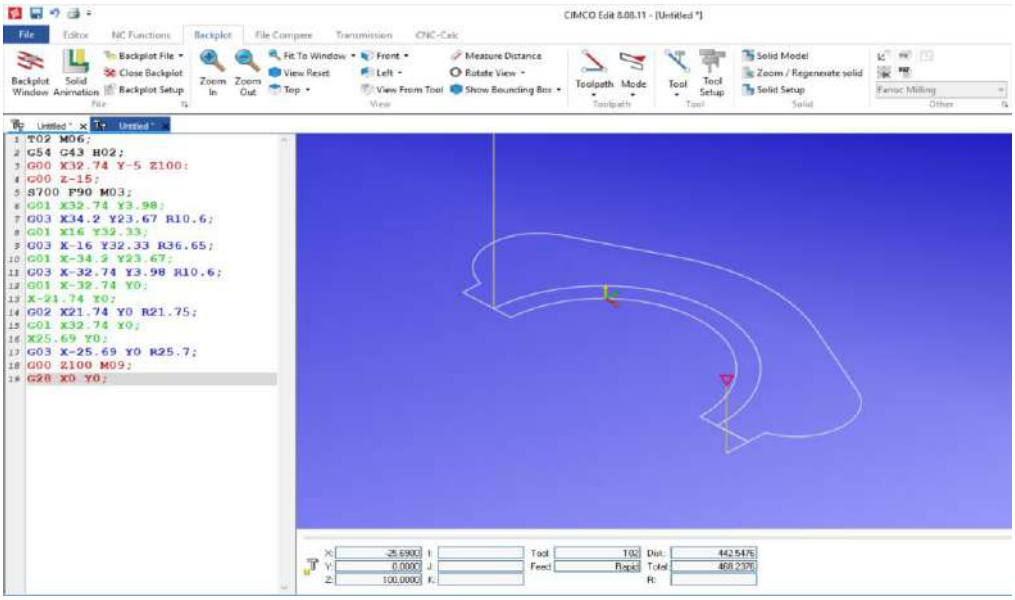

Fig. 8. - Product contour machining codes (finger cutter)

The main difference between the commands for this operation is the G02 and G03 commands. These commands provide movement along the contour of the device along a trajectory specified by radius R (Figure 9).

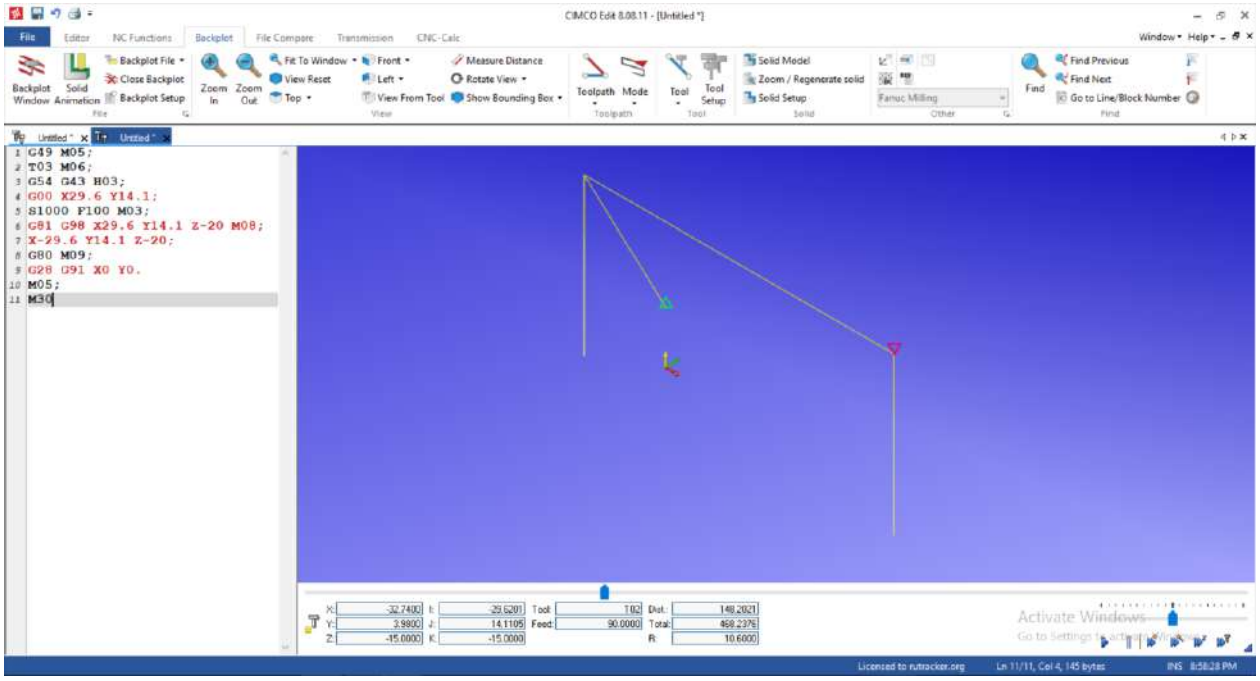

Fig. 9. - Processing codes for drilling holes in the product

The drilling operation code, like the machining operation codes above, after replacing the device, when the device arrives at the machining point at a certain safe height, after entering the spindle rotation modes using the S1000 F100 M03 command, the drilling code is written using the G81 G98 command. After recording the main drilling codes, the coordinates of the holes being machined are entered. After the holes are machined, the spindle will move to the reference point. Then the spindle is stopped through the M05 command, and the operation code is completed through the M30 command.

The code written in the CIMKO program is loaded via media into the machine control processor. After loading the program onto the machine, the workpiece is mounted on the clamp, the zero point of each tool relative to the workpiece is determined, and composition deviations are entered into the machine's CPU (Figure 10, a).

a) b)

Fig. 10. - The process of processing a workpiece on a milling machine

After the written program is entered on the machine and the zero points of the devices are determined, the operation of the codes according to the written program at a certain safe distance from the workpiece is first checked. Only after passing this check will the program start and the machine will begin processing the workpiece. During the processing of the workpiece, the movement of the tool is controlled, as shown on the screen (Fig. 10, b) in the control center of the FANUC machine. Processing operations are carried out using the commands for turning on the coolant (TCJ) M08 and turning off M09. (Fig. 10, b) the reason is that coolants are an important process in preventing overheating and tool failure.

Conclusions

During the work on the AKIRA SEIKI machine in the Japanese FANUC control system, work was carried out to process a Sketch of a part such as a composite bearing housing. During the article, the structure of the machine was discussed and a brief information about its activities was given. In order to carry out the machining operation, first of all, a plan was drawn up, according to which the operation codes were written in the CIMKO program, the correctness of the code written by the simulation was checked and installed on the machine.

As a result of the work, a sketch of a part such as a composite bearing housing was made on a milling machine. An image of the finished product is shown (Figure 11).

Fig. 11. - The result of processing the product on a milling machine

References

[1] Sherov, K., Mardonov, B., Zharkevich, O., Mirgorodskiy S., Gabdyssalyk R., Tussupova S., Tussupova A, Smakova N., Akhmedov, K., Imanbaev, Y. Studying the process of tooling cylindrical gears //Journal of Applied Engineering Science, 2020, 18(3), P. 327–332

[2] Azretbergenova G., Nakipbekova S., Turysbekova G. Direction of development of Kazakhstan in accordance with the fourth industrial revolution // Economic series of the bulletin of Gumilyov ENU, volume 141, № 4, 2022.

[3] ST 20999-83. Numerical control devices for metalworking equipment. Coding of control program information. – Enter. 1984-07-01. – M.: Standards Publishing House, 1983. – 26 p.

[4] ST 23597-79. Metal-cutting machines with numerical control. Designation of coordinate axes and directions of movement. General provisions. – Enter. 1980-07-01. – M.: Standards Publishing House, 1980. – 14 p.

[5] Programming processing on CNC machines using a specialized editor: a tutorial. – 2010. – 74 p.

[6] FANUC Series 0i – MC: instruction manual. – 936 p.

[7] Programming and operation of Fanuc-0i CNC milling machines. / ANO «Training Center Profi»; comp. Dolinin A. A., Talipov A. A., Selyaninova V. A. Sysoeva S. A. – Perm, 2014. – 62 p.

[8] Dolinin A. A., Selyaninova V. A. Programming and operation of Fanuc-0i CNC milling machines: Textbook. – Perm: ANO DPO «Center for Advanced Training «Becoming, 2015. – 64 p.

Information of the authors

Nikonova Tatyana Yuryevna, c.t.s, associate professor, Abylkas Saginov Karaganda Technical University
e-mail: nitka82@list.ru

Kabidenov Duman, doctoral student, Abylkas Saginov Karaganda Technical University
e-mail: miko-20-03@mail.ru

Abdugalieva Gulnur Baymurzayevna, c.t.s, associate professor, Abylkas Saginov Karaganda Technical University
e-mail: gulnura84@mail.ru

Berg Alexandra Sergeevna, PhD, assistant, Abylkas Saginov Karaganda Technical University
e-mail: kibeko_1995@mail.ru

Imasheva Kulzhan Imashevna, senior teacher, Abylkas Saginov Karaganda Technical University
e-mail: imasheva-gulzhan@mail.ru

DOI 10.52209/2706-977X_2024_1_29 IRSTI 55.69.99 UDC 628.5

Design of Scrubber for Sedimentation and Dissolution of Milk Dust

Raitsky G. E.*, Drobyazgo Yu. V.
Grodno State Agrarian University, Grodno, Belarus
*corresponding author

Abstact. In the work, the necessity of creating a device for settling the dispersed phase of milk dust - dry milk product, at the section of the coolant outlet to the environment is investigated. The quality of dry product deposition in the used devices: cyclones and filters has been evaluated. Technological factors occurring in scrubbers during sedimentation and dissolution of milk product are considered. The design of scrubber, providing the use of patented technology of return of precipitated dispersed phase of milk dust into a full commercial product, is offered.

Keywords: spray drying, cyclones, bag filters, finished product losses, heat energy recovery, scrubber design requirements.

Introduction

Spray dryers are the only alternative for drying dairy products. They have been widely used in the world since 1930, when a workable spraying disk device was developed and a specialized European company "Niro – Atomizer" was established. Subsequently, the designs of drying plants were improved, their productivity increased, the quality and range of the produced product improved, but inevitably remains the main disadvantage of the technology - high energy consumption and significant losses of the finished product into the environment [1]. Drying in general is the most energy-consuming process among dehydration technologies. For one kilogram of evaporated moisture from evaporated dairy product during drying, an average of three kilograms of saturated water vapor is consumed. Even higher costs are incurred during contact heating of air - heat carrier in heat generators directly burning combustible materials (gas, oil products). When dust with product quantity 275÷800 mg/m^3 [1,2] of heat carrier is discharged into the environment, there is no possibility of reuse of heat energy introduced into the air - heat carrier during primary heating, before letting it into the drying tower, as the dispersed phase of dust in contact with heat-exchange structures will quickly contaminate them [3]. It should be borne in mind that the humidity of the coolant at direct air intake from the environment, with its average humidity (for the Republic of Belarus) more than 80 %, significantly exceeds the moisture content of the exhausted, absorbing secondary moisture from the dried product [1,4].

Thus, with the high cost of thermal energy resources, the challenge is acute: to ensure good product deposition performance from milk dust.

1. Methodology

Modern drying plants of average productivity are chosen as objects of research. In the Republic of Belarus, it is the equipment of the Slovak company "Vzduchutorg" of VRA-4, VRC, VRD types, with heat carrier capacity of 46 ÷50 thousand m^3/hour and installations of the concern "GEO", having capacity up to 130 thousand m^3/hour. At medium-sized plants the aspiration system is initially limited to one or two cyclones. In addition, dairies can purchase bag filters from the named company with the number of 340 pcs. of bags, each 6 m long, 0, 18 m in diameter. The cost of the filter is more than 300 thousand dollars. The bags are replaced every 9 months. The firm directs potential buyers of new drying equipment to the use of filters, supplying, for example, in the VRD plant one cyclone of larger size. It should be borne in mind that the size of the cyclone has a decisive influence on the quality of sedimentation. These indicators are in an inverse relationship, i.e. with a large dust flow entering a large cyclone the quality indicators deteriorate. At the principled attitude of environmental protection structures to the established norms of product losses (10 mg/m^3) the owners of such installations have no choice but to use the proposed filters. It is fair to assess the quality of filtration as satisfactory. During a day filters installed after cyclones capture 250÷300 kg of finished product. Their disadvantage is impossibility of drying WMS (whole milk substitutes) for livestock farming using fat additives. Besides, the lint from bag filters is intensively lost and gets into the product, which reduces its grade. Even in a more difficult situation are the owners of drying plants with high capacity, although the company "Niro – Atomizer" also produces filters "Sanicryptm". Summarizing, it should be concluded that a significant improvement in the quality of product capture at the output to the environment, does not provide for the use of filters environmental requirements and the more so does not approach the possibility of heat recovery by repeated cyclic return of the coolant to the heating heat exchangers.

The only apparatus, fundamentally capable of solving these problems, should be recognized special scrubbers, devices for wet dust cleaning [3].

In the dairy industry, there have been attempts to use Y9-OMP volumetric scrubbers and Venturi scrubbers [1]. In the former, raw milk was used as the precipitating liquid. Large volumes of milk with captured dry product, the subsequent cycle of processing of such raw material along the entire technological line, starting from storage

tanks, made the technology unacceptable, although the quality of coolant purification was much better than when using cyclones.

Venturi scrubbers, widely used in various industries, with excellent quality indicators, did not continue to be used in the dairy industry due to the incompatibility of the device with the drying tower due to high hydraulic resistance - 35 kPA at permissible - 3 kPa.

Thus, a scrubber should be designed to overcome the effects of hydraulic resistance, with an irrigation density at the level of the Venturi scrubber.

2. Results and discussion

2.1 Hydraulic resistance of scrubber design depends on two main indicators: local and hydraulic resistances. In order to reduce the indicators of local resistances it is necessary to refrain from sharp changes in the area of dust flow along the trajectory of its movement from the discharge centrifugal fan to the solution outlet to the intermediate tanks, where the flow velocity is sharply reduced. The main requirement is the absence of shut-off and control valves on the pressure line of the flow.

Hydraulic resistance is due to the dimensions of the scrubber vessel, the viscosity of the liquid, which will increase as the concentration of solids in the reconstituted milk product increases. This means that it is necessary to avoid deposits on the internal surfaces of the scrubber, formed on dead-end sections, changes in the flow regime. Provision should be made for scouring of deposits in such areas not only during cleaning and washing, but also during scrubber operation. Thus, the inlet and outlet pipelines and the main scrubber vessel should have smooth outlines of internal surfaces, without sharp constrictions, preferably cylindrical in shape. The volume of the scrubber vessel should not impede the free passage of the flow, without local areas of increasing velocity head.

2.2 Flow velocity

When cycloning dry dust there is a requirement to limit the flow velocity to 20 m/s, because of the resulting effect of blowing off the settled product and involving it in the movement to the outlet pipe, i.e. to the exit to the environment. Wetting of the product particles by the precipitating liquid eliminates this effect. The adhesion of the wet dust-liquid mixture is more likely to be so high that there is a need to ensure that there is no deposit. Thus, an increase in velocity to the level of flow turbulization will be useful until a critical velocity head occurs, an undesirable increase in hydraulic head. When calculating the cross-sectional area of the inlet nozzle based on the design velocity value:

$$\vartheta_v = \frac{Q}{S}\ (m/s) \tag{1}$$

where $\boldsymbol{\vartheta}_v$ – flow velocity in the inlet pipe, m/s;

Q – fan supply, m^3/s;

S – cross-sectional area of the inlet branch, m^2.

It should be kept in mind that when cycloning wetted dust, there is a Coriolis acceleration as it approaches the deposition surface, which should be accounted for in the overall flow velocity balance.

Thus, we propose the main device of the scrubber - dust wetting zone, a device in the form of a wet cyclone, with the size ratio recommended by NIIOGAZ.

The recommended value of D, not more than 1.2 m and the flow thickness at the cyclone inlet 0.2 D can be increased based only on the limitation of hydraulic resistance, but taking into account more effective settling due to wetting of dust by a special slotted nozzle installed at the point of adjoining the inlet pipe to the cylindrical body of the scrubber (Figure 1).

The slot nozzle is introduced into the cyclone from above. The slit has a width sufficient for outputting a continuous flow of wetting liquid on the dust surface and a length equal to the length of the inner part of the outlet pipe (Figure1). Liquid velocity at the outlet of the slot is equal to the velocity of dust at the cyclone inlet. A solid film of liquid covers the surface of the dust flow and due to relatively high density, under the action of centrifugal force presses the dust to the deposition surface, simultaneously wetting it in the film-drop mode. In addition to the centrifugal action, the wetted dust in its downward movement strikes the liquid surface at the bottom of the cyclone.

This provides a centrifugal-impact mechanism for contacting the dust with the wetting liquid.

2.3 Foam in the scrubber.

The protein in the milk product will form foam when in contact with the liquid and the agitating motion of rotation. Foam in itself is a useful phase to ensure wetting, but at significant volume is a detrimental factor, increasing hydraulic resistance and preventing the separation of air from the liquid as it moves to the outlet. At the same time, the impact of the flow as it moves from above to the liquid surface on the bottom is one of the technical methods of foam destruction. In addition, it is necessary to arrange foam overflow from the scrubber through a special vertical pocket connected with the drainage system by a special overflow channel.

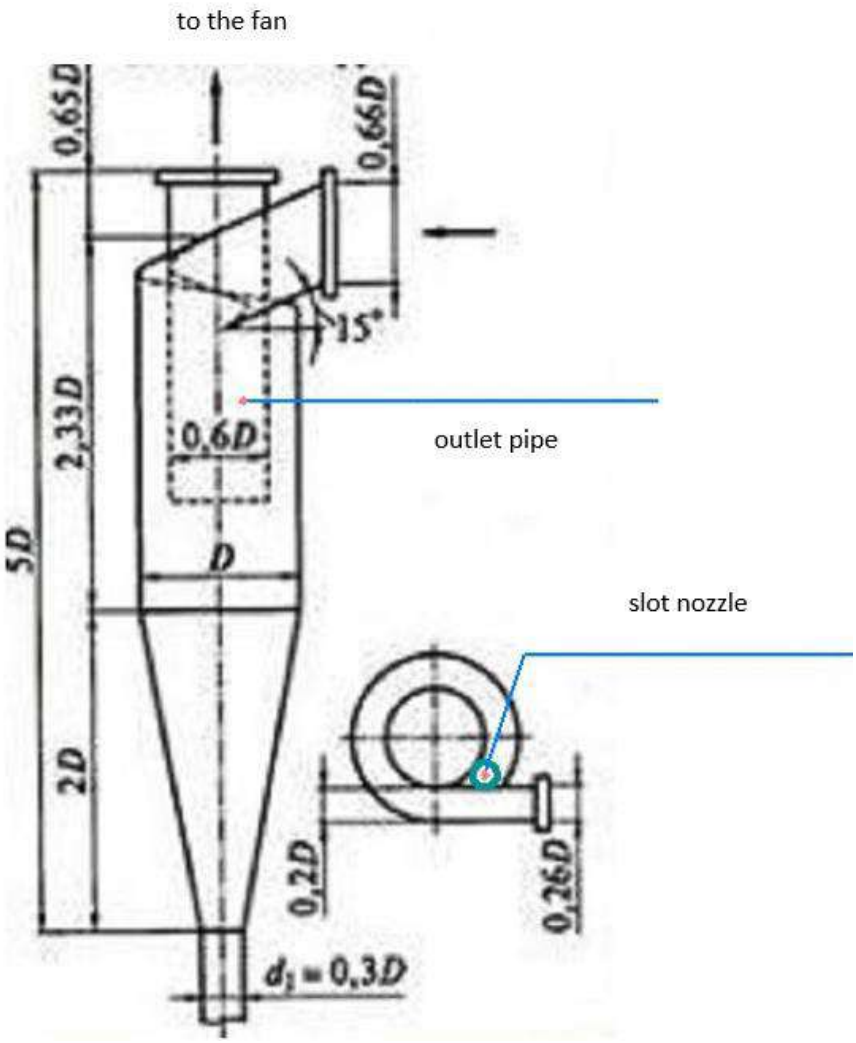

Fig.1. - Schematic diagram of the NIIOGAZ cyclone

The operation of the scrubber as part of the spray dryer is as follows:

In the scrubber body *7*, foam tank *9*, and level tank *11* is poured hot water *(t=70°C)* drinking quality, pump *12* through three-way automatic valve *14* until reaching the level of the pocket for foam in the scrubber body and the working level of the WL in the level tank *11*. The centrifugal fan *3* is switched on together with the exhaust fan *3* of the drying unit. Diverter *5* closes the air outlet on the exhaust pipe of the drying plant to the environment. Dust after leaving the cyclones enters through two successively installed, in order to overcome the hydraulic resistance of the scrubber, fan *3* and the inlet pipe of the scrubber *6* and is cyclonized in the body *7* of the scrubber. At the same time, the pump *12* in the cycloning zone supplies hot water from the level tank *11* to the slotted nozzle *18*. The water from the slit nozzle *18* irrigates the dust stream from its inner side. Water and wetted product particles due to increased density intensively approach to the outer wall of the scrubber body, on the way wetting and involving in this movement the entire dust stream. This mixture in a vortex motion enters the lower part of the scrubber body, hits the liquid surface, the level of which corresponds to the lower edge of the overflow channel for foam and is set using the valve *16* and water glass *17*. The flow of the cleaned coolant is then separated. Partially it flows through the crossflow pocket together with the foam into the foam container *9*. The main flow in contact with the cone *8* forms an upward spiral flow to the outlet of the casing *7* and outlet pipe *4* and is discharged into the environment outside the room. Foam from the container *9* is discharged to the drain *10.*

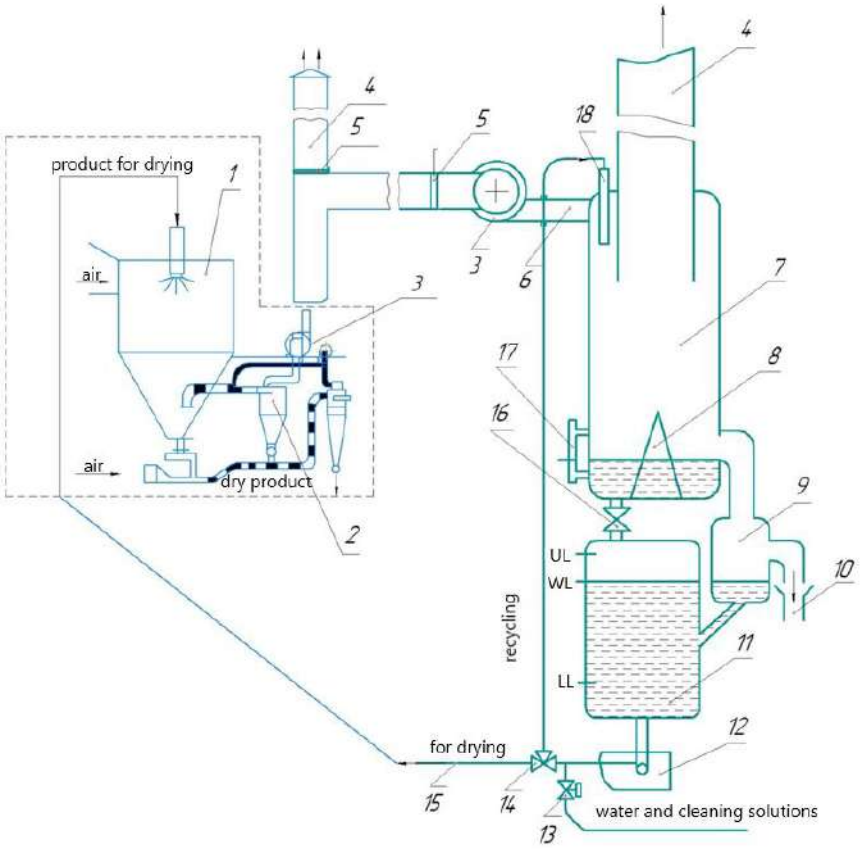

1 - drying plant; 2 - cyclone; 3 - fans; 4,6 - air ducts, dust pipelines; 5 - shibers; 7 - case of scrubber; 8 - case for the formation of ascending helical flow; 9-capacity for foam; 10 - drainage; 11-capacity of levels; 12 - pump-dispersant; 13 - automatic valve for water, cleaning solutions; 14 - automatic valve; 15 – pipeline to drying unit; 16 - regulating valve; 17 - water meter glass; 18-slit nozzle; LL-lower level; WL-working level; UL-upper level

Fig.2. - Schematic diagram of centrifugal-impact scrubber as a part of spray drying plant for dairy products

After reaching the upper level of WL in the level vessel during circulation, the automatic valve 14 closes the access of the solution to the scrubber and opens the supply to drying. When the lower level of LU is reached, the solution supply to drying is stopped. The automatic valves 13 and 14 are opened and hot water is again supplied to the scrubber until the operating level of WL is reached. The recirculation process is resumed.

Washing and disinfection of equipment after stopping dust supply from cyclones, similar to the process of hot water supply and solution circulation, using slotted and ball nozzles (not shown in the diagram).

2.4 Calculation of level capacity

There are three automatic levels in the level tank, which switch the liquid supply for recirculation, until obtaining the designed solids concentration in the solution and for supplying it after laboratory analysis for drying. The operating level of the WL gives permission to recirculate hot water, and then the solution of milk product, until reaching the upper level of UL, at which point the tank should contain a solution with a concentration of solids suitable for drying. The upper level of UL gives the command to open the valve of solution supply for drying. When reaching the lower level of LU solution supply for drying is stopped and allowed by the pump in the scrubber body, the container for foam and the container of hot water levels until reaching the working level of WL in the container of levels and the level of the lower edge of the overflow pocket for foam in the scrubber body. In this case, the liquid level in the level tank is equal to the level in the foam tank. Recirculation of liquid along the route pump - scrubber body - level tank - pump is carried out until the time of level rise from the WL to the UL due to the dispersed phase of dairy product dust that entered the solution. Consequently, it should be known, at the established frequency of feeding the received solution for drying, the volume of the part of the tank of levels between the working level of the RU and the upper level of the VU. In the process of recirculation during 20 hours (the usual duration of the drying process), the solution will not be spoiled by microbial causes, because the temperature of the solution when feeding dust with a temperature of 70 and more ºC, exceeds the temperature of the mode of long-term pasteurization.

From the point of view of production organization of preparation of the product for drying by evaporation at vacuum evaporator plants (VEP) and accordingly drying, the optimal is the arrival of the obtained solution for drying after the end of the VEP operation and transition to its washing. In other words, it is necessary to calculate the volume sufficient to contain the solution received in the scrubber for 20 hours.

3.1. The calculation is made according to the standardized indicators of the Ministry of Agriculture of the Republic of Belarus for some dry products.

Table 1. Indicators of dairy products during processing

Name of finished products	Mass of evaporated moisture during thickening kg/1000kg of raw material	Weight of condensed milk products kg/1000kg of raw materials	Mass of evaporated moisture during drying kg/1000kg of raw material	Weight of dry product kg/1000kg of raw material, moisture content 5%
Skimmed milk powder, SMP	807,3 thickening to solids concentration 45%, density 1190 kg/m^3	191,6	101,4	87,6
Whole milk powder 20%	738,76 Thickening to solids concentration 45%, density 1120 kg/m^3	260,8	133,3	119,2
Dried whey	880,4 Thickening to solids concentration of 50%, density 1209 kg/m^3	119,6	58,8	60,8

Since the purpose: technology of drying of the product obtained by dissolution in the scrubber, let's calculate the ratio of thickened products to dry ones:

- for SMP $191{,}6/87{,}6 = 2{,}180$;
- for whole milk powder $260{,}8/119{,}2 = 2{,}187$;
- for dried whey $191{,}6/60{,}8 = 1{,}967$.

The obtained figures for the ratio of dry products to condensed products allow us to determine the volume of product dissolved in the scrubber at its calculated concentration of 45% by dry matter, suitable for direct drying.

According to [1] Niro-Atomizer, Schwarte average losses of dry product with coolant at the outlet of the drying plant are 250 mg/m^3. Then the losses per hour of operation of the dryer will be for the drying plant VRA-4 with the volume of heat carrier 42000 m^3/hour

$$42000 \times 250 = 10500000mg = 10{,}5\ \ kg/hour\ of\ dry\ product.$$

respectively for 1 hour we get for SMP$_m$ = $10{,}5 \times 2{,}18 = 22{,}89\ \ solution/hour$.

Based on the density of the solution 1190 kg/m^2 find the volume of solution

$$V = \frac{m}{\rho} = \frac{22.89}{1190} = 0.019\ m^3/hour.$$

here m – is the mass of the solution, kg;
ρ – density of the solution, kg/m^3;
for 10 hours of work - 0,19 m^3;
for 20 hours of work - 0,38 m^3.
Similarly, for the solution of whole milk powder we obtain
for 1 hour of work – V = 0,02 m^3/hour;
for 10 hour of work – V = 0,2 m^2;
for 20 hour of work – V = 0,4 m^3/hour.

When calculating by serum, it should be taken into account that its losses in cyclones can be up to 800 mg/m^3, since all particles in its composition are very fine.

Conclusions

To reduce losses of dry dairy products during spray drying except traditional devices - cyclones and filters should be used scrubbers, which in combination with the previously developed technology of achieving the desired concentration of solids in the solution, provide drying of the resulting solution without other intermediate technological operations.

Active centrifugal-impact scrubber, taking into account the circulation mode of operation, can use not limited volume of irrigation liquid supplied to the milk dust by several slotted nozzles.

One should expect a high quality of the coolant cleaning, allowing its heat to be used repeatedly, after condensation of excessive moisture [4].

The considered features of operation of scrubbers for milk dust can be useful in the development of new designs.

References

[1] Raitsky G. E. Energy efficiency of drying dairy products: a monograph / G. E. Raitsky, I. S. Leonovich. - Grodno: GSAU, 2019. - 234 p.
[2] Varvarov V. V., Polyansky K. K. K. Efficiency of improving the means of cleaning emissions of spray dryers // Pub. of universities. Food technology,No. 2, 1988, P. 138.
[3] Method of liquid cleaning of the air stream from milk dust particles at the outlet of a spray drying plant. Patent of RB for invention No. 22658., B 01D 47/16/ G.E. Raitsky, I.S. Leonovich, N.V. Dubrovskaya; applicant and patentee G.E. Raitsky, I.S. Leonovich, N.V. Dubrovskaya. appl. 05.02.2015; publ. 30.08.2019.
[4] Method of conditioning air used as a drying agent in a spray drying plant. Patent of RB for invention No.20296., IPC F24F 3/00/ I.S. Leonovich, G.E. Raitsky, O.P. Shabunko, A.S. Kolomiets; applicant and patentee EI Grodno State Agrarian University. appl. 17.12.2012; published 30.08.2016.

Information of the authors

Raitsky Georgy Evgenievich, c.t.s., associate professor, Grodno State Agrarian University
e-mail: itftehmeh@ggau.by

Drobyazgo Yulia Viktorovna, master student, Belarus Grodno State Agrarian University
e-mail: itftehmeh@ggau.by

DOI 10.52209/2706-977X_2024_1_35 **IRSTI 55.31.01** **UDC 621.9**

Ways to Optimize the Kinetic Parameters of Tricone Drill Bits

Toshov J.[1], Baratov B.[1], Sherov K.[2], Mussayev M.[3]*, Baymirzaev B.[1], Esirkepov A.[2], Ismailov G.[4], Abdugaliyeva G.[3], Burieva J.[5]

[1]Tashkent state technical university named after I.Karimov, Tashkent, Uzbekistan
[2]Seifullin Kazakh Agrotechnical University, Astana, Kazakhstan
[3]Abylkas Saginov Karaganda Technical University, Karaganda, Kazakhstan
[4]Tomsk State Pedagogical University, Tomsk, Russia
[5]Tashkent State University of Economics, Tashkent, Uzbekistan
*corresponding author

Abstract. The improvement of the operation of roller cone bits, only drilling indicators are optimized, which include axial load, frequency of rotation, borehole diameter and rock fortress coefficient. The use of one or another roller bit can be justified by the physical-mechanical properties of rocks, which can have different values depending on the depth of drilling and the horizon. However, while resolving energy costs on the basis of the quality of the drill bits' interaction with the physical-mechanical properties of rocks and the condition of the cutters at the bottom of the well, which require high-tech solutions with scientific bases, it is possible to make the choice and justify a more efficient design of the drill bit. The article discusses a new method for determining the patency of a drilling cone bit using the determination of the workload of teeth and crowns based on kinematic calculations. Based on the kinematic parameters, the gear ratio of the cones, the specific indicators of contact and operation of the teeth on the bit crowns are determined, which in turn show the most loaded crowns. Based on these indicators, it is possible to determine crowns that are prone to breakage during the operation of bits. By this calculation was made a new program which by geometrical parameters of the tricone drill bit can show graphics of the work cones and crowns.

Key words: destruction, drilling, drill bit, kinetics, specific contact work, specific volume work

Introduction

Drill bit-the main tool with which the destruction of rock on the face and is the construction of deep wells in the oil and gas industry, as well as drilling wells in the mining industry and exploration. Drill bits are also widely used in the construction of complex engineering structures-bridges, tunnels, mines and other facilities [2]. A drill bit is a complex mechanism, rigidly limited in volume by the diameter of the wells. The supports of its sections contain multi-row radial and thrust rolling and sliding bearings, in the most critical designs of the bits, the supports are sealed and oil-filled. Roller bits perform 90-95% of the total drilling volume. To solve the problem of increasing the volume of work on drilling with roller bits, it is necessary to study not only the mechanical improvement of the bits, but it is necessary to apply the theoretical basis for a more detailed analysis of the drilling process.

Due to the variety of drilling methods and physical and mechanical properties of rocks, rock-breaking tools are made of different types of impact on the rock and structural design. The roller bit is a complex mechanism, in the production process of which the performance of 414 sizes is observed. Dimensional chains of bits consist of 224 links, geometrically connected by linear and angular dimensions, performed according to different systems of tolerances and landings (Figure1).

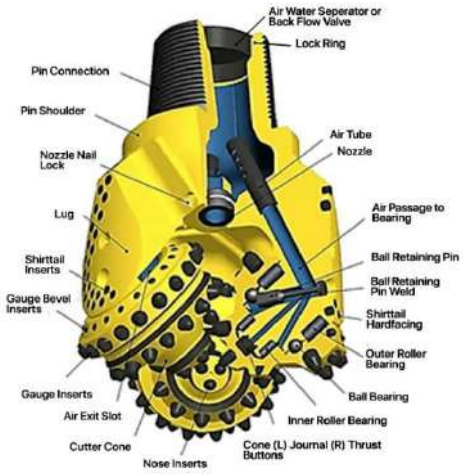

Fig. 1. - Tricone drill bits' elements

1. Methods and Materials

The roller bit is a one-time tool and in the process of operation undergoes significant statistical and dynamic axial loads and the action of alternating torque, in connection with which its design must be designed for an economically justified service life. The bit must meet the following basic requirements:

- to provide the maximum mechanical speed of drilling, the maximum penetration on a bit, operational reliability of riggings and a support of a bit, and durability of a support has to be higher since to 80% of cone bits fail owing to premature wear of elements of supports of drilling bits;
- to provide a receiving bore of a given diameter;
- have sufficient strength, excluding the destruction or deformation of parts under the action of maximum load;
- to have an optimal support design at the specified parameters of the drilling mode;
- to provide reliable lubrication system bearings cones;
- have a radial runout of the cones relative to the thread axis of not more than 0.8·10-3m and different heights of the cones relative to the thrust ledge of not more than 0.9·10-3 m;
- to have durable riggings cutters;
- to provide the necessary interaction time of the teeth with the rock.

The optimal drilling mode is understood as a harmonious combination of axial load, speed, torque and power on the bit, ensuring the maximum value of the mechanical drilling speed. The choice of operating parameters depends on the conditions of the well wiring, drilling method, design features of the bit used, its diameter, arrangement. Therefore, the drilling mode should be chosen on the basis of a comprehensive analysis of the available data, taking into account the obtained theoretical and experimental dependences. Optimization of drilling modes. In this case, the empirical dependence of the mechanical drilling speed on the axial pressure and the number of revolutions of the bit is constructed, i.e.:

$$V_M=f(P,n) \quad (1)$$

where V_M – mechanical drilling speed, m/h;

P – axial load, kN;

n – the number of revolutions of the bit, rpm.

Table 1. Drilling speed determination methods

Name of method	Formula	Indication
By V. Maurer	$V_M=\frac{nP^2}{D^2}K_d$ (2)	D - the bit diameter, m; K_d - the coefficient of drillability, depending on the rock properties, parameters of the washing fluid, the differential pressure type bits, wear his riggings, etc.
By G. Woods	$V_M=an(\frac{P}{D})^b$ (3)	b varies from 1.1 to 2.4
By R. Kanningham	$V_M=a\frac{n^{0,5}P}{D}$ (4)	Where a is the experimental coefficient, for the determination of which the corresponding experiments are required.
By B.S. Fedorov	$V_M=an^xP^y$ (5)	
B.N. Kutuzov used the elliptic law for the function V(t)	$V=V_o\sqrt{1-(\frac{h}{h_k})^2}$ (6)	V_0 - the initial drilling speed of the new bit, m/min; h - the current total depth of penetration of the bit, m; h_k - the maximum total depth of penetration (maximum resistance of the bit), m.
According to M.Bingham	$\frac{V_M}{n}=a(\frac{P}{D})^d$ (7)	a - the experimental coefficient, d-exponents does not fully take into account the influencing factors and does not have a sufficiently strict mathematical justification of the obtained functional relationship [3].
By Y.F. Potapov and V.V. Simonov	$V_M=knP^{1,4-0,0002n}$ (8)	
By Woods	$V_M=an\left(\frac{P}{D}\right)^4$ (9)	
According to Eckel, Canon and Bingstein	$V_M=aPn^{0,5}$ (10)	
By Kathleen	$V_M=a+bPn^y$ (11)	

Name of method	Formula	Indication
Most foreign researchers have come to the conclusion that the ratio that determines the mechanical speed of V_m with the amount of washing liquid providing the process should have the form proposed by M. G. Bingham	$V_M = k_b \cdot P^{\delta} \cdot n^{\alpha}$ (12)	P - the axial load on the bit, n - the bit rotation speed, k_b, δ and α - the parametric coefficients. The k_d - coefficient in the literature is called the "coefficient of drillability", because it characterizes the ability of the rock to drill. It takes values of 0.2-0.8, can reach a value of 2.5 units [4]. The coefficients δ and α have different values for different authors [5]. The value δ is most often assumed to be equal to one, but there is also δ =0,6. The coefficient α mainly lies in the range of 0.4-0.75, for particular conditions can be equal to 0.1 or 1. For the above equation, it is assumed that the flow rate Q and the pressure of the drilling fluid provide high-quality (complete) cleaning of the face from the drilled rock without re-grinding it.
The Halley-Woods-Lubinsky model is common in the United States, the state of the well wiring process for any given time is determined by a three-dimensional vector in the state space - the current values of V_M, the degree of tooth wear and the degree of wear of the bit support [6].	$V_M = k_\alpha \frac{\bar{P}^{\beta} \cdot r}{[a \cdot (D_t)]^b}$ (13)	Where: $\bar{P}^{\beta}$ - the axial load reduced to the bit diameter, $\bar{P}^{\beta} = P / D$; r – coefficient determining the type of rock: - for hard rocks $r = e^{\frac{100}{n^2}} \cdot n^{0.428} + 0.2(1 - e^{\frac{100}{n^2}})$ (14) - for soft rocks $r = e^{\frac{100}{n^2}} \cdot n^{0.75} + 0.5(1 - e^{\frac{100}{n^2}})$ (15) $a(D_t) = 0.928 \cdot D_t^2 + 6 \cdot D_t + 1$ (16) where β - exponent of axial load; D_t - the relative wear of the teeth of the bit; b-exponent of the bit arrangement wear function
Model of the company "Tenneco oil company". In determining the optimal combinations of bit load and rotor speed to ensure minimum drilling cost, it is assumed that the mechanical speed and wear of the bit are functions of the bit load, rotation speed, rock characteristics, bit type and washing fluid	$V_M = \frac{k_d \cdot (P - P_0) \cdot n^a}{f(h)}$ (17)	P_0 – the load on the bit at which the penetration of the tooth into the rock begins, $f(h)$ - characteristic of the state of the bit.
Model of Pogarskii A. A. for mechanical speed V_M allows to take into account the influence of flow and pressure of the washing liquid and has the form [5]	$V_M = \frac{a \cdot \bar{P}^2 \cdot n^{\alpha}}{1 + b^4 \cdot \bar{P}^4}$ (18)	a - the corresponding k_b, α - coefficient that have the same meaning as in other dependencies, but take different values. The coefficient b depends on the flow rate of the solution Q and the hydraulic power applied to the bit N_b and for the maximum speed $V_M=max$ is defined as $b=1/P$.

Currently, attempts to build such dependencies are ongoing. However, it is quite obvious that there can be no universal dependence of such a plan, because, firstly, the conditions of rock destruction are constantly changing as the depth of drilling wells increases, and secondly, there is always an intensive re-equipment of drilling enterprises with bits of new, more advanced designs. Therefore, it is possible to take any of these dependencies and each time under changed conditions to determine experimentally the coefficients of ignorance. But in this case, there can be no question of forecasting and, therefore, of optimizing the process of destruction of the rock in General. From the joint analysis of the formulas, it follows that to predict the cost of a meter of penetration, it is necessary to predict the variables T and H, which is associated with the V_M ratio

$$V_M = \frac{H}{T} \tag{19}$$

It follows that V_M prediction should be sought through these variables. As you know, the total penetration of the bit depends on the efficiency of drilling when transferring optimal parameters to the drill bit. To determine the speed of drilling plays an important role in the introduction of the teeth of the roller on the rock. Theoretical studies

of the characteristics of the introduction of teeth are based not only on the axial load but also on the shape of the teeth of the bit. Rotary drill bits are armed cutter in a gear or disk rims. Arrangement elements can be steel, milled in the body of the roller, or carbide, pressed into holes on the crown surfaces of the rollers. During designing roller bits, the placement of crowns on the surface of the balls is made so as to provide the necessary amount of overlap of the face and sufficient gaps between the crowns. Arrangement tends to be placed on the balls evenly. However, this is not enough to ensure a uniform loading of the crowns and the overall balls. The relative load of the various crowns of the bit balls depends on their vertical stiffness, determined mainly by the design of the support unit and the position of the crown on the ball [7].

The steel gear arrangement of the crowns is carried out in the form of blunted wedges by milling. The main parameters of riggings: the initial blunting, the length of the teeth (coincides with the width of the crown), the initial height of the teeth, the angle at the top of the wedge, the pitch of the teeth in the crown [8]. The carbide toothed arrangement of the crowns is made in the form of insert teeth made of tungsten cobalt alloy. Depending on the configuration of the working surface and the method of attachment in the body of the cones, carbide teeth of the following types are developed and manufactured: spherical, wedge-shaped straight, wedge-shaped inclined, polyhedral, conical, peripheral with a bevel, sub-caliber, corrugated, semi-corrugated, cap, sector, etc. [9]. An increase in rotation speed will bring about an increase in penetration rate, but within certain limits. In soft formations, where chips are produced by cutting/tearing actions, the increase in penetration rate is nearly proportional to the change in rotation speed (if the chips are all being cleared as soon as they are produced). The sliding of teeth complicates the operation of rollers on hard rocks as the rock breaks unevenly (Figure 2). Failing to completely clear the cuttings can also become a large problem at high speeds. The result is that there is little advantage in increasing the rotary speed above recommended levels. However, bit wear increases rapidly as rotation speed is increased, both for rollers and for hammer bits.

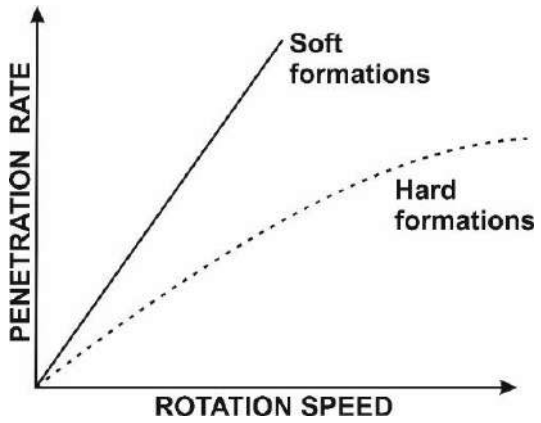

Fig. 2. - Relation between rotation speed and penetration rate for different formations [10]

The tooth of the bit is pressed into the rock by axial force and simultaneously makes a complex movement depending on the parameters of rotation of the roller and the bit, sliding along the face. At the same time, the adjacent tooth moves to the surface of the rock and strikes it. In the following moments of time, the load is redistributed from the first tooth to the second, and then the first tooth comes out of contact with the rock. Experimental studies of the interaction of individual elements of the drill bit with rock are performed according to the scheme of drilling with one tooth (Figure 3).

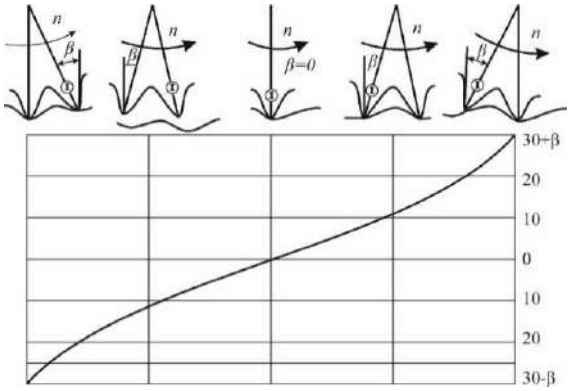

Fig. 3. – The scheme of interaction of a tooth of a roller with a face of a well [11]

Toothed crowns on the cones are arranged in such a way that they provide a complete defeat of the drilled surface. The teeth are formed in the form of wedges, the tops of which are located either in the axial planes of the cones, or are displaced relative to them at a certain angle. The main lateral surfaces of the teeth, as a rule, are flat with equal working surfaces in area, while the displacement of the axes of the cones relative to the axis of rotation of the bit is provided. Currently used methods of design of the roller drilling tool working with sliding gear arrangements, do not allow to ensure uniformity of distribution of volume work of destruction of the bottom face rock, between all crowns of arrangements taking into account the geometry of the teeth, their orientation, direction and slippage committed by them. In most experimental studies, the angular velocity of the cone was averaged within one revolution. However, as a result of experimental studies conducted on a special stand that allows to study the power and kinematic parameters of serial roller bits during direct drilling of the rock, it was established that the instantaneous gear ratios of the cones change in 1.4...1.75 times within one revolution [12]. At the same time, the minima of the instantaneous gear ratio fall on the vertical positions of the teeth relative to the face.

Drilling optimization: according to the proposed invention, the aforementioned goals can be reached by simultaneously implementing the following concepts, which allow for the mathematically determined optimal positioning of cutting elements on the surface of each cutter rotatably placed on a drill tool or drill bit:

1. By using an independent rolling cutter and varying the pitch between neighboring cutting parts, tracking while drilling on the bottom hole is completely eliminated;

2. The most effective spacing between succeeding penetrations while taking into account the mechanical characteristics of the rock to be drilled, the geometry of the cutting elements, and the orientation of the centerline of the cutting elements with regard to the surface of the cutter;

3. Through careful arrangement of cutting elements along cutter generatrices, harmful axial resonance frequency vibration of the drill bit or tool that restricts drilling the formation is significantly reduced [7].

In this regard, there was not a little change in the design of drill bits, which were justified only by the application of one or another type of change in the surface parts of the bits. But since the change in the location and number of teeth is of great importance, it should be borne in mind that the cost of the bit also depend on these indicators. Also, when changing these parameters, the change accounted for the load of other elements of the roller. From the diagram in Figure 3 it is seen that the teeth strike the face at the first pass with a step s close to the step of their placement in the crown. When re-passing, one part of the crowns strikes the face at the same points, and the other-with some offset along the step Δs (Figure 4). Step offset will be measured in the direction of rotation of the bit. Denote s0=Δs/s and call it the relative step offset. The value of s0 varies from 0 to 1. At s0, equal to 0 and 1, the face is affected "trace to trace". Tooth marks do not lie on the same radius of the bit. This means that at different times with the face interact different number of teeth and the actual coefficient of overlap of the face - a variable value in time. Let's estimate the actual overlap coefficient (ηf). For convenience, consider its relative value:

$$\eta' = \frac{\eta_f}{\eta} = \frac{\sum l}{\sum l_i} \tag{20}$$

where $\sum l$ is the number of teeth in contact at the moment. Definition η' is a statistical problem.

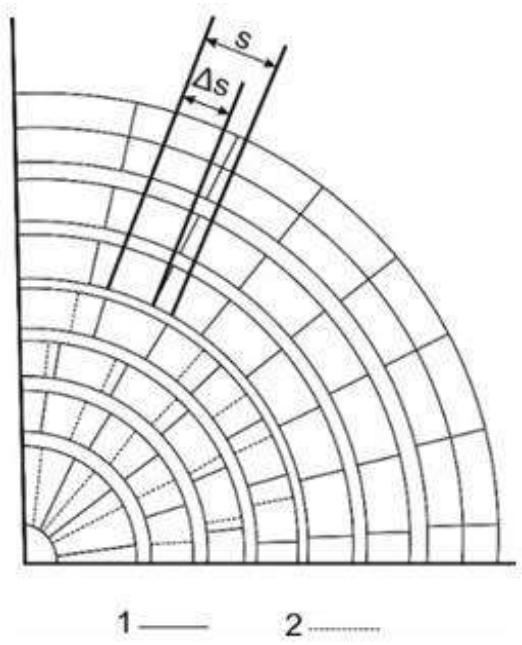

Fig. 4. - The scheme of defeat of a face by teeth of a bit of type T: 1-at the first pass; 2-at the second pass

The physical meaning of η' is the proportion of $\sum l$ rigging simultaneously involved in the destruction of the bottom hole. The completeness of the destruction of the bottom hole is characterized by the defeat of the bottom, which is equal to the ratio of the face area, covered by the teeth of all the cones for one revolution of the bit, to the face area of the well:

$$\eta_c = \frac{\sum_{i=1}^{z} F_i \cdot \bar{l}}{\pi \cdot R_b^2} \tag{21}$$

where Fi - the cross-sectional area of the tooth; z - the number of teeth except for the cone pressed into reverse cones; i - the average gear ratio of the bit. This indicator is used to characterize the bits with carbide riggings.

A roller bit from the point of view of kinematics is a part of a spatial gear or friction mechanism with movable axes of working links-cones. The mechanism includes a leading element in the form of interconnected legs, the slave units - cutters and non-rotating component, for slaughter. The study of such a mechanism would not be difficult if the transfer relations, both average and instantaneous, from the body of the bit to each of the cones were known, that is, the ratio of the bit is:

$$i_j = \frac{\omega_j}{\omega_b} \tag{22}$$

where i_j - the ratio of the bit body to the *j*-th cone; ω_j - the angular velocity of the *j*-th cone; ω_b - the angular velocity of the bit.

Analytically, it is very difficult to determine i_j. At destruction of firm rocks of frequency of rotation of cones are inversely proportional to numbers of teeths on peripheral crowns. This character of rotation is due to the fact that the teeth of the peripheral rims, destroying the face, form a toothed rack on it, which further determines the law of rotation of the cones. The step of the breaking line is close to the largest pitch of the peripheral S_{max} crowns. It allows to estimate approximately the number of teeth of a rack the $z_t : z = \frac{2\pi R_b}{s_{\max}}$. Received result is rounded up to the whole in the big party. Then the gear ratios of the cones are approximately equal

$$i_I = \frac{z_t}{z_I} \quad i_{II} = \frac{z_t}{z_{II}} \quad i_{III} = \frac{z_t}{z_{III}} \tag{23}$$

The total number of cutter teeth is selected from the conditions to achieve effective destruction of rocks and taking into account the set of teeth on the cutters. As a result of studies on this issue proposed the calculation of the number of teeth on the cutters produce in the following formulas [8]:

for plastic and elastic-plastic rocks:

$$Z = 3.14 \cdot \sqrt{\frac{R_b \cdot b \cdot (\frac{tgd}{2+\mu_1}) \cdot \sigma_{com}}{q_z}} \tag{24}$$

for elastic and elastic-brittle rocks:

$$Z = 3.14 \cdot \sqrt{\frac{E \cdot R_b \cdot c}{3 \cdot (1-\mu_1^2) \cdot q_z}} \tag{25}$$

where σ_{com} – rock hardness corresponding to the tensile strength, kN/m^2.

q_z – load acting on one tooth when it is introduced into the rock, kN;

d – the angle of sharpening of the teeth of the cones, deg;

b – the length of the sides of the tooth, m;

R_b – the radius of the cutter, m;

E – modulus of rock elasticity, kN/m^2;

μ_1 – the Poisson's ratio for rocks;

c – the width of the root face of the tooth, m.

Insufficiently studied, there is a question of influence of placement of crowns on cones on radius of a face on efficiency of drilling and durability of riggings of bits. Currently, the placement of crowns on the cones is made on the basis of the requirement of the necessary overlap of the face, taking into account the need for uniform placement of riggings on the cones. The strength characteristics of carbide teeth are significantly influenced by the quality of their surfaces. The presence of defects in the surface layer, which are stress concentrators, leads to an intensification of the tooth destruction process. The strength of carbide teeth depends on other technological factors, such as the

method of pressing teeth [9]. It is also established that the durability of carbide teeth affects the stiffness of the connection "tooth-bit" [10]. Reducing this stiffness can improve the durability of carbide riggings. Thus, the durability of carbide riggings, limited by the destruction of teeth, depends on a large number of design and technological factors. In known studies, the general nature of the destruction of carbide teeth of roller bits has been studied in detail. However, most researchers did not set themselves the task of analyzing the number of destroyed teeth on each crown of each bit. In addition, research works have been conducted in different years on bits of different types and sizes, with significant differences in the design of riggings and support units, so even the data available in the literature is difficult to use.

3. Results

Many researchers also include uneven wear and failure of components of riggings and support assemblies of the cutters. Uneven wear is observed both when working off bits with milled riggings, and when working off bits with pin carbide riggings. At industrial working off of the first designs of spherical bits with carbide riggings their uneven wear was noted. The bits failed mainly due to the wear of the top of the first cone, chipping teeth on the peripheral crowns and jamming of the supports of the cones. In subsequent designs of bits due to changes in the geometric shape of the cones, increasing the diameter of the teeth and the manufacture of vertices on all three cones, it was possible to reduce the uneven wear and destruction of carbide riggings and improve the efficiency of the bits. However, it is not possible to completely eliminate the uneven wear and destruction of carbide riggings. The proportion of destroyed teeth, accounting for an average of each cone, also varies. The largest number of destroyed teeth in bits of both types falls on the first cone. Research works have shown that although in most cases the performance of the bits is limited by the stability of the support, the durability of the bits is also insufficient [11].

The main goal of many works was to increase the efficiency of tricone bits, seen on the way to optimize the process of destruction of rock during drilling. For this at the first must compose mathematical model of describing the mechanism of interaction between the riggings of the rollers adequately to the real dynamics at the bottom [12]. In some cases, a 3d model of the drill bit, which was created by EDEM software, was used to optimize the operation of the drill bit using mathematical modeling, force was applied to the center and body, vibration, penetration rate and wear were studied [13].

The factors that can be studied are three main groups of parameters that include drilling equipment properties, rock properties, and environmental conditions. The properties of the equipment and environmental conditions are variable parameters, as the characteristic properties of the rock cannot be changed. In addition, the abrasiveness of the rock also affects the ability to drill the rock. Parameters used to predict drilling capacity include rock physical properties, rock chemical properties and rock drillability [14]. As a result of the detailed analysis of the conducted researches concerning dynamics of riggings, it is established that the complex approach to research of dynamics of a drill bit as a whole is necessary. The design of a drill bit with excellent dynamic characteristics in terms of arrangement can show worse results during drilling wells, if it will have a less stable sealing of the supports of the cones or a less effective system of cleaning the bottom of the well from the drilling fluid. In connection with the above, the drill bit must be considered as an element of a complex dynamic system, i.e. the dynamics of the drill bit.:

– dynamics of arrangement taking into account fluctuations at the bottom of the well;

– washing fluid dynamics;

– the dynamics of the thrust bearing.

The dynamics of the support bearings is inherent only in the drill bits of the roller type. When considering the dynamic aspects of the components of the overall dynamics of the drill bit, it is necessary to have a clear understanding of both relationships. In the case of partial optimization of the above components of the overall dynamics of the drill bit, it is necessary to know: are these optimization tasks overlay tasks or not? Are they contradictory or complementary? What is common in the methodology of their formulation and solution? The solution of these problems should be based on the classical provisions of theoretical mechanics. To date, the goal - to increase the efficiency of tricone bits is viewed by optimizing the process of rock destruction during drilling. For this, an appropriate mathematical model is needed that describes the mechanism of interaction between the cutter armament adequately to their real dynamics in the bottom hole. The destruction of rock by drill bits can be assessed through the definition of two parameters, as specific contact and specific volumetric work of destruction and are presented as follows [16]:

$$A_s = \frac{A_{tw}}{S} \tag{26}$$

where, A_s - specific contact work of destruction, kg.mm/mm;

A_{tw} - the total work spent on the deformation and destruction of the rock during the indentation of the stamp, kg.mm;

S - area of the flat base of the cylindrical stamp, mm^2.

$$A_v = \frac{A_{tw}}{V} \tag{27}$$

where, A_v - specific volumetric work of destruction, kg.mm/mm^3, V - volume of deformed rock, mm^3.

The following rules are designed in order to address these issues throughout long-term theoretical and experimental study on the effectiveness of tricone drill bits.

1. Using tricone roller bits, the effectiveness of rock destruction is functionally dependent on two kinetic criteria. [15]:

- from the relative specific contact work of destruction.

$$\left(A_j^{'}\right)_I = \frac{S_j F_j i}{\Delta S_j},\ \left(A_j^{'}\right)_{II} = \frac{S_j F_j i}{\Delta S_j}, \left(A_j^{'}\right)_{III} = \frac{S_j F_j i}{\Delta S_j} \tag{28}$$

where $A_j^{'}$ -relative specific contact work of destruction of teeth of j-th conditional crown, N*mm/mm^2 [17];

S_j - the contact path of the tooth of the unit area of the j-th conditional crown at the same contact with the face of the well, mm;

F_j - the force of resistance to the movement of the teeth of the unit area of the j-th conditional crown in contact with the rock at the bottom of the well;

N; i - gear ratio of the roller; ΔS_j - contact area of the tooth apex of the j-th crown of the cone of unit length and width, mm^2.

– from the relative specific volume work of destruction

$$A_k^{''} = \left(\frac{S_{j,k} F_j z_j d_j i}{V_k}\right)_I + \left(\frac{S_{j,k} F_j z_j d_j i}{V_k}\right)_{II} + \left(\frac{S_{j,k} F_j z_j d_j i}{V_k}\right)_{III} \tag{29}$$

where $A_k^{''}$ -relative specific volume work destruction of teeth of the j-th crown on the k-th ring face of the well, N*mm / mm^3 [16], $S_{j,k}$ - the contact path of the teeth of the j-th rings on the k-th ring faces of the well, mm; z_j - number of teeth on the j-th crown, PCs; d_j - number of conventional crowns of unit width on the j-th crown, PCs; V_k - volume of the destroyed rock on the k-th ring face, mm^3.

2. Kinetic criteria for evaluating the performance of drill bits in the form of (28) and (29) are generally functions of the parameters of the bit-rock-energy triad. Under the parameters of the triad is accepted [15]:

- bit -a complete list of geometric parameters of the rock-breaking tool, which depend on its kinetic model and strength properties of its components and parts;

- rock - physical and mechanical properties of rock, taking into account the conditions of its destruction, depending, for example, on the shape of the bottom hole, the quality of cleaning the bottom-hole zone of sludge, etc.;

- energy - the parameters of the drilling mode taking into account the transformation of energy components when feeding them to the rock-breaking elements (teeth).

3. The kinetic criteria are explicit functions of the geometric parameters of the drill bits (28) and (29).

4. According to the physical sense, the relative specific contact work of destruction in the form (1) determines the intensity of abrasive wear of the teeth of the j-th crowns of the cones [17]:

$$A_j' = \frac{1}{T_2} \tag{30}$$

where T_2 – time of mechanical drilling, hour;

5. On physical sense relative specific volume work of destruction in the formula defines intensity of destruction of a rock by teeth of j-th crowns of cones on k-th ring faces of a well [18]:

$$A_k'' = V_M \tag{31}$$

where V_M – mechanical drilling speed, m/h.

6. The penetration of the bit also depends on the relative specific contact work and the relative specific volumetric work, since:

$$H = V_M \cdot T_2 = A_K'' \cdot \frac{1}{A_j'} \tag{32}$$

The first and second provisions demonstrate the objectivity of the kinetic criteria, the third shows the possibility of actually changing the kinetic criteria by altering the geometric parameters of drill bits, the fourth and fifth establish the necessity of changing the kinetic criteria in order to improve drill bits, and the sixth establishes the economic criteria for evaluating drill bit performance [19].

During one cycle of axial reciprocating motion of the bit body, the angular velocity of the bit under the influence of changing in magnitude and direction of the dynamic load changes slightly, even in the steady-state drilling mode [20].

Keep in mind that the teeth working on the ring faces of the well, which are covered by the crowns of adjacent cones, have distinct values for particular contact and volumetric works of destruction. As a result, attention must be drawn to the extreme values of a particular contact and a certain volume of destructive activity.

The experience of solving optimization problems on the basis of comparative analysis of kinetic (dynamic) criteria showed the following.

1. The geometric properties of the teeth and their number must be used initially when optimizing practically any roller bit design.

2. The issue of guaranteeing equal load of supports of neighboring cones on the alignment of minimal volume operations of destruction of crowns of adjacent cones is the most promising optimization challenge.

With its more precise geometry and logical functioning under the defined geological and technological parameters, the roller bit will perform more effectively thanks to these recommendations.

The above recommendations have two aspects: technical-the recommendation of a more perfect geometry (design) of the bit, technological-the recommendation of a more rational design of the bit for given geological and technical conditions of drilling.

Drilling tricone bits fail, having exhausted their potential capabilities or the arrangement of the cones, or their supports. As is known, the level of penetration of the teeth of the cones into the rock is also an important parameter determining the efficiency of drilling [21]. Wear of the teeth of the cones is observed when the load on the bit is insufficient for the introduction of the tooth into the rock [22]. And the specified phenomena-wear (chip) of teeth of bits and wear of supports, as a rule, have local character, i.e. wear of riggings of bits and their supports comes with advance, respectively, on one of crowns at one of bit.

The above is in full accordance with the kinetic characteristics:

- the specific relative contact work of destruction;
- the specific relative volume work of destruction, or rather with the relations of their extreme values.

Specific contact work of destruction characterizes relative intensity of abrasive wear of teeth of crowns of adjacent cones, and specific volume work of destruction characterizes relative intensity of destruction of rock on adjacent ring faces of a well (Figure 5).

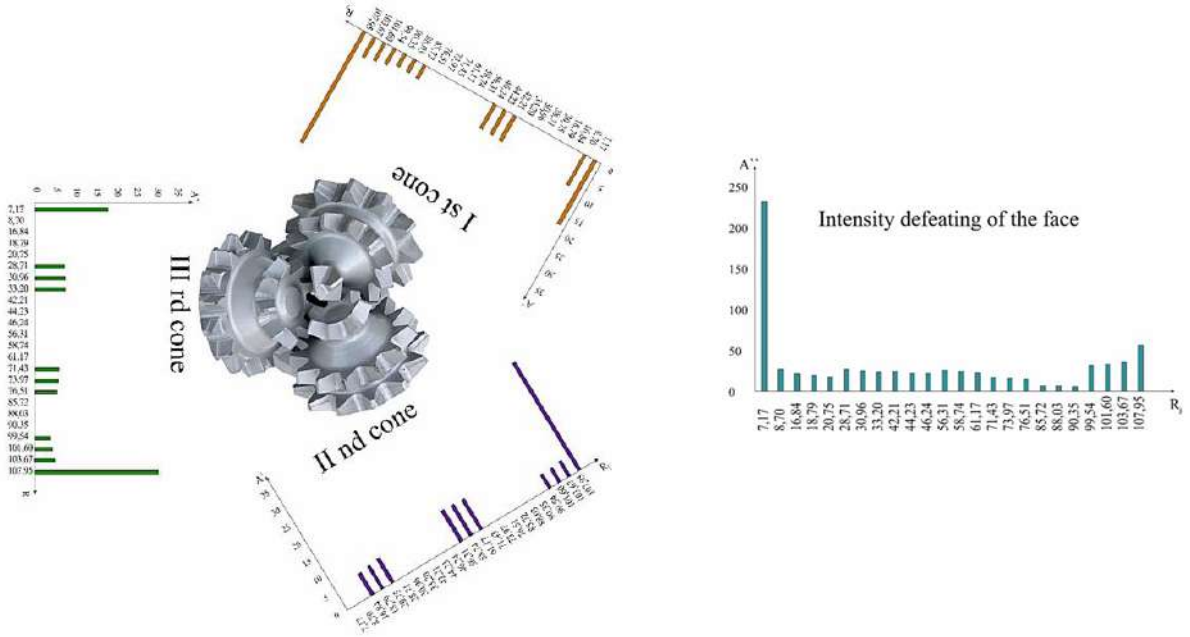

Fig. 5. - Kinetic passport of tricone bit 215.9

Values can accurately predict which of the crowns of adjacent cutters of the bit will wear out ahead and by a set of teeth which cutters have a greater chance of a chip and which one of the crowns defines the upper bound of the real mechanical speed of drilling, which foot the adjacent cutters will be more loaded and, therefore (Table 2), will have rapid wear [23].

Table 2. Analysis of the kinetic passport of the drill bit

Ring sections on the face from the periphery to the center			The intensity of wear of the crowns (in arbitrary units) A'						The intensity of the stope lesion (in conventional units
			First cone (gear ratio i = 1,458)		Second cone (gear ratio i = 1,427)		Third cone (gear ratio i = 1,442)		
j	R	D	Z	A'	Z	A'	Z	A'	A"
1	107,95	3,248	11,0	31,492	14,0	29,464	16,0	30,431	57,414
2	103,67	2,067	11,0	5,711	14,0	4,223	16,0	4,949	36,855
3	101,60	2,066	11,0	5,114	14,0	3,884	16,0	4,438	33,964
4	99,54	2,066	11,0	4,572	14,0	3,699	16,0	4,016	31,751
5	90,35	2,317	11,0	3,538					7,180
6	88,03	2,317	11,0	3,592					7,483
7	85,72	2,316	11,0	3,734					7,990
8	76,51	2,538					13,0	5,606	15,195
9	73,97	2,538					13,0	5,839	16,372
10	71,43	2,538					13,0	6,084	17,665
11	61,17	2,431			11,0	8,222			23,687
12	58,74	2,430			11,0	8,397			25,199
13	56,31	2,430			11,0	8,580			26,867
14	46,24	2,017	9,0	7,008					22,616
15	44,23	2,016	9,0	7,049					23,797
16	42,21	2,014	9,0	7,094					25,107
17	33,20	2,248					6,0	7,685	24,359
18	30,96	2,245					6,0	7,566	25,763
19	28,71	2,240					6,0	7,451	27,406
20	20,75	1,971			3,0	6,644			19,391
21	18,79	1,959			3,0	6,262			20,315
22	16,84	1,942			3,0	5,973			21,812
23	8,70	1,622	1,0	8,638					27,728
24	7,17	1,404	1,0	18,074			2,0	18,020	234,820

Conclusions

The bit arrangement is designed unsatisfactorily. The peripheral crown of the third cone, the second from the periphery of the crown of the second cone, and the second from the periphery of the crown of the first cone are where the minimal values of particular volume works fall. Uneven distribution of the drilling's maximum load will have a negative impact on the bit's stability. After analyzing the existing bit, it is possible to determine the main directions for increasing the efficiency of the bits, using kinetic data, which are possible in three consistent solutions:

1. By equidistant load of supports of adjacent cones.
2. On the way to increase the overall (minimum) intensity of rock destruction.
3. On the way of saving carbide riggings. Structure sketch

The economic effect will be determined:

- in the first case - by increasing the durability of the bit;
- in the second case - by increasing the mechanical speed of drilling;
- in the third case - by reducing the cost of the drill bit. In the General case, an effective solution can be found at the intersection of these paths.

The development of recommendations is based on solving the following sequence of tasks:

1. Analysis of the kinetic passport of the drill bit's basic design.
2. Calculation of ways to improve its design.
3. Calculation of a novel geometric parameter combination for the bit that provides the best kinetic passport.
4. Comparative evaluation of the bit's performance based on the kinetic passports of the suggested design.

References

[1] Norov Y.D., Toshov J.B., Shemetov P.A., Improving the efficiency of drilling blastholes in open pits, Tashkent: Fan, 2009.
Kirshenbaum V.Y. and Torgashov A.V., International translator-Handbook, Moscow: International Engineering Academy, 2000.
[2] Shevtsov V.D., Pressure regulation in boreholes, Moscow: Nedra, 1984.
[3] Pogarskii A.A., Automatization of drilling deep wells, Moscow: Nedra, 1972.
[4] Pogarskii A.A., Chefranov K.A. and Shishkin O.P., Optimization of drilling deep wells, Moscow: Nedra, 1981.

Tsuprikov A.A., “Analysis of mathematical models of mechanical penetration rate for optimization of oil and gas drilling”, Scientific journal of Kubgau, vol. 107, no. 3, 2015.
[5] Aaron A.V. and Lytvienko V., Anti-tracking earth boring bit with selected varied pitch for overbreak optimization and vibration reduction, US 2007.
[6] Baratov B., Toshov J., Baynazov U., “Method of calculating the gear ratios of the cones of tricone drill bits”, E3S Web Conf., vol. 201, 01012, 2020.
[7] Baratov B.N., Umarov F.Y., Toshov Z.H., “Tricone drill bit performance evaluation”, Gornyi Zhurnal, Moscow, vol. 12, pp. 60-63,2021.
[8] Mikhailin Y.G., Research and development of roller bits with teeth of hard alloy, Moscow, 1980.
[9] Toshov J.B., Toshov B.R., Baratov B.N., Haqberdiyev A.L., “Designing new generation drill bits with optimal axial eccentricity”, Mining Informational and Analytical Bulletin, vol. 9, pp. 133-142, 2022.
[10] Palchenkov V.A., “Criteria for the efficiency of the cutting structure of the drill bit”, Oil and gaz, vol.1, pp. 110-116, 2016.
[11] Naganawa S., “Dynamics modeling of roller cone bit axial vibration”, Journal of the japanese association for petroleum technology, pp. 333-337, 2005.
[12] Sousani M., Predicting Drill Wear using the Discrete Element Method// 2017. [Online]. Available: https://www.edemsimulation.com/blog/predicting-drill-wear-using-discrete-element-method.
Niyazi B. and Bilgehan K., “Investigation of the Effect of Drill Bit Rotation Speed on Sustainable Drilling” in Proceedings of the 8th International Conference on "Sustainable Development in the Minerals Industry, Canada, 2017.
[13] Steklyanov B. L., Studies of the mechanism of interaction of working protrusions of the rollers with the face of the wells, Tashkent, 1973.
[14] Toshov J.B., “Improving the efficiency of drilling blast wells on the ways of optimizing the three components of the dynamics of drill bits”, Mining bulettein, vol. 6, pp. 281-285, 2014.
[15] Morozov L.V., Improving the durability of drill bits on the basis of computer analysis of structural elements and their assembly, Samara, 2003.
[16] Blinkov O.G., Ways to improve the efficiency of drill bits, Moscow, 2007.
Steklyanov B.L., Steinert V.A. and Rakhimov R.M., “Dynamic components of rock-breaking drilling tools”, Construction of oil and gas wells on land and at sea, vol. 6, pp. 19-21, 2008.
[17] Balitsky P.V., Interaction of the drill string with the bottom of the well, Moscow: Nedra, 1975.
[18] Travkin V.S., Rock-breaking tool for rotational cavernless drilling of wells, Moscow: Nedra, 1982.
[19] Toshov J. B., “Research kinematics gear crown of cone bits” Mining bulletin, vol. 6, pp. 13-15, 2005.
[20] Nurzhanova O., Zharkevich O., Berg A., Zhukova A., Mussayev M, Buzauova T., Abdugaliyeva G., Shakhatova A. Evaluation of the Structural Strength of a Prefabricated Milling Cutter with Replaceable inserts During Machining // Material and Mechanical Engineering Technology, №4, 2023, pp. 10-17

Information of the authors

Javokhir Toshov, Doctor of Technical Sciences, Professor, Tashkent State Technical University named after I. Karimov.
e-mail: javokhir.toshov@yandex.ru

Bakhtiyor Baratov, PhD, Tashkent State Technical University named after I. Karimov
e-mail: bakhtiyor.baratov@yandex.ru

Karibek Sherov, Doctor of Technical Sciences, Professor, Seifullin Kazakh Agro-Technical Research University
e-mail: shkt1965@mail.ru

Medgat Mussayev, PhD, associate professor, Abylkas Saginov Karaganda Technical University
e-mail: mussayev.medgat@gmail.com

Bakhtiyor Baymirzaev, Head of educational and methodological department, Tashkent State Technical University named after I. Karimov
e-mail: b.baymirzayev76@gmail.com

Azimbek Esirkepov, Doctoral student, Seifullin Kazakh Agro-Technical Research University
e-mail: azimbek.esirkepov@mail.ru

Gafurzhan Ismailov, Candidate of Technical Sciences, Associate Professor, Tomsk State Pedagogical University
e-mail: gmismailov@rambler.ru

Gulnur Abdugaliyeva, Candidate of Technical Sciences, Associate Professor, Abylkas Saginov Karaganda Technical University
e-mail: gulnura84@mail.ru

Jasmina Burieva, Student, Tashkent State University of Economics
e-mail: bjasmina0109@icloud.com

DOI 10.52209/2706-977X_2024_1_46 **IRSTI 67.09.29** **UDC 699.86**

Bench Studies of Sound Insulation Materials and Vacuum Sound Insulation Panel

Lemeshko M.A.*, Zanina I.A.[1], Kostromina E.I.[1], Salikova N.S.[2]
[1]Institute of Service and Entrepreneurship (branch) of Don State Technical University
[2]Abay Myrzakhmetov Kokshetau University
*corresponding author

Abstract. There is a problem of protection from high-level sound of city residents, employees of enterprises; to a greater extent, in the workshops of machine-building factories, for example, during stamping, forging and other metalworking processes. Specialists and maintenance personnel are exposed to high-intensity noise near powerful agitators, pumps, engines and other power equipment. Due to these circumstances, it is necessary to constantly improve systems, devices, materials, coatings that reduce the negative impact of high noise levels on people. For this purpose, various soundproof walls, panels, screens, plates are being developed. One of the directions of modernizing sound-proofing fences is the method of using vacuum to design these protective devices. The article discusses the use of vacuum in special sound-insulating panels developed by the authors. The information about bench experimental studies of some sound-proofing materials is given, some results of testing of vacuum sound-proofing panels are presented. The research stand and research methodology are described. The features of the stand for the study of sound-proofing properties of flat samples of sound-proofing materials of the same size and thickness are given.

Keywords: sound insulation research, vacuum sound insulation, sound-proofing materials, panels, screens, experimental method, research automation, stand with software control.

Introduction

Often, noises from machines, apparatuses and other equipment operating at enterprises or technological noises of production reach a level exceeding not only the norms of comfortable work for a person, but also legally permissible indicators. However, a relatively low noise level of 50-55 dBA negatively affects performance, causes faster fatigue of working people. As is known, the equivalent noise level for all types of work in workshops and on the territory of manufacturing enterprises is an acceptable noise level of 80 dBA, while the maximum level is 107 dBA. For concentrated work in rooms with noisy equipment, the maximum permissible noise level is 103 dBA, and the equivalent is 75 dBA. However, the requirements for the noise level at enterprises are not always met and often due to the lack of necessary means and sound insulation systems. Due to the high noise level, healthy people suffer and their ability to work decreases. Therefore, it is obvious that the task of improving sound-proofing structures and panels with effective sound insulation is urgent. The need for such developments is also explained by the fact that with the development of technology and technology, the intensity of machine work increases, the power of the equipment used increases and, as a result, the power of sound effects on humans increases [1].

In various industries, for example, in mechanical engineering, in light industry, problems with high noise levels in the area of human presence are very significant [2, 3]. And the solution of these problems is very relevant. This explains the relatively large number of publications in the field of noise abatement and the development of various methods and means of protecting people from industrial noise. In patent funds, for example in FIPS, a large number of patents for various methods and devices for noise control can be noted - engineers, scientists are actively trying to solve the problem under consideration [4 – 13].

From the wide variety of engineering solutions to the noise problem, we will single out several characteristic ones, close to the method of noise control by using soundproof fences in the form of walls, fences, panels, screens, etc.

1. Materials and Methods

The purpose of the research is to create effective sound insulation, taking into account the trends of its improvement. To achieve the goal, the analytical method of research, analysis of patent materials, planning and conducting experimental studies were used. Based on the results of the study of literary and patent materials, trends in the improvement of soundproof structures have been established.

This knowledge served as a basis for planning experimental studies. Taking into account the peculiarities of the research process of sound-insulating materials, a method of automated research of these materials is proposed and developed. A special automated stationary stand for experimental research was developed, and later the concept of robotization of some experimental works was formed. This concept is limited to those experimental studies in which the experimental plan includes a set of values of one or more parameters under study.

The experience of using such a stand has established its effectiveness with the "intelligent" control of the experimental program. When according to preliminary results, the program clarifies the experiment plan. In these studies, the frequency of sound emission and sound power were varied to determine sound reflection and sound absorption for various porous and fibrous materials. And also for various designs of soundproof panels.

2. Results and discussion

A review of the methods of sound insulation, the designs of sound-proofing panels revealed some trends in their modernization. For example, the development of flexible sound insulation. As an example, we will give the device of a sound-proofing panel (Kalinin, 2019), which is made of upper and lower steel plates in the form of separate geometric shapes. The plates are fixed together on both sides on a flexible material. The panel is made of two layers of geometric shapes. In addition, the plates have a cutout h by an amount equal to half the thickness of the plate to ensure the flexibility of the panel during operation.

Another direction of creating sound-insulating fences is the creation of diverse sandwich panels, with elements to increase strength, durability, etc. It is necessary to single out developments in which both fibrous and porous materials are used simultaneously to solve the problems of sound insulation. When the directions of the fibers in the mineral wool insulation panels are combined.

For example, to solve the problems of sound insulation, a special construction sandwich panel has been developed (Kalinin, 2006), which uses two surface layers of metal and a central part made of pieces of mineral wool that make up longitudinal strips. The longitudinal axes of the pieces are parallel to the longitudinal axis of the panel, and the orientation of the fibers in the pieces is perpendicular to the plane of the surface layers, the ends of the pieces are displaced longitudinally with respect to each other. Between the strips of pieces of mineral wool, longitudinal strips of filler foam, polyurethane, etc. are additionally introduced), and they are introduced sequentially between groups of strips of mineral wool. The essence of such a combination is explained in Figure 1, by the layout of materials in the panel.

A heat and sound insulation honeycomb sandwich panel is also known [12], which includes two identical surface layers and an inner layer of equal area placed between them, which is honeycomb cells in the form of regular hollow prisms with hexagonal bases facing the surface layers. In this panel, hexagonal recesses are symmetrically made on the inner sides of the surface layers to form a base inside the layers, and the inner layer is made with holes that symmetrically coincide with the recesses and is shifted diagonally relative to the surface layers. Of course, interesting developments in which vacuum is used to improve sound insulation. For example, a sound–proofing structure is known - a "Sound-proofing element" in which sound insulation is provided by vacuuming the enclosed cavity with hemispherical surfaces [5].

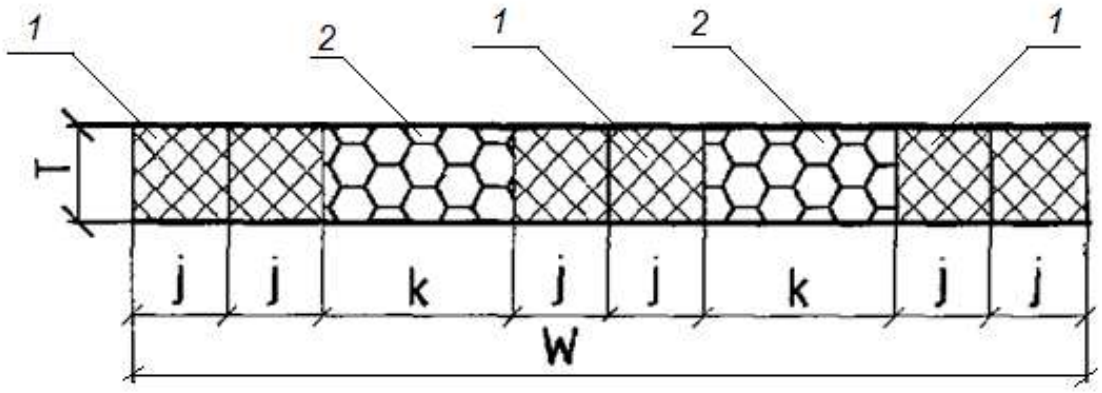

1 - filled polyurethane foam, 2 - mineral (stone) wool

Fig. 1. - Layout of panel materials

There are also known designs of vacuum sound-proofing flat panels in which the evacuated cavity is filled with a form-forming and sound-proofing filler made of porous material. For example, a vacuum sound-proofing design according to the patent [11]. This flat panel is made in the form of a sound-proofing wall panel, which uses filler between the enclosing walls (Figure 2).

In the specified source, the evacuated panel contains a formative incompressible element with the formation of a porous internal space for its evacuation.

The sealed shell 1 is covered from the outside with a sound-absorbing material 3, a sealant, rubber or a rubber-like material (polyurethane, thiocol and others).

Metal foil 1, laminated with a polymer film, has flexibility and there are no cracks in it, it is technologically advanced in the assembly stage of the vacuum constructions. The tightness of the structure is provided by a welded or soldered joint 4.

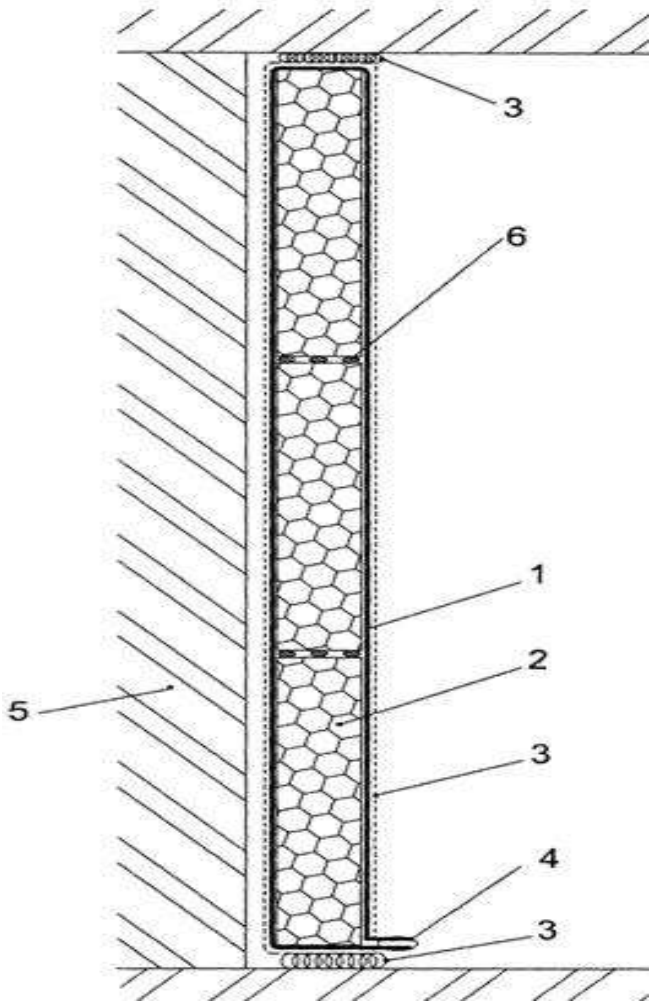

1 – shell, 2 – filler, 3 – reflective coating, 4 – nipple, 5 – wall, 6 – partitions

Fig. 2. - Vacuum wall panel [11]

In other similar designs of sound-proofing panels, it is proposed to use flat, rigid covering sheets; between which plates of sound-proofing porous material are placed. At the same time, this material is used as a support for flat, rigid cover sheets.

The application for the invention "Electrified Vacuum Panel" [4] describes a vacuum panel in which a porous filler is used as sound insulation, enclosed between two flat sheets connected at the edges of the vacuum panel. In such a design of a vacuum panel with rigid protective sheets, an intermittent or porous filling material is located between these sheets, which is also a conductor of sound vibrations and therefore the disadvantage of such a design is its relatively low sound-proofing ability.

We have developed a design of a vacuum sound-proofing panel [10], which has advantages in comparison with known similar vacuum sound-proofing panels (Figure 3).

In the developed design, two limiting walls are cylindrical in shape and oriented with bulges in one direction. At the same time, a connecting belt made of an elastic vacuum-dense material is located between the limiting walls along the perimeter, to which the limiting walls are firmly fixed, forming a closed vacuum cavity between them.

Another development of the authors is a vacuum sound-proofing panel in which stiffeners and coating layers are used [8]. Reinforcement of the covering sheets with ribs in the panel design provides rigidity of the limiting walls (covering sheets), since the stiffening ribs prevent the deflection of the limiting walls after vacuuming the cavity between them.

In this case, a "quasi-plate" is formed with a high deflection resistance. The membrane effect disappears and the proportion of energy of the reflected sound wave from the front surface facing the sound source increases significantly.

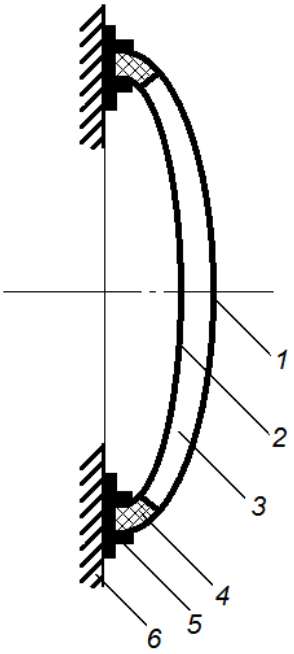

1,2 – limiting walls, 3 – vacuumed cavity, 4 – connecting belt, 5 – fasteners, 6 – panel support

Fig. 3. - Vacuum sound-proofing panel [10]

The disadvantage of such a panel is the ribbing of the front surface. We have also developed a sound-proofing panel with internal stiffeners [9], in which this disadvantage has been eliminated. And the sound-reflecting properties of the panel with internal ribs have been significantly increased, therefore, the sound-insulating characteristics of such a panel have been significantly improved.

Figure 4 shows a diagram of a panel with stiffeners inside the panel. The vacuum sound-proofing panel consists of two limiting walls 1, frame 2, stiffeners 3. The elements of the vacuum sound-proofing panel 1,2 form a closed vacuumed cavity 4 with the possibility of deep discharge up to 0.1...0.2 atm., while the elements 1,2 are interconnected motionlessly and vacuum-tight, and the stiffeners 3 are fixed along their entire length to the inner the surfaces of the bounding walls 1 are integral.

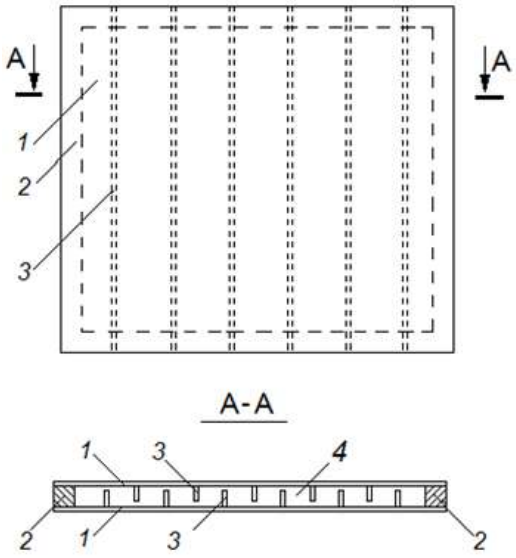

1 – covering sheets, 2 – spacer frame, 3 – stiffeners

Fig. 4. - Vacuum sound-proofing panel with internal stiffeners [9]

To evaluate ideas for improving sound-proofing structures, modeling or experiments are usually resorted. To

test the effectiveness of vacuum sound insulation and compare the sound insulation performance of other known sound-insulating materials, experimental studies were conducted on a stationary stand. A research acoustic stand has been developed and used, allowing to study and compare various sound-proofing materials, including samples of a vacuum sound-proofing panel.

A stand has been developed with software control and with the possibility of autonomous individual experiments in the study of sound-insulating materials with varying sound frequency and sound pressure power, programmatically, without human participation.

The scheme of the stand on which the research was carried out is shown in Figure 5.

The stand consists of: sensitive microphones – 4,6, a rigid body – 2, a soundproof coating – 3, a tray for installing the samples under study – 5, low-frequency and high-frequency speakers – 7. The stand is provided by: a system for changing the frequency and power of sound – 1. It includes a sound oscillator and an adjustable sound power amplifier, as well as a software controller for changing the frequency and power of the sound effect. To control the measurement algorithm of the parameters under study and record the measurement results, a personal computer is used, to which the microphone output is connected and which controls the operation of the controller for changing the frequency and power of the sound effect.

During experimental studies of sound-insulating materials on a stand with software control, a stable mono frequency and stable radiated sound power are established. According to the research plan, it is planned to generate different sound wave spectra and adjust their power (sound pressure) at different frequencies. The use of recording the noise of real machines for which sound insulation is being developed is provided.

Here are some research results obtained at the stand for various sound-insulating materials and for an experimental vacuum sound-insulating device. The experiments were carried out on samples in the form of flat panels with the same dimensions: 400x500 mm, 80 mm thick (Figure 5).

Table 1 shows the data of sound power measurements after a sound-proofing sample, under the same other measurement conditions.

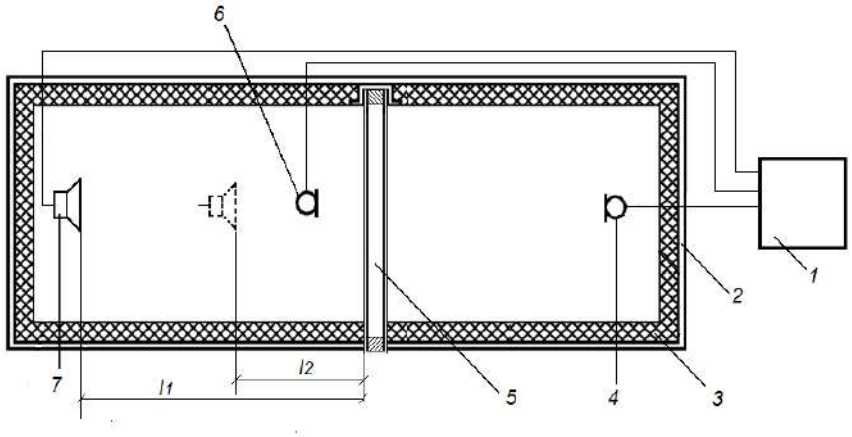

1 – measurement unit, 2 – stand housing, 3 – sound insulation, 4 – microphone after sound insulation, 5 – test sample, 6 – microphone of reflected sound, 7 – sound emitters

Fig. 5. - Diagram of the stand for automated studies of sound insulation materials

As can be seen from Table 1, despite the different structure of sound-proofing materials and their physical and mechanical features, the materials studied differ markedly in sound-proofing properties. Along with this, the dependence of the degree of sound absorption of the studied materials on the frequency of the main sound wave is established. For better absorption of sound power with a large frequency range, it is obviously necessary to design multilayer fences made of various materials.

The camera without a partition, in Table 1, understands the mode when the maximum power of the sound source is measured at the installation site of the first microphone. In this case, the reflection of sound waves is equal to "0". So for acoustic felt, with a speaker power of 2 watts, the sound radiation power was 69.9 dBA, and the microphone measured the sound power after sound insulation equal to – 38.1 dBA. The sound power in front of the test sample, made of acoustic felt, on microphone 2 was 75.4 dBA, therefore, the reflected sound power for this experiment was 5.3 dBA. The greatest reflected sound power was found when measuring the sound-insulating properties of the vacuum panel, it was 28.5 dBA.

Table 1. Results of measurements of the sound-insulating properties of the materials under study at a generator frequency of 1000 Hz

Material	Sound level on the microphone, dBA		
	Gain 1 (P=2W)	**Gain 2 (P=5W)**	**Gain 3 (P=10W)**
Acoustic felt	38.1	40.2	61.5
Foam	39.1	59.4	63.5
Basalt cotton	40.9	52.2	63.9
Household felt	44.7	54.0	68.5
Isolon	45.4	56.2	66.1
Foam rubber (impregnated)	46.7	66.3	68.6
Corrugated cardboard	48.1	64.4	65.7
Wood chips	41.6	54.1	68.0
Sawdust	49.4	59.9	67.0
A camera without a partition	69.9	80.9	85.6
Vacuum panel	34. 6	38.2	57.0

When analyzing the results of sound level measurements on the first microphone, after a sample of a sound-insulating material, at a frequency of 1000 Hz and a sound source power of 2, 5, 10 Watts, it was found that the materials have the best sound-insulating properties: acoustic felt, foam, basalt wool. Table 2 shows the values of these levels at those settings of the power amplifier of the stand, at 2, 5 and 10 watts. The levels are given as a percentage of the maximum level for each gain.

Table 2. The effect of sound level on the sound-insulating properties of the materials under study

Amplifier power, watts	Materials under study			
	Foam	**Basalt wool**	**Acoustic felt**	**Wood shavings**
2	56.0 %	58.5 %	64.0%	59.5%
5	73.0%	64.5%	66.7%	66.8%
10	74.0 %	74.2%	74.2%	74.4%

As can be seen from the data in Table 2, the greater the sound power, the less the sound insulation ability.

Discussion

In automated studies, the measurement results are recorded in the memory of a personal computer and can be transmitted for analysis remotely from the place of experiments. The developed and considered method of experimental research provides a significant simplification of the process of long-term multiparametric studies, reducing research costs, improving their quality. In addition, it becomes possible to automatically change the research program.

The possibility of conducting automated "intellectual research" using the criteria of a Student, Fisher, etc. is provided. "Intelligent research" is when the experiment plan can be adjusted based on the results of a certain amount of research already performed. For example, if there is an extremum in the studied range, the experiment control program can automatically increase the number of experiments in the critical area. In combination with software-controlled manipulators, it becomes possible to automatically change the test samples, and automatically change the experimental conditions, in a wide range and in working conditions with hazardous substances.

Conclusions

1) The developed research stand allows measuring the power transmitted through the sound-insulating material and the power of the sound reflected from the sound-insulating material.

2) Comparative characteristics of sound-proofing panel samples were obtained at different mono frequencies of the sound emitter and at three power levels of the sound source.

3) It was established that of the studied samples, the acoustic felt used for the noise insulation of automobiles has the best sound-insulating characteristics.

4) The study of the sound insulation properties of the vacuum panel showed results close to the properties of acoustic felt insulation.

5) The results of the study of the sound insulation vacuum panel turned out to be worse than expected, the authors will continue to research and improve the vacuum sound insulation structures from now on.

6) For experimental conditions, it was found that the sound permeability through sound-insulating materials increases with increasing power of the sound source.

References

[1] Butuzov, A. B. & Sukhov, V. N. (2016). From the experience of reducing noise in the workplace from engineering equipment (blender). *Technology of the textile industry, 4* (364), 140-146.
[2] Gusev, V. P., Zhogoleva, O. A. & Ledenev, V. I. (2017). Design of noise protection in buildings with suspended ceilings for technological purpose. *Construction and reconstruction*, 3, 49-57.
[3] Gorbunova, O. A., Pavlov, G. I. & Nakoryakov, P.V. (2017). Development of Design and Engineering Solutions to Reduce Noise from the Boiler Room to Protect the Residents. *Ecology and industry in Russia, 21*(10), 44-49. DOI: 10.18412/1816-0395-2017-10-44-49
[4] Giannantonio, R., Fumagalli, A. & Galliani, G. (2005). *Electrified vacuum panel*. (Application for invention of the Russian Federation No 2004107130 A). Russian Federation: Federal Service for Intellectual Property, Potentials and Trademarks.
[5] Bogolepov, I. I. (1984). *Sound-proofing element*. (Patent RU No. 1270251). USSR: State committee for inventions and discoveries
[6] Kalinin, I. N. (2006). *Building sandwich panel.* (Patent RU No. 2280132 C1). Russian Federation: Federal service on intellectual property.
[7] Kalinin, I. N. (2019). *Sound proofing panel*. (Patent RU No. 194873 U1). Russian Federation: Federal Service for Intellectual Property, Potentials and Trademarks.
[8] Lemeshko, M. A., Baklakova, V. V. & Galdin, D. V. (2020). *Vacuum sound insulation panel*. (Patent RU No. 198761 U1). Russian Federation: Federal service on intellectual property.
[9] Lemeshko, M. A. & Lemeshko, A. M. (2021). *Vacuum sound insulation panel.* (Patent RU No. 205795 U1). Russian Federation: Federal service on intellectual property.
[10] Lemeshko, M. A., Zanina, I. A., Baklakova, V. V. & Babenko, L. G. (2020). *Vacuum cylindrical sound insulation panel.* (Patent RU No. 201291 U1). Russian Federation: Federal service on intellectual property.
[11] Pilyagin, M. V. & Menyashkin, D. (2014). *Vacuum sound-proofing design.* (Patent RU No. 2582149 C1). Russian Federation: Federal service on intellectual property.
[12] Sergeeva, N. V. (2013). *Thermal and sound-insulating honeycomb sandwich panel.* (Patent RU No. 131756 U1). Russian Federation: Federal service on intellectual property.
[13] Zhivkovich, T. & Draganovich, M. (2015). Protection from noise in the environment of the city of Belgrade. *International scientific journal life and ecology, 1,* 36.

Information of the authors

Lemeshko Mikhail Alexandrovich, c.t.s, docent, Institute of Service and Entrepreneurship (branch) of Don State Technical University
e-mail: lemeshko.ise-dstu@mail.ru

Zanina Irina Alexandrovna, c.t.s, docent, Institute of Service and Entrepreneurship (branch) of Don State Technical University
e-mail: zanina.ise-dstu@mail.ru

Kostromina Evgenia Igorevna, teacher, Institute of Service and Entrepreneurship (branch) of Don State Technical University
Institute of Service and Entrepreneurship (branch) of Don State Technical University
e-mail: kostromina.ise-dstu@mail.ru

Salikova Natalia Semenovna, c.ch.s, docent, Abay Myrzakhmetov Kokshetau University
e-mail: salikova.amku@mail.ru

DOI 10.52209/2706-977X_2024_1_53 **IRSTI 55.13.17** **UDC 316.343.653**

Investigating the Time Spent on Manufacturing Parts of Complex Geometry Using Additive and Traditional Technologies

Zhetessova G.S.[1], Škamat Je.S.[2], Tattimbetova G.B.[3], Mateshov A.K.[4]
[1,3,4] Abylkas Saginov Karaganda Technical University, Karaganda, Kazakhstan
[2] Vilnius Gediminas Technical University, Vilnius, Lithuania
*corresponding author

Abstract. The research objective is to conduct a comprehensive analysis of the time spent on the production of parts of complex geometry using additive and traditional technologies. In modern industrial production, especially in the field of mechanical engineering, the manufacture of parts with complex shapes is becoming more and more in demand. These parts often have a high degree of complexity and require precise and efficient processing. The use of additive and traditional technologies in the production of parts can present various advantages and disadvantages, including production speed, manufacturing quality and overall time costs. However, there is insufficient research comparing the time costs of these two production methods, especially in the context of manufacturing parts of complex geometry. This work aims to fill this knowledge gap by analyzing and comparing the time spent on manufacturing parts using additive and traditional technologies. The results of this research can be useful for both the scientific community and industrial enterprises, helping them make informed decisions when choosing production technology for specific tasks.

Keywords: additive technologies, 3D printing, prototyping, milling, model.

Introduction

Prototyping is an integral part of product pre-production. Prototyping allows you to obtain valuable technical information, conduct a marketing research of a new product on the market, check some functional properties of the CAD model and the future product, and much more. Before starting mass production of a product, it is necessary to produce one, and sometimes even several versions of prototypes. In the latter case, this leads to additional costs, but they cannot be avoided when working with new or unfamiliar materials, designing products of complex geometric shapes or individual loaded, load–bearing parts - in practice, it is necessary to find out the real shrinkage characteristics of plastic, assess the possibilities of maintaining dimensional tolerances, etc. The above applies equally to two groups of prototypes: exact facsimile copies of products (for evaluating appearance and other applications) and technological (obtained in an experimental injection mold to evaluate the process and some properties of castings [1]).

Various technologies can be used to manufacture master models for casting (hereinafter referred to as parts) having a complex geometric shape:

– machining;
– photopolymerization;
– stereolithography;
– laser sintering of powder materials;
– layered application of molten polymer filament;
– gluing (lamination) of layers;
– casting into elastic silicone molds;
– low pressure casting;
– creating solid - state objects using printers;
– production of models from foamed plastics;
– casting of prototypes in experimental molds.

This article discusses in more detail two manufacturing technologies for such parts: milling on a CNC machine and 3D printing.

The rapid proliferation of Additive Manufacturing (AM) in the last 50 years has seen the developing manufacturing sector integrated into design and modelling as a rapid prototyping technique [2]. 3D printing (Three Dimension Printing, 3DP) technology is a rapid prototyping technology, also known as additive manufacturing technology. It is a technology based on digital model files, using powdered plastics, metals or bondable materials to build objects by layer-by-layer printing [3]. Compared with the traditional processing and manufacturing technology that removes materials, 3D printing technology is a brand-new manufacturing technology. With the maturity and promotion of computer-aided design (CAD) technology, 3D printing technology is becoming more and more perfect [4]. The ability to fabricate complex parts in one machine and job, has businesses determined to establish AM as a certified end-user product manufacturing technique. AM research and company integration of the

technologies has progressed AM from rapid prototyping to rapid tooling and now to a future in Direct Manufacturing [5].

The additive technology market consists of segments of equipment, materials, services and software. According to forecasts of world experts, the global market for additive technologies will reach $41.6 billion by 2027, and 3D printing services will be in high demand [6] (Fig. 1).

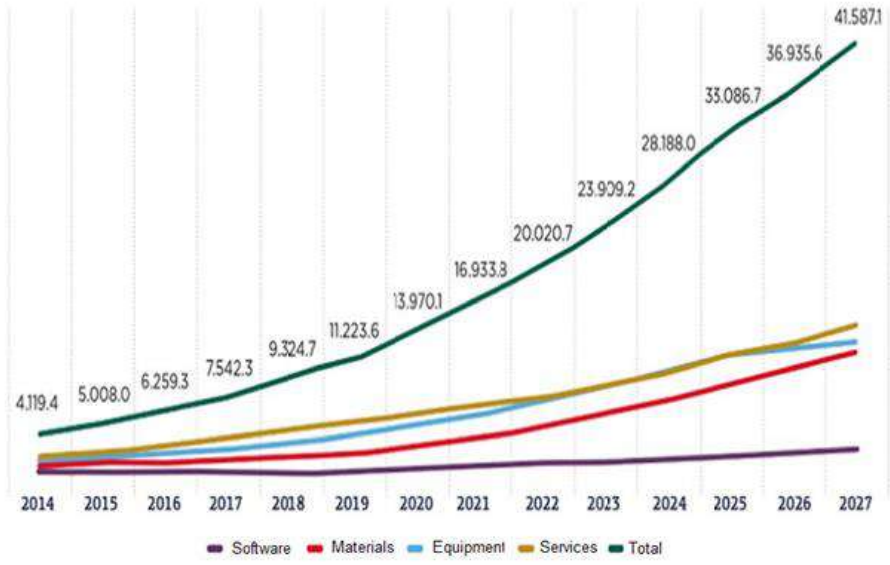

Fig. 1. – Dynamics and forecast of the total volume of the additive technologies market (by application areas), billion dollars. Source: SmarTech Publishing

1. Methods and experimental research

During the experiments, general methods of scientific cognition were used: analysis and synthesis of information on the research topic; methods of mathematical modeling in the analysis of experimental results; experiment planning; 3D modeling of parts and their manufacture on a 3D printer with maintenance of the required technological parameters, as well as calculation of time costs for the production of parts using additive and traditional technologies.

The process of manufacturing a part using additive (3D printing) and traditional (milling) technologies can be presented in the following sequence of works (Table 1)

Table 1. Stages of manufacturing a part of complex geometry

No.	Stages	Traditional technologies (milling)	Additive technologies (3D printing)
1	Designing	Creating a model	Creating a model
2	Postprocessing	Creating a blank Development of the technological process Tool Selection Code generation Check	Exporting a 3D model to STL format G-code generation
3	Production preparation	Preparation of the machine Setting up Preparation of the tool Debugging	Preparing a 3D printer
4	Production	Milling	3D printing
5	Post-production processing	Finishing (on demand)	Finishing (on demand)

The rational use of time in the process of creating parts allows you to optimize the entire production cycle. This may include improving design processes, reducing hardware setup time, and optimizing the execution time of operations.

We will experimentally calculate the time spent on creating a pump body using additive technologies. To begin with, a three-dimensional model is created in a special Siemens NX software module. The result of designing a 3D model is shown in Fig. 2. The resulting file is exported to STL format. STL is a graphical standard for representing model data for rapid prototyping systems. It is based on the method of three-dimensional triangulation of the model surface, which is carried out by triangles and can be smoothed by geometric shapes of a higher order, thereby achieving high accuracy and reproducibility of the synthesized surface [7].

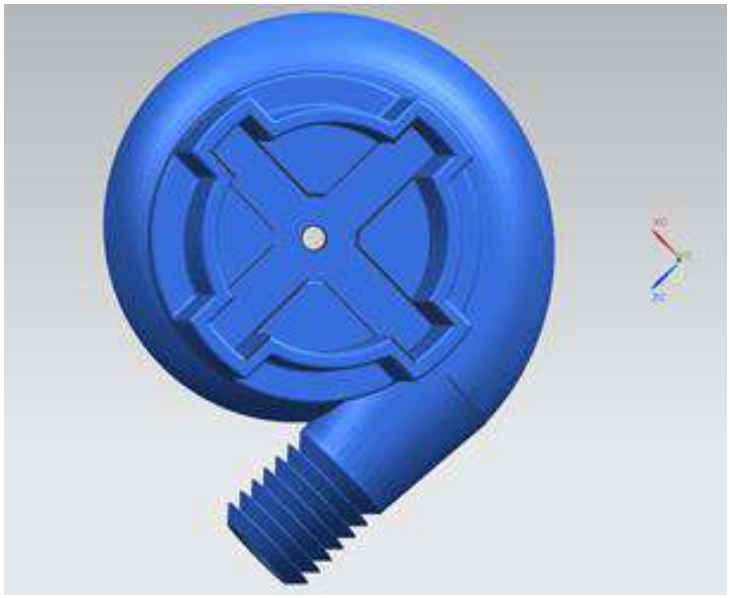

Fig. 2. – 3D model of the pump housing in Siemens NX

In the next step, using the Polygon software, the two-dimensional fragments, in turn, are converted into a G-code that controls the movement of the print head and printing conditions such as temperature and speed [8]. In addition, at this stage, the optimal parameters for the direct printing process of the product are determined. According to the received G-code, the approximate printing time of the product with dimensions 57 x 41 x 60 mm is 2 hours and 12 minutes (Fig. 3).

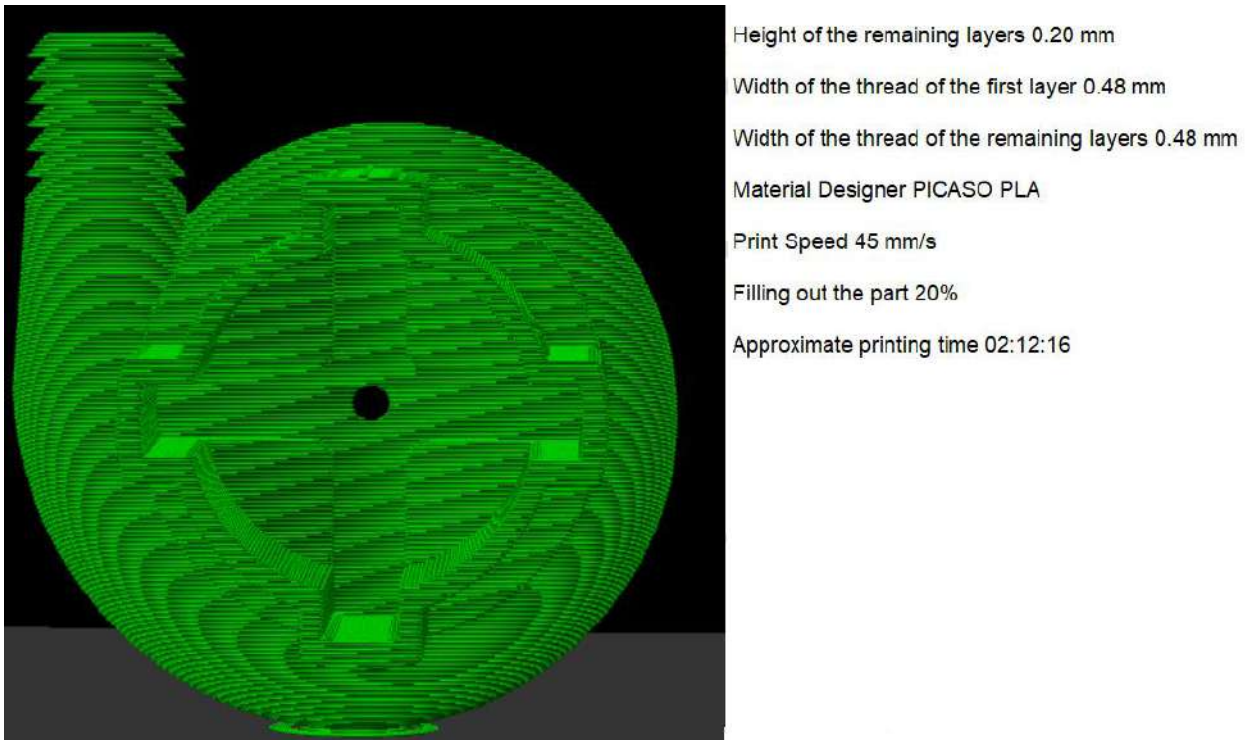

Fig.3. – Setting up a print job

The part was printed on a Designer Classic 3D printer based on the laboratory of the Abylkas Saginov Karaganda Technical University. Designer Classic is a 3D printer using FFF technology (fused filament fabrication). Typical feedstock materials for FFF are thermoplastics or thermoplastic-matrix composites in the form of filaments having a tightly controlled diameter of 1.75 or 2.85 mm, depending on the printing hardware [9]. As illustrated in Fig. 2, the filament is fed into the printhead by the action of two counter-rotating gears. The core of the printhead is the liquefier, where the feedstock material is heated and melted. The filament at the liquefier's entrance works like a

piston and pushes the melt out of the print nozzle. While the extrudate is being deposited on the base platform, the printhead moves on a X–Y gantry following a computer-controlled toolpath defined by the G-code, so that the extrudate draws the cross section of the part. When the first layer is completed, the base platform moves downward along the Z (growth) direction (or, vice versa, the printhead moves upward), and a second layer is added on top of the previous one. The process is then repeated layer by layer until completion of the desired 3D geometry [10]. The technical specifications of the 3D printer are shown in Table 2.

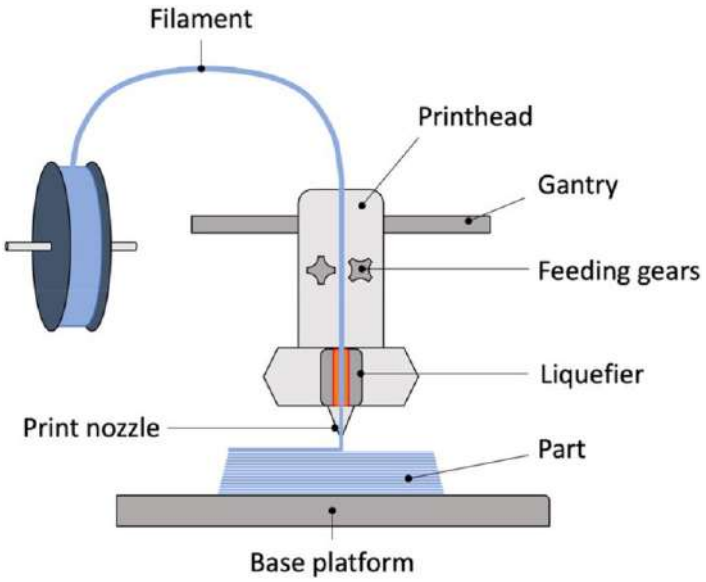

Fig. 4. – Schematic representation of an FFF printer

Table 2. Technical specifications of the Designer Classic 3D printer

№	Name of the parameter	Value
1	Printing technology	Fused Filament Fabrication (FFF)
2	Printing area, mm	201 x 201 x 210
3	Printing speed, cm^3/h	Up to 100
4	Minimum layer thickness, mm	0.01 mm
5	Diameter of the plastic thread, mm	1.75±0.1
6	Nozzle diameter, mm	0.5 mm (0.2 – 0.8 mm)
7	Printing material	PLA, PVA, ABS, PETG, TPE, SEBS etc.
8	Printing temperature, ºC	Up to 250
9	Platform temperature, ºC	150
10	Software	Polygon X

In the process of manufacturing a part on a 3D printer, the following time costs were experimentally recorded for the entire production process (Table 3).

Table 3. Numerical values of time spent during the manufacture of a part by 3D printing

No.	Name of the parameter	Value
1	Creating a digital model, min	60
2	Exporting a 3D model to STL format, min	3
3	G-code generation, min	3
4	Preparing the 3D printer for operation, min	40
5	3D model printing, min	132
6	Finishing of the part, min	60
	Total, min	298

If 100% of the total time spent from the beginning of the creation of the digital model to the finishing of the part is taken into account, then the distribution of time costs has the form shown in Fig. 5.

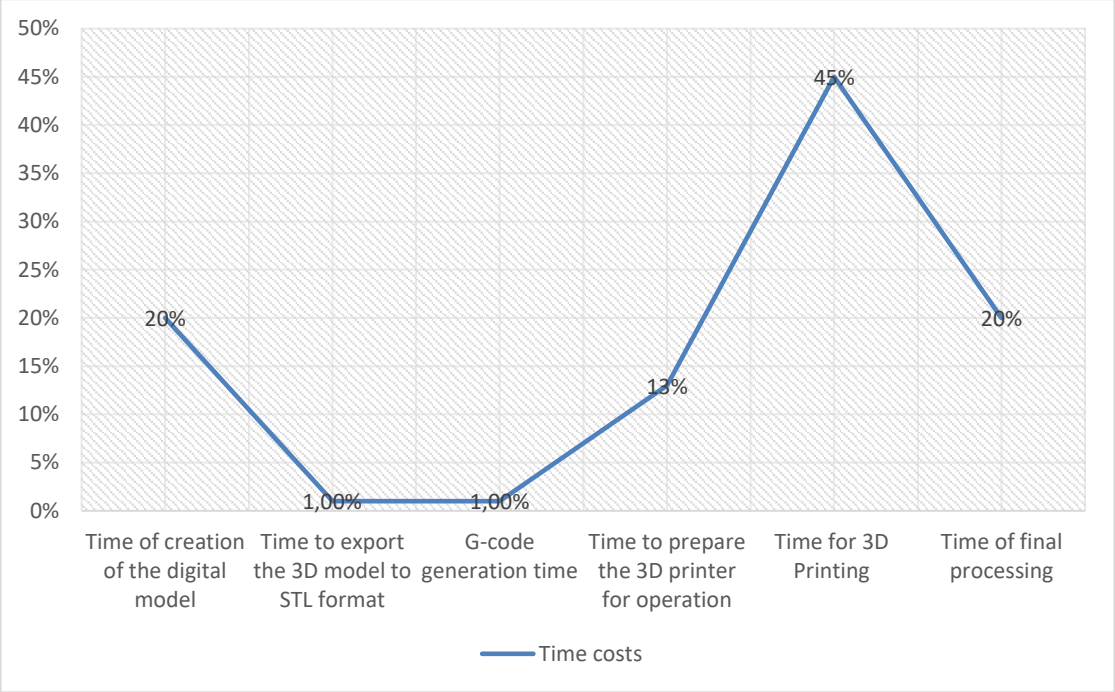

Fig. 5. – Time spent on the process of manufacturing a part by 3D printing

According to Fig. 5, the longest stage in the manufacture of a part is the stage of direct 3D printing of the part.

To conduct a comparative analysis of time costs, we will also consider the manufacture of a part in the traditional way – by milling on a CNC machine.

As can be seen from Table 1, the milling process on a CNC machine includes several important steps:

– Development of the control program;

– Preparation of the CNC machine;

– Manufacturing of the part.

For milling on a CNC machine, the same digital model was adopted, which is shown in Fig. 2. Next, it is necessary to develop a control program for the CNC. Currently, there are 2 ways to write control programs for CNC machines:

1. The manual method.

2. Development of control programs using automated CAD/CAE/CAM systems.

The manual method of developing a control program is impractical when developing a program for manufacturing parts of complex geometry.

To calculate the time to create programs to start the milling process on a CNC machine, we will use the Standard Time standards for preparing control programs for CNC machines using a computer (hereinafter – standard). According to the standard, the manufactured part belongs to the group of complexity of technological operations – 6.

Before programming, it is necessary to develop a technological process for processing a part on a CNC milling machine, which includes the following types of work:

– studying the drawing of the part, linking the projected technological operation with the functionality of the machine;

– choosing the optimal variant of the technological operation;

– selection of the basing scheme, technological equipment, cutting, measuring and auxiliary tools;

– drawing up and drawing a sketch of the processing and adjustment scheme with the calculation of tool departures;

– rationing of the technological operation;

– development of operational technology;

– control of technological preparation, standard control [11].

Based on the data in Table 3 [11], 14.07 hours are spent to develop the technological process of processing a part belonging to the complexity group 6.

Next, it is necessary to encode information for input into the CNC system (CP for a CNC milling machine), which includes the following types of work:

- construction of a mathematical model of the workpiece;

- building a technological model of the projected operation;

- development of the CP;
- CP control.

Based on the data in Table 7 [11], 3.41 hours are spent to encode information, 0.53 hours are spent to control the control program (Table 12 [11]). The total time spent on CNC programming is 18.01 hours.

According to table 14 [11], it takes 5.2 hours to debug the control program on a CNC machine. Debugging includes the following types of work:

- verification and control of compliance of the machine setup and the developed technological documentation (selection and installation of cutting, measuring and auxiliary tools, installation of the device and the workpiece);
- working out the control program on the machine outside the part and making the necessary changes;
- processing of the part in frame-by-frame mode, monitoring and making necessary changes [11].

As a result of computer modeling of milling in NX [12], it was found that the average milling time on a CNC machine of the part under study is 235 minutes (on both sides), quality control is 30 minutes. The part is not subjected to final processing

In the process of manufacturing a part on a CNC machine, the following time costs were analytically recorded for the entire production process (Table 4). If we take the total time spent from the beginning of the design of the model to the finishing of the part as 100%, then the distribution of time costs has the form shown in Fig. 6.

Table 4. Numerical values of time spent during the manufacture of a part by milling

No.	Parameter	Value
1	Model design, min	60
2	CNC programming, min	1081
3	Machine preparation, min	312
4	Milling of the workpiece, min	235
5	Quality control, min	30
6	Finishing of the part, min	0
	Total, min	1718

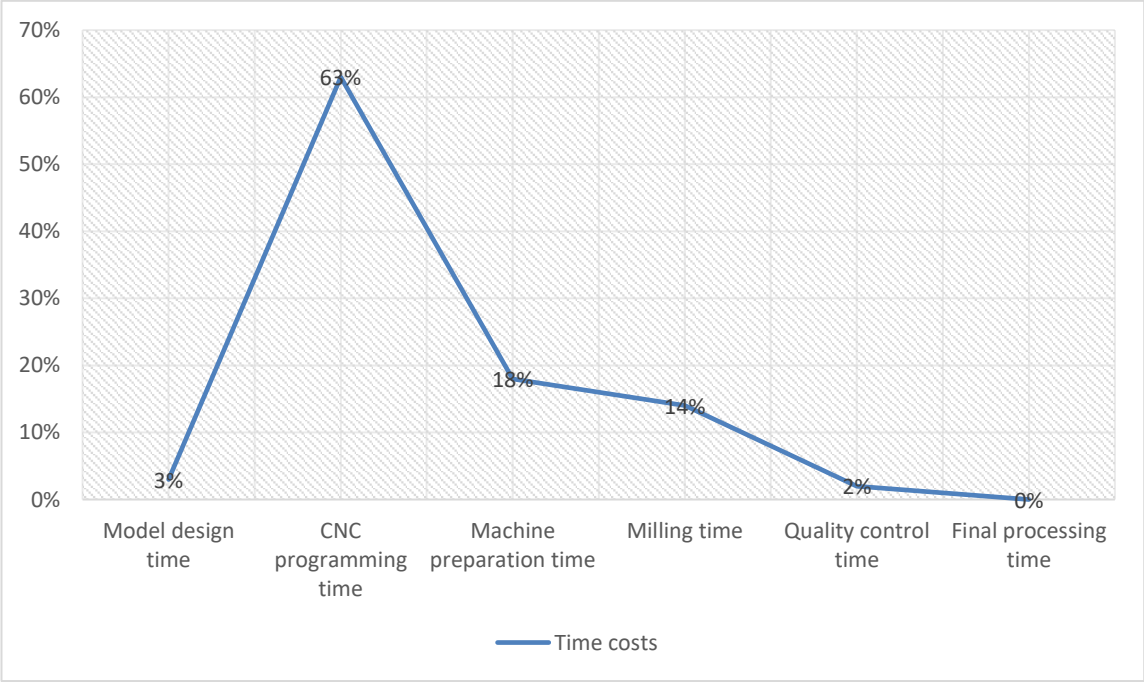

Fig. 6. – Time spent on the process of manufacturing a part by milling

According to the data shown in Fig. 6, the longest stage in the manufacture of a milling part is the programming stage of the control program for a CNC machine.

When using 3D printing to manufacture a part, the main work is done by the designer and the operator of the 3D printer. While the milling process requires qualified employees: a designer, a technologist, an adjuster and a machine operator. This means that choosing milling instead of 3D printing requires additional labor costs for qualified specialists, which may affect the economic side of the issue.

Conclusions

As a result of the analysis of empirical and analytical data, it was found that the most time-consuming operations are the following:

- in the process of 3D printing, the main amount of time (45% of the total process time) is spent directly on the printing process of the part;

- in the milling process, the largest share of time (63% of the total process time) is occupied by the development of a control program for a CNC machine.

The study showed that the preparation and completion time of the milling process (1718 minutes) exceeds the time spent on the 3D printing process (298 minutes) by 5.76 times. This is due to the fact that the main efforts during milling are aimed at developing a control program and initial setup of the machine, which makes the use of milling unprofitable in conditions of single and repair production.

References

[1] Melloy R.A. Konstruirovaniye plastmassovykh izdeliy dlya lit'ya pod davleniyem / per. s angl. yaz. pod. red. V.A. Braginskiy, Ye.S. Tsobkallo, G.V. Komarova – SPb.: Professiya, 2006. - 512 s.

[2] Gao, W., et al., The status, challenges, and future of additive manufacturing in engineering. Computer-Aided Design, 2015. 69. - P. 65-89.

[3] Guan Yunqin. Application of 3D printing technology in 3D modeling course [J]. Quality Education in West China, 2018 (6): 169

[4] Kianoush Haghsefat, Liu Tingting. 3D Printing and traditional manufacturing technology analysis and comparison

[5] Gausemeier, J., et al., Thinking ahead the Future of Additive Manufacturing–. Future Applications, 2011.

[6] Novikov S. V., Ramazanov K. N. Additive technologies: state and prospects : textbook [Electronic resource] / Ufa State University. aviac. tech. Ufa University: UGATU, 2022.

[7] P.P. Serebrenitsky. Rapid prototyping technologies // Rhythm. – 2008, № 6 (36). – p. 27

[8] C.K. Chua, C.H. Wong, W.Y. Yeong, 4 – software and data format, in: Standards, Quality Control, and Measurement Sciences in 3D Printing and Additive Manufacturing, Academic Press, Elsevier, London, UK – San Diego, CA, United States – Cambridge, MA, United States – Kidlington, Oxford, UK, 2017, pp. 75–94.

[9] L. Koester, H. Taheri, L.J. Bond, D. Barnard, J. Gray, Additive manufacturing metrology: state of the art and needs assessment, AIP Conf. Proc. 1706 (2016).

[10] L.S. Moura, G.D. Vittoria, A.H.G. Gabriel, E.B. Fonseca, L.P. Gabriel, T.J. Webster, E.S.N. Lopes, A highly accurate methodology for the prediction and correlation of mechanical properties based on the slimness ratio of additively manufactured tensile test specimens, J. Mater. Sci. 55 (2020) 9578–9596.

[11] Typical time standards for the preparation of control programs for CNC machines using a computer: approved The Central Bureau of Labor Standards of the USSR State Committee. – Moscow, 1991. – 43 p.

[12] Vedmid P.A., Sulinov A.V. Programming processing in NX CAM. – M.: DMK Press, 2014. – 304 p.: ill. ISBN 978-5-97060-143-3

[13] Savelyeva N.A., Zhetessova G.S., Ibatov M.K., Nikonova T.Yu., Reshetnikova O.S., Berg A.S., Berg A.A., Yassakov Yu.D. Prerequisites for developing a technological preparation database of small- and medium-scale machine-building industries //Material and mechanical engineering technology

Information of the authors

Zhetessova Gulnara Santaevna, d.t.s., professor, Karaganda Abylkas Saginov Karaganda Technical University
e-mail: zhetesova@mail.ru

Škamat Jelena, d.t.s., associate professor, Vilnius Gediminas Technical University
e-mail: jelena.skamat@vilniustech.lt

Tattimbetova Gulim Bolatovna, doctoral student, Karaganda Abylkas Saginov Karaganda Technical University
e-mail: tattimbetova@mail.ru

Mateshov Arman Karievich, Senior lecturer, Karaganda Abylkas Saginov Karaganda Technical University
e-mail: makashka_m@mail.ru